

On Statistical Rates and Provably Efficient Criteria of Latent Diffusion Transformers (DiTs)

Jerry Yao-Chieh Hu^{†*1} Weimin Wu^{†*2} Zhao Song^{‡3} Han Liu^{†§4}

[†] Department of Computer Science, Northwestern University, Evanston, IL 60208 USA

[‡] Adobe Research, Seattle, WA 98103 USA

[§] Department of Statistics and Data Science, Northwestern University, Evanston, IL 60208 USA

We investigate the statistical and computational limits of latent **D**iffusion **T**ransformers (**DiTs**) under the low-dimensional linear latent space assumption. Statistically, we study the universal approximation and sample complexity of the DiTs score function, as well as the distribution recovery property of the initial data. Specifically, under mild data assumptions, we derive an approximation error bound for the score network of latent DiTs, which is sub-linear in the latent space dimension. Additionally, we derive the corresponding sample complexity bound and show that the data distribution generated from the estimated score function converges toward a proximate area of the original one. Computationally, we characterize the hardness of both forward inference and backward computation of latent DiTs, assuming the Strong Exponential Time Hypothesis (SETH). For forward inference, we identify efficient criteria for all possible latent DiTs inference algorithms and showcase our theory by pushing the efficiency toward almost-linear time inference. For backward computation, we leverage the low-rank structure within the gradient computation of DiTs training for possible algorithmic speedup. Specifically, we show that such speedup achieves almost-linear time latent DiTs training by casting the DiTs gradient as a series of chained low-rank approximations with bounded error. Under the low-dimensional assumption, we show that the convergence rate and the computational efficiency are both dominated by the dimension of the subspace, suggesting that latent DiTs have the potential to bypass the challenges associated with the high dimensionality of initial data.

¹ jhu@u.northwestern.edu

² weiminwu2023@u.northwestern.edu

³ zsong@adobe.com

⁴ hanliu@northwestern.edu

*These authors contributed equally to this work.

Contents

1	Introduction	2
2	Background	4
2.1	Score-Matching Denoising Diffusion Models	4
2.2	Score Decomposition in Linear Latent Space	5
2.3	Score Network and Transformers	5
3	Statistical Rates of Latent DiTs with Subspace Data Assumption	6
3.1	DiT Score Network Class	7
3.2	Score Approximation of DiT	7
3.3	Score Estimation and Distribution Estimation	9
4	Provably Efficient Criteria	11
4.1	Computational Limits of Backward Computation	11
4.2	Computational Limits of Forward Inference	14
5	Discussion and Conclusion	15
A	More Discussion on Low-Dimensional Linear Latent Space	18
B	Nomenclature Table	19
C	Related Works	20
D	Supplementary Theoretical Background	23
D.1	Diffusion Models	23
D.2	Proof of Lemma 2.1	24
D.3	Preliminaries: Strong Exponential Time Hypothesis (SETH) and Tensor Trick	28
E	More Background and Auxiliary Lemmas:	
	Universal Approximation of Transformers via Piecewise Approximation	30
E.1	Piecewise-constant Function Approximates Compact-Supported Continuous Function	30
E.2	Modified Transformer Approximates Piece-Wise Constant Function	31
E.3	Standard Transformers Approximate Modified Transformers	36
E.4	All Together: Standard Transformers Approximate Compact-Supported Continuous Functions	36
E.5	Supplementary Proofs	37
F	Proofs of Section 3	50
F.1	Proof of Theorem 3.1	50
F.2	Proof of Corollary 3.1.1	57
F.3	Proof of Corollary 3.1.2	63
G	Proofs of Section 4	67
G.1	Auxiliary Theoretical Results for Theorem 4.1	67
G.2	Proof of Theorem 4.1	75

1 Introduction

We investigate the statistical and computational limits of latent diffusion transformers (DiTs), assuming the data is supported on an unknown low-dimensional linear subspace. This analysis is not only practical but also timely. On one hand, DiTs have demonstrated revolutionary success in generative AI and digital creation by using Transformers as score networks [Esser et al., 2024, Ma et al., 2024, Chen et al., 2024, Mo et al., 2023, Peebles and Xie, 2023]. On the other hand, they require significant computational resources [Liu et al., 2024], making them challenging to train outside of specialized industrial labs. Therefore, it is natural to ask whether it is possible to make them lighter and faster without sacrificing performance. Answering these questions requires a fundamental understanding of the DiT architecture. This work provides a timely theoretical analysis of the fundamental limits of DiT architecture, aided by the analytical feasibility provided by the low-dimensional data assumption.

Empirically, Latent Diffusion is a go-to design for effectiveness and computational efficiency [Rombach et al., 2022, Liu et al., 2021, Pope et al., 2021, Su and Wu, 2018]. Theoretically, it is capable of hosting the assumption of low-dimensional data structure (see [Assumption 2.1](#) for formal definition) for detailed analytical characterization [Chen et al., 2023a, Bortoli, 2022]. In essence, diffusion models with low-dimensional data structures manifest a natural lower-dimensional diffusion process through an encoder/decoder within a robust and informative latent representation feature space [Rombach et al., 2022, Pope et al., 2021]. Such lower-dimensional diffusion improves computational efficiency by reducing data complexity without sacrificing essential information [Liu et al., 2021]. With this assumption, Chen et al. [2023a] decompose the score function of U-Net based diffusion models into on-support and orthogonal components. This decomposition allows for the characterization of the distinct behaviors of the two components: the on-support component facilitates latent distribution learning, while the orthogonal component facilitates subspace recovery.

In our work, we utilize low-dimensional data structure assumption to explore statistical and computational limits of latent DiTs. Our analysis includes the characterizations of statistical rates and provably efficient criteria. Statistically, we pose two questions and provide a theory to characterize the statistical rates of latent DiT under the assumption of a low-dimensional data:

Question 1. What is the approximation limit of using transformers to approximate the DiT score function, particularly in the low-dimensional data subspace?

Question 2. How accurate is the estimation limit for such a score estimator in practical training scenarios? With the score estimator, how well can diffusion transformers recover the data distribution?

Computationally, the primary challenge of DiT lies in the transformer blocks’ quadratic complexity. This computational burden applies to both inference and training, even with latent diffusion. Thus, it is essential to design algorithms and methods to circumvent this $\Omega(L^2)$ where L is the

latent DiT sequence length. However, there are no formal results to support and characterize such algorithms. To address this gap, we pose the following questions and provide a fundamental theory to fully characterize the complexity of latent DiT under the low-dimensional linear subspace data assumption:

Question 3. Is it possible to improve the $\Omega(L^2)$ time complexity with a bounded approximation error for both forward and backward passes? What is the computational limit for such an improvement?

Contributions. We study the fundamental limits of latent DiT. Our contributions are threefold:

- **Score Approximation.** We address [Question 1](#) by characterizing the approximation limit of matching the DiT score function with a transformer-based score estimator. Specifically, under mild data assumptions, we derive an approximation error bound for the score network, sub-linear in the latent space dimension ([Theorem 3.1](#)). These results not only explain the expressiveness of latent DiT (under mild assumptions) but also provide guidance for the structural configuration of the score network for practical implementations ([Theorem 3.1](#)).
- **Score and Distribution Estimation.** We address [Question 2](#) by exploring the limitations of score and distribution estimations of latent DiTs in practical training scenarios. Specifically, we provide a sample complexity bound for score estimation ([Corollary 3.1.1](#)), using norm-based covering number bound of transformer architecture. Additionally, we show that the learned score estimator is able to recover the initial data distribution ([Corollary 3.1.2](#)).
- **Provably Efficient Criteria and Existence of Almost Linear Time Algorithms.** We address [Question 3](#) by providing provably efficient criteria for latent DiTs in both forward inference and backward computation/training. For forward inference, we characterize all possible efficient DiT algorithms using a norm-based efficiency threshold for both conditional and unconditional generation ([Proposition 4.1](#)). Efficient algorithms, including almost-linear time algorithms ([Proposition 4.2](#)), are possible only below this threshold. For backward computation, we prove the existence of almost-linear time DiT training algorithms ([Theorem 4.1](#)) by utilizing the inherent low-rank structure in DiT gradients through a chained low-rank approximation.

Interestingly, both our statistical and computational results are dominated by the subspace dimension under the low-dimensional assumption, suggesting that latent DiT can potentially bypass the challenges associated with the high dimensionality of initial data.

Organization. [Section 2](#) includes background on score decomposition and Transformer-based score networks. [Section 3](#) presents the statistical rates of DiTs. [Section 4](#) provides provably efficient criteria. We defer discussions of related works to [Appendix C](#) due to space constraints.

Notations. We use lower case letters to denote vectors, e.g., $z \in \mathbb{R}^D$. $\|z\|_2$ and $\|z\|_\infty$ denote its Euclidean norm and Infinite norm respectively. We use upper case letters to de-

note matrix, e.g., $Z \in \mathbb{R}^{d \times L}$. $\|Z\|_2$, $\|Z\|_{\text{op}}$, and $\|Z\|_F$ denote the 2-norm, operator norm and Frobenius norm respectively. $\|Z\|_{p,q}$ denotes the p, q -norm where the p -norm is over columns and q -norm is over rows. Given a function f , let $\|f(x)\|_{L^2} := (\int \|f(x)\|_2^2 dx)^{1/2}$, and $\|f(\cdot)\|_{Lip} = \sup_{x \neq y} (\|f(x) - f(y)\|_2 / \|x - y\|_2)$. With a distribution P , we denote $\|f\|_{L^2(P)} = (\int_P \|f(x)\|_2^2 dx)^{1/2}$ as the $L^2(P)$ norm. Let $f_{\#}P$ be a pushforward measure, i.e., for any measurable Ω , $(f_{\#}P)(\Omega) = P(f^{-1}(\Omega))$. We use ψ for (conditional) Gaussian density functions.

2 Background

This section reviews the ideas we built on, including an overview of diffusion models (Section 2.1), the score decomposition under the linear latent space assumption (Section 2.2), and the transformer backbone in DiT (Section 2.3).

2.1 Score-Matching Denoising Diffusion Models

We briefly review forward process, backward process and score matching in diffusion models.

Forward and Backward Process. In the **forward** process, Diffusion models gradually add noise to the original data $x_0 \in \mathbb{R}^D$, and $x_0 \sim P_0$. Let x_t denote the noisy data at time stamp t , with marginal distribution and destiny as P_t and p_t . The conditional distribution $P(x_t|x_0)$ follows $N(\beta(t)x_0, \sigma(t)I_D)$, where $\beta(t) = \exp(-\int_0^t w(s)ds/2)$, $\sigma(t) = 1 - \beta^2(t)$, and $w(t) > 0$ is a nondecreasing weighting function. In practice, the forward process terminates at a large enough T such that P_T is close to $N(0, I_D)$. In the **backward** process, we obtain y_t by reversing the forward process. The generation of y_t depends on the score function $\nabla \log p_t(\cdot)$. However, this is unknown in practice, we use a score estimator $s_W(\cdot, t)$ to replace $\nabla \log p_t(\cdot)$, where $s_W(\cdot, t)$ is usually a neural network with parameters W . See Appendix D.1 for the details.

Score Matching. To estimate the score function, we use the following loss

$$\min_W \int_{T_0}^T \gamma(t) \mathbb{E}_{x_t \sim P_t} [\|s_W(x_t, t) - \nabla \log p_t(x_t)\|_2^2] dt,$$

where $\gamma(t)$ is the weight function, and T_0 is a small value to stabilize training and prevent score function from blowing up [Vahdat et al., 2021]. However, it is hard to compute $\nabla \log p_t(\cdot)$ with available data samples. Therefore, we minimize the equivalent denoising score matching objective

$$\min_W \int_{T_0}^T \gamma(t) \mathbb{E}_{x_0 \sim P_0} [\mathbb{E}_{x_t|x_0} [\|s_W(x_t, t) - \nabla_{x_t} \log \psi_t(x_t | x_0)\|_2^2]] dt, \quad (2.1)$$

where $\psi_t(x_t|x_0)$ is the transition kernel, then $\nabla_{x_t} \log \psi_t(x_t|x_0) = (\beta(t)x_0 - x_t) / \sigma(t)$.

To train the parameters W in the score estimator $s_W(\cdot, t)$, we use the empirical version of (2.1).

We select n i.i.d. data samples $\{x_{0,i}\}_{i=1}^n \sim P_0$, and sample time t_i ($1 \leq i \leq n$) uniformly from interval $[T_0, T]$. Given $x_{0,i}$, we sample x_{t_i} from $N(\beta(t_i)x_{0,i}, \sigma(t_i)I_D)$. The empirical loss is

$$\min_W \hat{\mathcal{L}}(W) = \frac{1}{n} \sum_{i=1}^n \|s_W(x_{t_i}, t_i) - x_{0,i}\|_2^2. \quad (2.2)$$

For convenience of notation, we denote population loss $\mathcal{L}(W) = \mathbb{E}_{P_0}[\hat{\mathcal{L}}(W)]$.

2.2 Score Decomposition in Linear Latent Space

In this part, we review the score decomposition in [Chen et al., 2023a]. We consider that the D -dimensional input data x supported on a d_0 -dimensional subspace, where $d_0 \leq D$.

Assumption 2.1 (Low-Dimensional Linear Latent Space). Data point x can be written as $x = Bh$, where $B \in \mathbb{R}^{D \times d_0}$ is an unknown matrix with orthonormal columns. The latent variable $h \in \mathbb{R}^{d_0}$ follows the distribution P_h with a density function p_h .

Remark 2.1. By ‘‘Linear Latent Space,’’ we mean that each entry of a given latent vector is a linear combination of the corresponding input, i.e., $x = Bh$. This is also known as the ‘‘low-dimensional data’’ assumption in literature [Chen et al., 2023a].

Based on the low-dimensional data structure assumption, we have the following score decomposition theory: on-support score $s_+(B^\top x, t)$ and orthogonal score $s_-(x, t)$.

Lemma 2.1 (Score Decomposition, Lemma 1 of [Chen et al., 2023a]). Let data $x = Bh$ follow **Assumption 2.1**. The decomposition of score function $\nabla \log p_t(x)$ is

$$\nabla \log p_t(x) = \underbrace{B \nabla \log p_t^h(\bar{h})}_{s_+(\bar{h}, t)} - \underbrace{(I_D - BB^\top) x / \sigma(t)}_{s_-(x, t)}, \quad \bar{h} = B^\top x, \quad (2.3)$$

where $p_t^h(\bar{h}) := \int \psi_t(\bar{h}|h) p_h(h) dh$, $\psi_t(\cdot|h)$ is the Gaussian density function of $N(\beta(t)h, \sigma(t)I_{d_0})$, $\beta(t) = e^{-t/2}$ and $\sigma(t) = 1 - e^{-t}$. We restate the proof in **Appendix D.2** for completeness.

Additionally, our theoretical analysis is based on two following assumptions as in [Chen et al., 2023a].

Assumption 2.2 (Tail Behavior of P_h). The density function $p_h > 0$ is twice continuously differentiable. Moreover, there exist positive constants A_0, A_1, A_2 such that when $\|h\|_2 \geq A_0$, the density function $p_h(h) \leq (2\pi)^{-d_0/2} A_1 \exp(-A_2 \|h\|_2^2/2)$.

Assumption 2.3 (L_{s_+} -Lipschitz of $s_+(\bar{h}, t)$). The on-support score function $s_+(\bar{h}, t)$ is L_{s_+} -Lipschitz in $\bar{h} \in \mathbb{R}^{d_0}$ for any $t \in [0, T]$.

2.3 Score Network and Transformers

In this part, we introduce the score network architecture and Transformers. Transformers are the backbone of the score network in DiT. By **Assumption 2.1**, $\bar{h} = B^\top x \in \mathbb{R}^{d_0}$ with $d_0 < D$.

(Latent) Score Network. Following [Chen et al., 2023a], we rearrange (2.3) into

$$\nabla \log p_t(x) = B \underbrace{(\sigma(t) \nabla \log p_t^h(B^\top x) + B^\top x)}_{:=q(B^\top x, t): \mathbb{R}^{d_0} \times [T_0, T] \rightarrow \mathbb{R}^{d_0}} / \sigma(t) - x / \sigma(t). \quad (2.4)$$

We use $W_B \in \mathbb{R}^{D \times d_0}$ to approximate $B \in \mathbb{R}^{D \times d_0}$, and a neural network $f(W_B^\top x, t)$ to approximate $q(B^\top x, t)$. We adopt the following score network class for diffusion in latent space (i.e., in $h \in \mathbb{R}^{d_0}$)

$$\mathcal{S} = \{s_W(x, t) = W_B f(W_B^\top x, t) / \sigma(t) - x / \sigma(t), W = \{W_B, f\}\}, \quad (2.5)$$

where the columns in W_B are orthogonal, $f: \mathbb{R}^{d_0} \times [T_0, T] \rightarrow \mathbb{R}^{d_0}$ is a neural network. In our work, we focus on the diffusion transformers (DiTs), i.e., using Transformer for f [Peebles and Xie, 2023].

Transformers. A Transformer block consists of a self-attention layer and a feed-forward layer, with both layers having skip connection. We use $\tau^{r,m,l}: \mathbb{R}^{d \times L} \rightarrow \mathbb{R}^{d \times L}$ to denote a Transformer block. Here r and m are the number of heads and head size in self-attention layer, and l is the hidden dimension in feed-forward layer. Let $X \in \mathbb{R}^{d \times L}$ be the model input, then we have the model output

$$\text{Attn}(X) = X + \sum_{i=1}^r W_O^i W_V^i X \cdot \text{Softmax}\left((W_K^i X)^\top W_Q^i X\right), \quad (2.6)$$

$$\text{FF} \circ \text{Attn}(X) = \text{Attn}(X) + W_2 \cdot \text{ReLU}(W_1 \cdot \text{Attn}(X) + b_1 \mathbf{1}_L^\top) + b_2 \mathbf{1}_L^\top, \quad (2.7)$$

where $W_K^i, W_Q^i, W_V^i \in \mathbb{R}^{m \times d}, W_O^i \in \mathbb{R}^{d \times m}, W_1 \in \mathbb{R}^{l \times d}, W_2 \in \mathbb{R}^{d \times l}, b_1 \in \mathbb{R}^l, b_2 \in \mathbb{R}^d$.

In our work, we use Transformer networks with positional encoding $E \in \mathbb{R}^{d \times L}$. We define the Transformer networks as the composition of Transformer blocks

$$\mathcal{T}_P^{r,m,l} = \{f_{\mathcal{T}}: \mathbb{R}^{d \times L} \rightarrow \mathbb{R}^{d \times L} \mid f_{\mathcal{T}} \text{ is a composition of blocks } \tau^{r,m,l}_s\}.$$

For example, the following is a Transformer network consisting K blocks and positional encoding

$$f_{\mathcal{T}}(X) = \text{FF}^{(K)} \circ \text{Attn}^{(K)} \circ \dots \circ \text{FF}^{(1)} \circ \text{Attn}^{(1)}(X + E). \quad (2.8)$$

3 Statistical Rates of Latent DiTs with Subspace Data Assumption

In this section, we analyze the statistical rates of latent DiTs. Section 3.1 introduces the class of latent DiT score networks. In Section 3.2, we prove the approximation limit of matching the DiT score function with the score network class, and characterize the structural configuration of the

score network when a specified approximation error is required. Following this, in [Section 3.3](#), utilizing the characterized structural configuration, we prove the score and distribution estimation for latent DiTs.

3.1 DiT Score Network Class

In this part, we give the details about DiT score network class used in our analysis. In [\(2.5\)](#), f is a network with Transformer as the backbone, and $(h, t) \in \mathbb{R}^{d_0} \times [T_0, T]$ denotes the input data. Following [\[Peebles and Xie, 2023\]](#), DiT uses time point t to calculate the scale and shift value in the Transformer backbone, and it transforms an input picture into a sequential version. To achieve the transformation, we introduce a reshape layer.

Definition 3.1 (DiT Reshape Layer $R(\cdot)$). Let $R(\cdot) : \mathbb{R}^{d_0} \rightarrow \mathbb{R}^{d \times L}$ be a reshape layer that transforms the d_0 -dimensional input into a $d \times L$ matrix. Specifically, for any $d_0 = i \times i$ image input, $R(\cdot)$ converts it into a sequence representation with feature dimension $d := p^2$ (where $p \geq 2$) and sequence length $L := (i/p)^2$. Besides, we define the corresponding reverse reshape (flatten) layer $R^{-1}(\cdot) : \mathbb{R}^{d \times L} \rightarrow \mathbb{R}^{d_0}$ as the inverse of $R(\cdot)$. By $d_0 = dL$, R, R^{-1} are associative w.r.t. their input.

To simplify the self-attention block in [\(2.6\)](#), let $W_{OV}^i = W_O^i W_V^i$ and $W_{KQ}^i = (W_K^i)^\top W_Q^i$.

Definition 3.2 (Transformer Network Class $\mathcal{T}_p^{r,m,l}$). We define the Transformer network class as

$\mathcal{T}_p^{r,m,l}(K, C_{\mathcal{T}}, C_{OV}^{2,\infty}, C_{OV}, C_{KQ}^{2,\infty}, C_{KQ}, C_F^{2,\infty}, C_F, C_E, L_{\mathcal{T}})$, satisfying the constraints

- Model architecture with K blocks: $f_{\mathcal{T}}(X) = \text{FF}^{(K)} \circ \text{Attn}^{(K)} \circ \dots \circ \text{FF}^{(1)} \circ \text{Attn}^{(1)}(X)$;
- Model output bound: $\sup_X \|f_{\mathcal{T}}(X)\|_2 \leq C_{\mathcal{T}}$;
- Parameter bound in $\text{Attn}^{(i)}$: $\|(W_{OV}^i)^\top\|_{2,\infty} \leq C_{OV}^{2,\infty}, \|(W_{OV}^i)^\top\|_2 \leq C_{OV}, \|W_{KQ}^i\|_{2,\infty} \leq C_{KQ}^{2,\infty}, \|W_{KQ}^i\|_2 \leq C_{KQ}, \|E^\top\|_{2,\infty} \leq C_E, \forall i \in [K]$;
- Parameter bound in $\text{FF}^{(i)}$: $\|W_j^i\|_{2,\infty} \leq C_F^{2,\infty}, \|W_j^i\|_2 \leq C_F, \forall j \in [2], i \in [K]$;
- Lipschitz of $f_{\mathcal{T}}$: $\|f_{\mathcal{T}}(X_1) - f_{\mathcal{T}}(X_2)\|_F \leq L_{\mathcal{T}}\|X_1 - X_2\|_F, \forall X_1, X_2 \in \mathbb{R}^{d \times L}$.

Definition 3.3 (DiT Score Network Class $\mathcal{S}_{\mathcal{T}_p^{r,m,l}}$ ([Figure 1](#))). We denote $\mathcal{S}_{\mathcal{T}_p^{r,m,l}}$ as the DiT score network class in [\(2.5\)](#), replacing f with $R^{-1} \circ f_{\mathcal{T}} \circ R$, and $f_{\mathcal{T}}$ is from the Transformer class $\mathcal{T}_p^{r,m,l}$.

3.2 Score Approximation of DiT

Here, we explore the approximation limit of latent DiT score network class $\mathcal{S}_{\mathcal{T}_p^{r,m,l}}$ under linear latent space assumption. Recall that P_t is the distribution of x_t , $\sigma(t)$ is the variance of $P(x_t|x_0)$, d_0 is the dimension of latent space, L is the sequence length of transformer input, T is the stopping

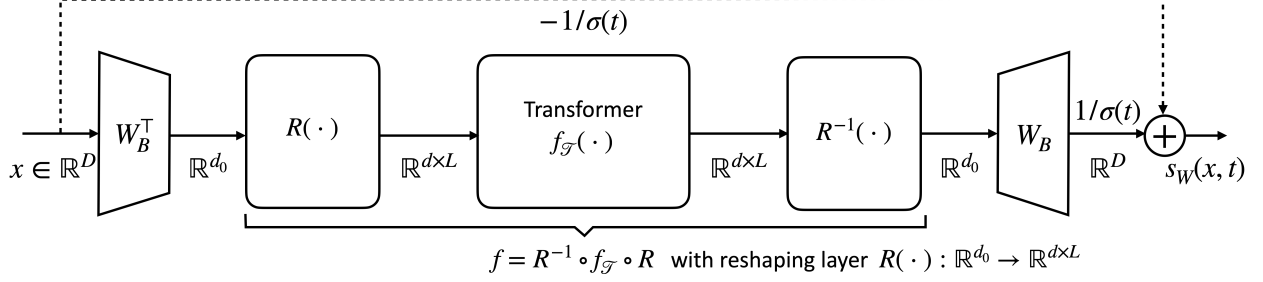


Figure 1: **Overview of DiT Score Network Architecture** $s_W(x, t)$. W_B^T denotes the linear layer from the input data space to the linear latent space. $f(\cdot) = R^{-1} \circ f_{\mathcal{T}} \circ R(\cdot)$ denotes the transformer network $f_{\mathcal{T}}(\cdot)$ with reshaping layer $R(\cdot)$, where $f_{\mathcal{T}}(\cdot) \in \mathcal{T}_p^{r,m,l}$. W_B denotes the linear layer from the linear latent space to the input data space. $\sigma(t)$ denote the variance of the conditional distribution $P(x_t | x_0)$.

time in forward process, T_0 is the early stopping time in backward process, and L_{s+} is the Lipschitz coefficient of on-support score function. Then we have the following **Theorem 3.1**.

Theorem 3.1 (Score Approximation of DiT). For any approximation error $\epsilon > 0$ and any data distribution P_0 under **Assumptions 2.1** to **2.3**, there exists a DiT score network $s_{\widehat{W}}$ from $\mathcal{S}_{\mathcal{T}_p^{2,1,4}}$ (defined in **Definition 3.2**), where $\widehat{W} = \{\widehat{W}_B, \widehat{f}_{\mathcal{T}}\}$, such that for any $t \in [T_0, T]$, we have:

$$\|s_{\widehat{W}}(\cdot, t) - \nabla \log p_t(\cdot)\|_{L^2(P_t)} \leq \epsilon \cdot \sqrt{d_0}/\sigma(t),$$

where $\sigma(t) = 1 - e^{-t}$, and the upper bound of hyperparameters in $\mathcal{S}_{\mathcal{T}_p^{2,1,4}}$ are

$$\begin{aligned} K &= \mathcal{O}(\epsilon^{-2L}), \quad C_{\mathcal{T}} = \mathcal{O}\left(d_0 L_{s+} \sqrt{d_0 \log(d_0/T_0) + \log(1/\epsilon)}\right), \\ C_{OV}^{2,\infty} &= (1/\epsilon)^{\mathcal{O}(1)}, \quad C_{OV} = (1/\epsilon)^{\mathcal{O}(1)}, \quad C_{KQ}^{2,\infty} = (1/\epsilon)^{\mathcal{O}(1)}, \quad C_{KQ} = (1/\epsilon)^{\mathcal{O}(1)}, \\ C_E &= \mathcal{O}(L^{3/2}), \quad C_F^{2,\infty} = (1/\epsilon)^{\mathcal{O}(1)}, \quad C_F = (1/\epsilon)^{\mathcal{O}(1)}, \quad L_{\mathcal{T}} = \mathcal{O}(d_0 L_{s+}). \end{aligned}$$

Proof Sketch. Our proof is built on the key observation that there is a tail behavior of the low-dimensional latent variable distribution P_h (**Assumption 2.2**). Recall that $\nabla \log p_t(x) = Bq(\bar{h}, t)/\sigma(t) - x/\sigma(t)$, where $\bar{h} = B^\top x$ (defined in (2.4)). By taking $\widehat{W}_B = B$, our aim reduces to construct a transformer network to approximate $q(\bar{h}, t)$. To achieve this, we firstly approximate $q(\bar{h}, t)$ with a compact-supported continuous function, based on the tail behavior of P_h . Then we construct a transformer to approximate the compact-supported continuous function using the universal approximation capacity of transformer [Yun et al., 2020]. See **Appendix F.1** for a detailed proof. \square

Intuitively, **Theorem 3.1** indicates the capability of the transformer-based score network to approximate the score function with precise guarantees. Furthermore, **Theorem 3.1** provides empirical

guidance for the design choices of the score network when a specified approximation error is required.

Remark 3.1 (Comparing with Existing Works). Theoretical analysis of DiTs is limited. Previous works that do not specify the model architecture assume that the score estimator is well-approximated [Benton et al., 2024, Wibisono et al., 2024]. To the best of our knowledge, this work is the first to present an approximation theory for DiTs, offering the estimation theory in Corollaries 3.1.1 and 3.1.2 based on the estimated score network, rather than a perfectly trained one.

Remark 3.2 (Latent Dimension Dependency). Theorem 3.1 suggests that the approximation capacity and Transformer network size primarily depend on the latent variable dimension $d_0 = d \times L$. This indicates that DiTs can potentially bypass the challenges associated with the high dimensionality of initial data by transforming input data into a low-dimensional latent variable.

3.3 Score Estimation and Distribution Estimation

Besides score approximation capability, Theorem 3.1 also characterizes the structural configuration of the score network for any specific precision, e.g., K, C_E, C_F , etc. This characterization enables further analysis of the performance of score network in practical scenarios. In Corollary 3.1.1, we provide a sample complexity bound for score estimation. In Corollary 3.1.2, show that the learned score estimator is able to recover the initial data distribution.

Score Estimation. To derive a sample complexity for score estimation using $\mathcal{S}_{\mathcal{T}_p^{2,1,4}}$, we rewrite the score matching objective in (2.2) as $\widehat{W} \in \operatorname{argmin}_{s_W \in \mathcal{S}_{\mathcal{T}_p^{2,1,4}}} \widehat{\mathcal{L}}(s_W)$, $\widehat{W} = \{\widehat{W}_B, \widehat{f}_T\}$.

Corollary 3.1.1 shows that as sample size $n \rightarrow \infty$, $s_W(\cdot, t)$ convergences to $\nabla \log p_t(\cdot)$.

Corollary 3.1.1 (Score Estimation of DiT). Under Assumptions 2.1 to 2.3, we choose $\mathcal{S}_{\mathcal{T}_p^{2,1,4}}$ as in Theorem 3.1 using $\epsilon \in (0, 1)$ and $L > 1$, With probability $1 - 1/\operatorname{poly}(n)$, we have

$$\frac{1}{T - T_0} \int_{T_0}^T \|s_{\widehat{W}}(\cdot, t) - \nabla \log p_t(\cdot)\|_{L^2(P_t)} dt = \tilde{\mathcal{O}} \left(\frac{1}{n^{1/2}} \frac{T}{T_0} \cdot 2^{(1/\epsilon)^{2L}} + \frac{1}{T_0 T} \epsilon^2 + \frac{1}{n} \right), \quad (3.1)$$

where $\tilde{\mathcal{O}}$ hides the factor about $D, d_0, d, L_{s+}, \log n$.

Proof. See Appendix F.2 for a detailed proof. □

Intuitively, Corollary 3.1.1 shows a sample complexity bound for score estimation in practice.

Remark 3.3 (Comparing with Existing Works). [Zhu et al., 2023] provides a sample complexity for simple ReLU-based diffusion models under the assumption of an accurate score estimator. To

the best of our knowledge, we are the first to provide a sample complexity for DiTs, based on the learned score network in [Theorem 3.1](#) and the quantization (piece-wise approximation) approach for transformer universality [[Yun et al., 2020](#)].

Remark 3.4. [Corollary 3.1.1](#) reports an explicit result on sample complexity bounds for score estimation of latent DiTs: a double exponential factor $2^{(1/\epsilon)^{2L}}$ in the first term. We remark that this arises from the required depth K is $\mathcal{O}(\epsilon^{-2L})$, and the norm of required weight parameters is $(1/\epsilon)^{\mathcal{O}(1)}$ as shown in [Theorem 3.1](#), assuming the universality of transformers requires dense layers [[Yun et al., 2020](#)]. This motivates us to rethink transformer universality and explore new proof techniques for DiTs, which we leave for future work.

Definition 3.4. For later convenience, we define $\xi(n, \epsilon, L) := \frac{1}{n^{1/2}} \frac{T}{T_0} \cdot 2^{(1/\epsilon)^{2L}} + \frac{1}{T_0 T} \epsilon^2 + \frac{1}{n}$.

Distribution Estimation. In practice, DiTs generate data using the discretized version with step size μ , see [Appendix D.1](#) for details. Let \hat{P}_{T_0} be the distribution generated by $s_{\hat{W}}$ in [Corollary 3.1.1](#). Let $P_{T_0}^h$ and $p_{T_0}^h$ be the distribution and density function of on-support latent variable \bar{h} at T_0 . We have the following results for distribution estimation.

Corollary 3.1.2 (Distribution Estimation of DiT, Modified From Theorem 3 of [[Chen et al., 2023a](#)]). Let $T = \mathcal{O}(\log n)$, $T_0 = \mathcal{O}(\min\{c_0, 1/L_{s+}\})$, where c_0 is the minimum eigenvalue of $\mathbb{E}_{P_h}[hh^\top]$. With the estimated DiT score network $s_{\hat{W}}$ in [Corollary 3.1.1](#), we have the following with probability $1 - 1/\text{poly}(n)$.

- (i) The accuracy to recover the subspace B is $\|W_B W_B^\top - B B^\top\|_F^2 = \tilde{\mathcal{O}}(T_0 \xi(n, \epsilon, L)/c_0)$.
- (ii) $(W_B U)^\top \hat{P}_{T_0}$ denotes the pushforward distribution. With the conditions $\text{KL}(P_h || N(0, I_{d_0})) < \infty$, and step size $\mu \leq \xi(n, \epsilon, L) \cdot T_0^2 / (d_0 \sqrt{\log d_0})$. There exists an orthogonal matrix $U \in \mathbb{R}^{d \times d}$ such that we have the following upper bound for the total variation distance

$$\text{TV}(P_{T_0}^h, (W_B U)^\top \hat{P}_{T_0}) = \tilde{\mathcal{O}}(\sqrt{\xi(n, \epsilon, L)}), \quad (3.2)$$

where $\tilde{\mathcal{O}}$ hides the factor about $D, d_0, d, L_{s+}, \log n$, and $T - T_0$.

- (iii) For the generated data distribution \hat{P}_{T_0} , the orthogonal pushforward $(I - W_B W_B^\top)^\top \hat{P}_{T_0}$ is $N(0, \Sigma)$, where $\Sigma \preceq a T_0 I$ for a constant $a > 0$.

Proof. See [Appendix F.3](#) for a detailed proof. □

Intuitively, [Corollary 3.1.2](#) shows the estimation results including 3 parts: (i) The accuracy of recovering the subspace B . (ii) The estimation error between \hat{P}_{T_0} and $P_{T_0}^h$. (iii) The vanishing behavior of \hat{P}_{T_0} in the orthogonal space. These three parts indicate that the learned score estimator is capable of recovering the initial data distribution. Notably, [Corollary 3.1.2](#) is agnostic to details of $\xi(n, \epsilon, L)$.

Remark 3.5 (Comparing with Existing Works). [Oko et al. \[2023\]](#) analyze the distribution estimation under the assumption that the initial density is supported on $[-1, 1]^D$ and smooth in the boundary. Our [Assumption 2.2](#) demonstrates greater practical relevance. This suggests that our method of distribution estimation aligns more closely with empirical realities.

Remark 3.6 (Subspace Recovery Accuracy). (i) of [Corollary 3.1.2](#) confirms that the subspace is learned by DiTs. The error is proportional to the sample complexity for score estimation and depends on the minimum eigenvalue of the covariance of P_h .

4 Provably Efficient Criteria

Here, we analyze the computational limits of latent DiTs under low-dimensional linear subspace data assumption (i.e., [Assumption 2.1](#)). The hardness of DiT models ties to both forward and backward passes of the score network in [Definition 3.3](#). We characterize them separately.

4.1 Computational Limits of Backward Computation

Following [Section 2](#), suppose we have n i.i.d. data samples $\{x_{0,i}\}_{i=1}^n \sim P_d$, and time t_{i_0} ($1 \leq i \leq n$) uniformly sampled from $[T_0, T]$. For each data $x_{0,i} \in \mathbb{R}^D$, we sample $x_{t_{i_0}} \in \mathbb{R}^D$ from $N(\beta(t_{i_0})x_{0,i}, \sigma(t_{i_0})I_D)$. Let $(W_A R^{-1}(\cdot))^\dagger$ be the inverse transformation of $W_A R^{-1}(\cdot)$, and denote $Y_{0,i} := (W_A R^{-1})^\dagger(x_{0,i}) \in \mathbb{R}^{d \times L}$. We rewrite the empirical denoising score-matching loss [\(2.2\)](#) as

$$\frac{1}{n} \sum_{i=1}^n \left\| W_A R^{-1}(f_{\mathcal{T}}(\underbrace{R(W_A^\top x_{t_{i_0}})}_{d_0 \times 1})) - x_{0,i} \right\|_F^2 = \frac{1}{n} \sum_{i=1}^n \left\| \underbrace{W_A}_{D \times d_0} \underbrace{R^{-1}(\underbrace{f_{\mathcal{T}}(R(W_A^\top x_{t_{i_0}})})_{d_0 \times 1})}_{d \times L} - \underbrace{Y_{0,i}}_{d \times L} \right\|_F^2. \quad (4.1)$$

For efficiency, it suffices to focus on just transformer attention heads of the DiT score network due to their dominating quadratic time complexity in both passes. Thus, we consider only a single layer attention for $f_{\mathcal{T}}$, to simplify our analysis. Further, we consider the following simplifications:

- (S0) To prove the hardness of [\(4.1\)](#) for both full gradient descent and stochastic mini-batch gradient descent methods, it suffices to consider training on a single data point.
- (S1) For the convenience of our analysis, we consider the following expression for attention mechanism. Let $X, Y \in \mathbb{R}^{d \times L}$. Let $W_K, W_Q, W_V \in \mathbb{R}^{s \times d}$ be attention weights such that $Q = W_Q X \in \mathbb{R}^{d \times L}$, $K = W_K X \in \mathbb{R}^{s \times L}$ and $V = W_V X \in \mathbb{R}^{s \times L}$. We write attention mechanism of hidden size s and sequence length L as

$$\text{Att}(X) = \underbrace{(W_O W_V X)}_{V \text{ multiplication}} \underbrace{D^{-1} \exp(X^\top W_K^\top W_Q X)}_{K-Q \text{ multiplication}} \in \mathbb{R}^{d \times L}, \quad (4.2)$$

with $D := \text{diag}(\exp(X W_Q W_K^\top X^\top) \mathbf{1}_L)$. Here, $\exp(\cdot)$ is entry-wise exponential function,

i.e., $\exp(A)_{i,j} = \exp(A_{i,j})$ for any matrix A , $\text{diag}(\cdot)$ converts a vector into a diagonal matrix with the vector's entries on the diagonal, and $\mathbb{1}_L$ is the length- L all ones vector.

(S2) Since V multiplication is linear in weight while K - Q multiplication is exponential in weights, we only need to focus on the gradient update of K - Q multiplication. Therefore, for efficiency analysis of gradient, it is equivalent to analyzing a reduced problem with fixed $W_O W_V X = \text{const.}$.

(S3) To focus on the DiT, we consider the low-dimensional linear encoder W_A to be pretrained and to not participate in gradient computation. This aligns with common practice [Rombach et al., 2022] and is justified by the trivial computation cost due to the linearity of W_A ¹.

(S4) To further simplify, we introduce $A_1, A_2, A_3 \in \mathbb{R}^{s \times L}$ and $W \in \mathbb{R}^{d \times d}$ via

$$\begin{aligned} & \left\| W_A R^{-1} \left(\underbrace{f_{\mathcal{T}}(R(W_A^{\top} x_{t_{i_0}}))}_{:=X \in \mathbb{R}^{d \times L}} - \underbrace{Y_{0,i}}_{:=Y \in \mathbb{R}^{d \times L}} \right) \right\|_F^2 && \text{(By (S0), (S1) and (S2))} \\ &= \left\| W_A R^{-1} \left(\underbrace{W_O W_V}_{:=W_{OV} \in \mathbb{R}^{d \times d}} \underbrace{X}_{:=A_3 \in \mathbb{R}^{d \times L}} D^{-1} \exp \left(\underbrace{X^{\top}}_{:=A_1^{\top} \in \mathbb{R}^{L \times d}} \underbrace{W_K^{\top} W_Q}_{:=W \in \mathbb{R}^{d \times d}} \underbrace{X}_{:=A_2 \in \mathbb{R}^{d \times L}} \right) - Y \right) \right\|_F^2. \end{aligned} \quad (4.3)$$

Notably, A_1, A_2, A_3, X, Y are constants w.r.t. training above loss with gradient updates.

Therefore, we simplify the objective of training DiT into

Definition 4.1 (Training Generic DiT Loss). Given $A_1, A_2, A_3, Y \in \mathbb{R}^{d \times L}$ and $W_{OV}, W \in \mathbb{R}^{d \times d}$ following (S4), Training a DiT with ℓ_2 loss on a single data point $X, Y \in \mathbb{R}^{d \times L}$ is formulated as

$$\min_W \mathcal{L}_0(W) = \min_W \frac{1}{2} \left\| W_A R^{-1} (W_{OV} A_3 D^{-1} \exp(A_1^{\top} W A_2) - Y) \right\|_F^2. \quad (4.4)$$

Here $D := \text{diag}(\exp(A_1^{\top} W A_2) \mathbb{1}_n) \in \mathbb{R}^{L \times L}$.

Remark 4.1 (Conditional and Unconditional Generation). \mathcal{L}_0 is generic. If $A_1 \neq A_2 \in \mathbb{R}^{d \times L}$, Definition 4.1 reduces to cross-attention in DiT score net (for conditional generation). If $A_1 = A_2 \in \mathbb{R}^{d \times L}$, Definition 4.1 reduces to self-attention in DiT score net (for unconditional vanilla generation).

We introduce the next problem to characterize all possible gradient computations of optimizing (4.4).

¹The gradient computation is linear in W_A , and hence the computation w.r.t. W_A is cheap and upper-bounded by $L \cdot \text{poly}(d)$ time in a straightforward way.

Problem 1 (Approximate DiT Gradient Computation (ADITGC(L, d, Γ, ϵ))). Given $A_1, A_2, A_3, Y \in \mathbb{R}^{d \times L}$. Let $\epsilon > 0$. Assume all numerical values are in $\mathcal{O}(\log(L))$ -bits encoding. Let loss function \mathcal{L}_0 follow [Definition 4.1](#). The problem of approximating gradient computation of optimizing empirical DiT loss (4.4) is to find an approximated gradient matrix $\tilde{G}^{(W)} \in \mathbb{R}^{d \times d}$ such that $\|\tilde{G}^{(W)} - \frac{\partial \mathcal{L}}{\partial W}\|_{\max} \leq 1/\text{poly}(L)$. Here, $\|A\|_{\max} := \max_{i,j} |A_{ij}|$ for any matrix A .

In this work, we aim to investigate the computational limits of all possible efficient algorithms of ADITGC with $\epsilon = 1/\text{poly}(L)$. Yet, the explicit gradient of DiT denoising score matching loss (4.4) is too complicated to characterize ADITGC. To combat this, we make the following observations.

- (O1) Let $g_1(\cdot) := W_A R^{-1}(\cdot) : \mathbb{R}^{d \times L} \rightarrow \mathbb{R}^{d_0}$, $g_2(\cdot) := \text{Att}(\cdot) : \mathbb{R}^{d \times L} \rightarrow \mathbb{R}^{d \times L}$, and $g_3(\cdot) := R(W_A^\top \cdot) : \mathbb{R}^D \rightarrow \mathbb{R}^{d \times L}$ such that $g_3(x) = X$ for $x \in \mathbb{R}^D$ (with $D > d_0 = dL$).
- (O2) **Vectorization of $f_{\mathcal{T}}$** . For the ease of presentation, we use notation flexibly that $f_{\mathcal{T}}$ to denote both a matrix in $\mathbb{R}^{d \times L}$ and a vector in \mathbb{R}^{dL} in the following analysis. This practice does not affect correctness. The context in which $f_{\mathcal{T}}$ is used should clarify whether it refers to a matrix or a vector. Explicit vectorization follows [Definition D.1](#).
- (O3) **Linearity of g_1** . By linearity of $W_A R^{-1}(\cdot)$, we treat g_1 as a matrix in $\mathbb{R}^{d_0 \times dL}$ acting on vector $f_{\mathcal{T}}(\cdot) \in \mathbb{R}^{dL}$.

Therefore, we have $\mathcal{L}_0 = \|g_1 \cdot [g_2(g_3) - Y]\|_2^2$, such that its gradient involves $\frac{d\mathcal{L}_0}{dW} = g_1 \frac{dg_2}{dW}$. From above, we only need to focus on proving the computation time and error control of term $\frac{dg_2}{dW}$ for gradient w.r.t W . Luckily, with tools from fine-grained complexity theory [[Alman and Song, 2023](#)] and tensor trick (see [Appendix D.3](#)), we prove the existence of almost-linear time algorithms for [Problem 1](#) in the next theorem. Let $\text{vec}(W) := \underline{W}$ for any matrix W following [Definition D.1](#).

Theorem 4.1 (Existence of Almost-Linear Time Algorithms for ADITGC). Suppose all numerical values are in $\mathcal{O}(\log L)$ -bits encoding. Let $\max(\|W_{OV} A_3\|_{\max}, \|W_K A_1\|_{\max}, \|W_Q A_2\|_{\max}) \leq \Gamma$. There exists a $L^{1+o(1)}$ time algorithm to solve ADITGC($L_p, L, d = \mathcal{O}(\log L), \Gamma = o(\sqrt{\log L})$) (i.e., [Problem 1](#)) with loss \mathcal{L}_0 from [Definition 4.1](#) up to $1/\text{poly}(L)$ accuracy. In particular, this algorithm outputs gradient matrices $\tilde{G}^{(W)} \in \mathbb{R}^{d \times d}$ such that $\|\tilde{G}^{(W)} - \frac{\partial \mathcal{L}}{\partial W}\|_{\max} \leq 1/\text{poly}(L)$.

Proof Sketch. Our proof is built on the key observation that there exist low-rank structures within the DiT training gradients. Using the tensor trick [[Diao et al., 2019, 2018](#)] and computational hardness results of attention [[Hu et al., 2024c, Alman and Song, 2023](#)], we approximate DiT training gradients with a series of low-rank approximations and carefully match the multiplication dimensions so that the computation of $\frac{dg_2}{dW}$ forms a chained low-rank approximation. We complete the proof by demonstrating that this approximation is bounded by a $1/\text{poly}(L)$ error and requires only almost-linear time. See [Appendix G.2](#) for a detailed proof. \square

Remark 4.2. We remark that [Theorem 4.1](#) is dominated by the relation between L and d , hence by the subspace dimension² $d_0 = dL$. A smaller d_0 makes [Theorem 4.1](#) more likely to hold.

4.2 Computational Limits of Forward Inference

Since the inference of score-matching diffusion models is a forward pass of the trained score estimator s_W , the computational hardness of DiT ties to the transformer-based score network,

$$s_W(A_1, A_2, A_3) = W_A R^{-1} \left(\underbrace{W_{OV} A_3}_{d \times L} \underbrace{D^{-1}}_{L \times L} \exp \left(\underbrace{A_1^\top W_K^\top}_{L \times s} \underbrace{W_Q A_2}_{s \times L} \right) \right), \quad (4.5)$$

following notation in [Definition 4.1](#). For inference, we study the following approximation problem. Notably, by [Remark 4.1](#), (4.5) subsumes both conditional and unconditional DiT inferences.

Problem 2 (Approximate DiT Inference ADiTI(d, L, Γ, δ_F)). Let $\delta_F > 0$ and $B > 0$. Given $A_1, A_2, A_3 \in \mathbb{R}^{d \times L}$, and $W_{OV}, W_K, W_Q \in \mathbb{R}^{d \times d}$ with guarantees that $\|W_{OV} A_3\|_\infty \leq B$, $\|W_K A_1\|_\infty \leq B$ and $\|W_Q A_2\|_\infty \leq B$, we aim to study an approximation problem ADiTI(d, L, B, δ_F), that approximates $s_W(A_1, A_2, A_3)$ with a vector $\tilde{z} \in \mathbb{R}^{d_0}$ (with $d_0 = d \cdot L$) such that $\|\tilde{z} - W_A R^{-1} (W_{OV} A_3 D^{-1} \exp(A_1^\top W_K^\top W_Q A_2))\|_{\max} \leq \delta_F$. Here, $\|A\|_{\max} := \max_{i,j} |A_{ij}|$ for any matrix A .

By (O2) and (O3), we make an observation that [Problem 2](#) is just a special case of [\[Alman and Song, 2023\]](#). Hence, we characterize the all possible efficient algorithms for ADiTI with next proposition.

Proposition 4.1 (Norm-Based Efficiency Phase Transition). Let $\|W_Q A_2\|_\infty \leq B$, $\|W_K A_1\|_\infty \leq B$ and $\|W_{OV} A_3\|_\infty \leq B$ with $B = \mathcal{O}(\sqrt{\log L})$. Assuming SETH ([Hypothesis 1](#)), for every $q > 0$, there are constants $C, C_a, C_b > 0$ such that: there is no $O(n^{2-q})$ -time (sub-quadratic) algorithm for the problem ADiTI($L, d = C \log L, B = C_b \sqrt{\log L}, \delta_F = L^{-C_a}$).

Remark 4.3. [Proposition 4.1](#) suggests an efficiency threshold for the upper bound of $\|W_K A_1\|_\infty$, $\|W_Q A_2\|_\infty$, $\|W_{OV} A_3\|_\infty$. Only below this threshold are efficient algorithms for [Problem 2](#) possible.

Moreover, there exist almost-linear DiT inference algorithms following [\[Alman and Song, 2023\]](#).

Proposition 4.2 (Almost-Linear Time DiT Inference). Assuming SETH, the DiT inference problem ADiTI($L, d = \mathcal{O}(\log L), B = o(\sqrt{\log L}), \delta_F = 1/\text{poly}(L)$) can be solved in $L^{1+o(1)}$ time.

Remark 4.4. [Proposition 4.2](#) is a special case of [Proposition 4.1](#) under the efficiency threshold.

Remark 4.5. [Propositions 4.1](#) and [4.2](#) are dominated by the relation between L and d , hence by the subspace dimension $d_0 = dL$. A smaller d_0 makes [Propositions 4.1](#) and [4.2](#) more likely to hold.

²See [Assumption 2.1](#).

5 Discussion and Conclusion

We explore the fundamental limits of latent DiTs with 3 key contributions. First, we prove that transformers are universal approximators for the score functions in DiTs ([Theorem 3.1](#)), with approximation capacity and model size dependent only on the latent dimension, suggesting DiTs can handle high-dimensional data challenges. Second, we show that Transformer-based score estimators converge to the true score function ([Corollary 3.1.1](#)), ensuring the generated data distribution closely approximates the original ([Corollary 3.1.2](#)). Third, we provide provably efficient criteria ([Proposition 4.1](#)) and prove the existence of almost-linear time algorithms for forward inference ([Proposition 4.2](#)) and backward computation ([Theorem 4.1](#)). These results highlight the potential of latent DiTs to achieve both computational efficiency and robust performance in practical scenarios.

Practical Guidance from Computational Results. [Section 4](#) analyzes the computational feasibility and identifies all possible efficient DiT algorithms/methods for both forward inference and backward training. These results provide practical guidance for designing efficient methods:

- The latent dimension should be sufficiently small: $d = \mathcal{O}(\log L)$ ([Theorem 4.1](#), [Propositions 4.1](#) and [4.2](#)).
- Normalization of K , Q , and V in DiT attention heads enhances performance and efficiency:
 - For efficient inference: $\max \{\|W_K A_1\|, \|W_Q A_2\|, \|W_{OV} A_3\|\} \leq B$ with $B = o(\sqrt{\log L})$ ([Proposition 4.2](#)).
 - For efficient training: $\max \{\|W_K A_1\|, \|W_Q A_2\|, \|W_{OV} A_3\|\} \leq \Gamma$ with $\Gamma = o(\sqrt{\log L})$ ([Theorem 4.1](#)).

We remark that these conditions are necessary but not sufficient; sufficient conditions depend on the specific design of the methods used.

Limitations and Future Direction. As discussed in [Remark 3.4](#), the double exponential factor in our explicit sample complexity bound ([Corollary 3.1.1](#)) suggests a possible gap in our understanding of transformer universality and its interplay with DiT architecture. This motivates us to rethink transformer universality and explore new proof techniques for DiTs, which we leave for future work. Besides, due to its formal nature, this work does not provide immediate practical implementations. However, we expect that our findings provide valuable insights for future diffusion generative models.

Broader Impact

This theoretical work aims to shed light on the foundations of diffusion generative models and is not anticipated to have negative social impacts.

Acknowledgments

JH would like to thank to Minshuo Chen, Sophia Pi, Yibo Wen, Tim Tsz-Kit Lau, Chenwei Xu, Dino Feng and Andrew Chen for enlightening discussions on related topics, and the Red Maple Family for support.

JH is partially supported by the Walter P. Murphy Fellowship. HL is partially supported by NIH R01LM1372201. The content is solely the responsibility of the authors and does not necessarily represent the official views of the funding agencies.

Appendix

A	More Discussion on Low-Dimensional Linear Latent Space	18
B	Nomenclature Table	19
C	Related Works	20
D	Supplementary Theoretical Background	23
D.1	Diffusion Models	23
D.2	Proof of Lemma 2.1	24
D.3	Preliminaries: Strong Exponential Time Hypothesis (SETH) and Tensor Trick . .	28
E	More Background and Auxiliary Lemmas:	
	Universal Approximation of Transformers via Piecewise Approximation	30
E.1	Piecewise-constant Function Approximates Compact-Supported Continuous Function	30
E.2	Modified Transformer Approximates Piece-Wise Constant Function	31
E.3	Standard Transformers Approximate Modified Transformers	36
E.4	All Together: Standard Transformers Approximate Compact-Supported Continuous Functions	36
E.5	Supplementary Proofs	37
F	Proofs of Section 3	50
F.1	Proof of Theorem 3.1	50
F.2	Proof of Corollary 3.1.1	57
F.3	Proof of Corollary 3.1.2	63
G	Proofs of Section 4	67
G.1	Auxiliary Theoretical Results for Theorem 4.1	67
G.2	Proof of Theorem 4.1	75

A More Discussion on Low-Dimensional Linear Latent Space

Our analysis is based on the low-dimensional linear latent space assumption, here we give a further discussion about it with our theoretical results.

The low-dimensional data structure in [Assumption 2.1](#) indicates robust and informative latent representation feature space. Besides, it improves computational efficiency by reducing data complexity without sacrificing essential information. This is consistent with the analysis in our work. Similar to the results under [Assumption 2.1](#) ($d_0 < D$), it is easy to find that our theoretical results hold in other two settings: $d_0 = D$ and $d_0 > D$.

- Statistically, for score approximation, score estimation, and distribution estimation, the upper bound depends on the dimension of the latent variable d_0 , other than d . A smaller d_0 allows for a reduced model size to achieve a specified approximation error compared to a larger one ([Theorem 3.1](#)). Additionally, with a smaller d_0 , both score and distribution estimation errors are reduced relative to scenarios with larger ones ([Corollary 3.1.1](#) and [Corollary 3.1.2](#)).
- Computationally, smaller d_0 benefits the provably efficient criteria ([Proposition 4.1](#), almost-linear time algorithms for forward inference ([Proposition 4.2](#)) and backward computation ([Theorem 4.1](#)).

B Nomenclature Table

We summarize our notations in the following table for easy reference.

Table 1: Mathematical Notations and Symbols

Symbol	Description
$\ z\ _2$	Euclidean norm, where z is a vector
$\ z\ _\infty$	Infinite norm, where z is a vector
$\ Z\ _2$	2-norm, where Z is a matrix
$\ Z\ _{\text{op}}$	Operator norm, where Z is a matrix
$\ Z\ _F$	Frobenius norm, where Z is a matrix
$\ Z\ _{p,q}$	p, q -norm, where Z is a matrix
$\ f(x)\ _{L^2}$	L^2 -norm, where f is a function
$\ f(x)\ _{L^2(P)}$	$L^2(P)$ -norm, where f is a function and P is a distribution
$\ f(\cdot)\ _{Lip}$	Lipschitz-norm, where f is a function
$f_\#P$	Pushforward measure, where f is a function and P is a distribution
n	Sample size
x	Data point in original data space, $x \in \mathbb{R}^D$
h	Latent variable in low-dimensional subspace, $h \in \mathbb{R}^{d_0}$
p_h	The destiny function of h
B	The matrix with orthonormal columns to transform h to x , where $B \in \mathbb{R}^{D \times d_0}$
\bar{h}	$\bar{h} = B^\top x$
T	Stopping time in the forward process of Diffusion model
T_0	Stopping time in the backward process of Diffusion model
μ	Discretized step size in backward process
$p_t(\cdot)$	The density function of x for at time t
$p_t^h(\cdot)$	The density function of \bar{h} at time t
ψ	(Conditional) Gaussian density function
d	Input dimension of each token in the Transformer network of DiT
L	Token length in the Transformer network of DiT
X	Sequence input of Transformer network in DiT, where $X \in \mathbb{R}^{d \times L}$
E	Position encoding, where $E \in \mathbb{R}^{d \times L}$
$R(\cdot)$	Reshape layer in DiT, $R(\cdot) : \mathbb{R}^{d_0} \rightarrow \mathbb{R}^{d \times L}$
W_B	The orthonormal matrix to approximate B , where $W_B \in \mathbb{R}^{D \times d_0}$

C Related Works

Diffusion [Ho et al., 2020] and score-based generative models [Song and Ermon, 2019] have been particularly successful as generative models of images, video and biomedical data [Nichol et al., 2021, Ramesh et al., 2022, Liu et al., 2024, Zhou et al., 2024a,b, Wang et al., 2024a,b]. There are two popular directions in this direction. Empirically, diffusion transformers (DiTs) [Peebles and Xie, 2023] have emerged as a significant advancement, effectively combining the strengths of transformer architectures and diffusion-based approaches. Theoretically, the development of the approximation theory for diffusion models supports their practical success, providing a theoretical framework for understanding and enhancing their effectiveness in various applications [Chen et al., 2023a].

Organization. In the following, we first discuss recent developments in DiTs. Then, we discuss the main technique of our statistical results: the universality (universal approximation) of transformer. Next, we discuss recent theoretical developments in diffusion generative models. Lastly, we discuss other aspects of transformer in foundation models beyond diffusion models.

Diffusion Transformers. Recently, transformer-based diffusion models have garnered significant attention in research. The U-ViT model [Bao et al., 2022] incorporates transformer blocks into a U-net architecture, treating all inputs as tokens. In contrast, DiT [Peebles and Xie, 2023] utilizes a straightforward, non-hierarchical transformer structure. Models like MDT [Gao et al., 2023a] and MaskDiT [Zheng et al., 2023] improve the training efficiency of DiT by applying a masking strategy.

Universality and Memory Capacity of Transformers. The universality of transformers refers to their ability to serve as universal approximators. This means that transformers theoretically models any sequence-to-sequence function to a desired degree of accuracy. Yun et al. [2020] establish that transformers can universally approximate sequence-to-sequence functions by stacking numerous layers of feed-forward functions and self-attention functions. In a different approach, Jiang and Li [2023] affirm the universality of transformers by utilizing the Kolmogorov-Albert representation Theorem. Most recently, Kajitsuka and Sato [2023] show that transformers with one self-attention layer is a universal approximator.

The memory capacity of a transformer is a practical measure to test the theoretical results of the transformer’s universality, by ensuring the model can handle necessary context and dependencies. By memory capacity, we refer to the minimal set of parameters such that the model (i.e., transformer) approximates all input-output pairs in the training dataset with a bounded error. Several works address the memory capacity of transformers. Kim et al. [2022] show that transformers with $\tilde{O}(d+L+\sqrt{NL})$ parameters are sufficient to memorize N length- L and dimension- d sequence-to-sequence data points by constructing a contextual mapping with $\mathcal{O}(L)$ attention layers. Mahdavi et al. [2023] show that a multi-head-attention with h heads is able to memorize $\mathcal{O}(hL)$ examples

under a linear independence data assumption. [Kajitsuka and Sato \[2023\]](#) show that a single layer transformer with $\mathcal{O}(NLd + d^2)$ parameters is able to memorize N length- L and dimension- d sequence-to-sequence data points by utilizing the connection between the softmax function and Boltzmann operator. [Wang et al. \[2023\]](#) extend the results of [\[Yun et al., 2020\]](#) to prompt tuning and discuss the memorization of only the last token of each data sequence. Another line of research establishes a different kind of memory capacity for transformers by connecting transformer attention with dense associative memory models (modern Hopfield models) [\[Hu et al., 2024a,b,c, 2023, Wu et al., 2024a,b, Ramsauer et al., 2020\]](#). Notably, they define memory capacity as the smallest number of (length- L and dimension- d) data points the model (transformer attention) is able to store and derive exponential-in- d high-probability capacity lower bounds.

Our work is motivated by and builds on [\[Yun et al., 2020\]](#) to bridge the transformer’s function approximation ability with data distribution estimation. While we do not address the memorization of DiTs (or diffusion models in general), recent studies on dense associative models suggest viewing pretrained diffusion generative models as associative memory models [\[Hoover et al., 2023, Ambrogioni, 2023\]](#). We plan to explore this aspect in future work.

Theories of Diffusion Models. In addition to empirical success, there has been several theoretical analysis about diffusion models. [Chen et al. \[2023a\]](#) studies score approximation, estimation, and distribution recovery of U-Net based diffusion models. [Benton et al. \[2024\]](#) provide convergence bounds linear in data dimensions, assuming accurate score function approximation. [Zhu et al. \[2023\]](#), [Wibisono et al. \[2024\]](#) provide statistical sample complexity bounds for score-matching under the similar assumptions. [Oko et al. \[2023\]](#) analyze the distribution estimation under the assumption that the initial density is supported on $[-1, 1]^D$ and smooth in the boundary.

Among these works, our work is built on and closest to [\[Chen et al., 2023a\]](#), as both assume the data has a low-dimensional structure. However, our work differs in three key aspects. First, beyond the simple ReLU networks considered in [\[Chen et al., 2023a\]](#), we provide the first score approximation analysis for DiTs with a transformer-based score estimator. Second, our work is the first to provide the statistical rates of DiTs (score and distribution estimation) based on transformer universality [\[Yun et al., 2020\]](#) and norm-based converging number bound [\[Edelman et al., 2022\]](#), supporting the practical success of DiTs [\[Esser et al., 2024, Ma et al., 2024\]](#). Lastly, our work provides the first comprehensive analysis of the computational limits and all possible efficient DiT algorithms/methods for both forward inference and backward training. This offers timely insights into the empirical computational inefficiency of DiTs [\[Liu et al., 2024\]](#) and guidance for future DiT architectures.

Transformers in Foundation Models: Transformer-Based Pretrained Models. Transformer-based pretrained models utilize attention mechanisms to process sequential data, enabling the learning of contextual relationships for tasks like natural language understanding and generation. These models encompass three types: encoder-based, decoder-based, and diffusion transform-

ers. Encoder-based transformers, such as DNABERT [Zhou et al., 2024c, 2023, Ji et al., 2021], employ bidirectional attention to extract feature representations DNABERT shows great potential to capture complex patterns of genome sequences and improve tasks such as gene prediction. Decoder-based transformers generate output sequences from encoded information using unidirectional attention, such as ChatGPT [Radford et al., 2019, Floridi and Chiriatti, 2020, Brown et al., 2020] for natural language. The diffusion transformers generate a sequence toward a target distribution, such as Sora [Liu et al., 2024] and Videofusion [Luo et al., 2023] for video generation and DecompDiff [Guan et al., 2024] for drug design. In our paper, we present an early exploration of the statistical and computational limits of diffusion transformer models.

D Supplementary Theoretical Background

In this section, we provide some further background. We show the details about the forward and backward process in Diffusion Models in [Appendix D.1](#). Besides, we give the details of the proof about the score decomposition in [Appendix D.2](#).

D.1 Diffusion Models

Forward Process. Diffusion models gradually add noise to the original data in the forward process. We describe the forward process as the following SDE

$$dx_t = -\frac{1}{2}w(t)x_t dt + \sqrt{w(t)}dB_t, \quad x_t \in \mathbb{R}^D, \quad (\text{D.1})$$

where $x_0 \sim P_0$, $(B_t)_{t \geq 0}$ is a standard Brownian motion, and $w(t) > 0$ is a nondecreasing weighting function. Let P_t and p_t denote the marginal distribution and density of x_t . The conditional distribution $P(x_t|x_0)$ follows $N(\beta(t)x_0, \sigma(t)I_D)$, where $\beta(t) = \exp\left(-\int_0^t w(s)ds/2\right)$ and $\sigma(t) = 1 - \beta^2(t)$. In practice, [\(D.1\)](#) terminates at a large enough T such that P_T is close to $N(0, I_D)$.

Backward Process. We obtain the backward process $y_t := x_{T-t}$ by reversing [\(D.1\)](#). The backward process satisfies

$$dy_t = \left[\frac{1}{2}w(T-t)y_t + w(T-t)\nabla \log p_{T-t}(y_t) \right] dt + \sqrt{w(T-t)}d\bar{B}_t, \quad (\text{D.2})$$

where the score function $\nabla \log p_t(\cdot)$ is the gradient of log probability density function of x_t , and \bar{B}_t is a reversed Brownian motion. However, $\nabla \log p_t(\cdot)$ and P_T are both unknown in [\(D.2\)](#). To resolve this, we use a score estimator $s_W(\cdot, t)$ to replace $\nabla \log p_t(\cdot)$, where $s_W(\cdot, t)$ is usually a neural network with parameters W . Secondly, we replace P_T by the standard Gaussian distribution. Consequently, we obtain the following SDE

$$dy_t = \left[\frac{1}{2}w(T-t)y_t + w(T-t)s_W(y_t, T-t) \right] dt + \sqrt{w(T-t)}d\bar{B}_t, \quad y_0 \sim N(0, I_D). \quad (\text{D.3})$$

In practice, we use discrete schemes of [\(D.3\)](#) to generate data, following [\[Song and Ermon, 2019\]](#). We use $\mu > 0$ to denote the discretization step size, and for $t \in [k\mu, (k+1)\mu]$, we have

$$dy_t^\leftarrow = \left[\frac{1}{2}w(T-t)y_{k\mu}^\leftarrow + w(T-t)s_W(y_{k\mu}^\leftarrow, T-k\mu) \right] dt + \sqrt{w(T-t)}d\bar{B}_t. \quad (\text{D.4})$$

D.2 Proof of Lemma 2.1

Here we restate the proof of [Chen et al., 2023a, Lemma 1] for completeness.

Proof. Recall $x = Bh$ by Assumption 2.1 with $x \in \mathbb{R}^D$, $B \in \mathbb{R}^{D \times d_0}$ and $h \in \mathbb{R}^{d_0}$.

By the forward process (D.1), we have

$$p_t(x) = \int \psi_t(x | Bh) p_h(h) dh, \quad (\text{D.5})$$

where

$$\psi_t(x | Bh) = [2\pi h(t)]^{-D/2} \exp \left(-\frac{\|\beta(t)Bh - x\|_2^2}{2\sigma(t)} \right), \quad (\text{D.6})$$

is the Gaussian transition kernel.

Then we write the score function as

$$\begin{aligned} \nabla \log p_t(x) &= \frac{\nabla p_t(x)}{p_t(x)} && (\text{By log-derivative}) \\ &= \frac{\nabla \int \psi_t(x | Bh) p_h(h) dh}{\int \psi_t(x | Bh) p_h(h) dh} && (\text{By plugging in } p_t(x)) \\ &= \frac{\int \nabla \psi_t(x | Bh) p_h(h) dh}{\int \psi_t(x | Bh) p_h(h) dh}, && (\text{By interchanging } \int \text{ with } \nabla) \end{aligned}$$

where the last equality holds since $\psi_t(x | Bh)$ is continuously differentiable in x .

Plugging (D.6) into ((By log-derivative)), we have

$$\begin{aligned} &\nabla \log p_t(x) \\ &= \frac{[2\pi h(t)]^{-D/2}}{\int \psi_t(x | Bh) p_h(h) dh} \int \frac{1}{\sigma(t)} (\beta(t)Bh - x) \exp \left(-\frac{\|\beta(t)Bh - x\|_2^2}{2\sigma(t)} \right) p_h(h) dh. \end{aligned}$$

We then decompose above score function by projecting of x into $\text{Span}(B)$, i.e., replacing $-x$

with $-BB^\top x - (I_D - BB^\top)x$:

$$\begin{aligned}
& \nabla \log p_t(x) \\
&= \frac{[2\pi h(t)]^{-D/2}}{\int \psi_t(x | Bh) p_h(h) dh} \\
& \quad \cdot \int \frac{1}{\sigma(t)} \left[(\beta(t)Bh - BB^\top x) - (I_D - BB^\top) x \right] \exp \left(-\frac{\|\beta(t)Bh - x\|_2^2}{2\sigma(t)} \right) p_h(h) dh.
\end{aligned}$$

Absorbing the factor of $[2\pi h(t)]^{-D/2}$ into the Gaussian kernel $\psi_t(x | Bh)$, we have

$$\begin{aligned}
& \nabla \log p_t(x) \\
&= \frac{[2\pi h(t)]^{-D/2}}{\int \psi_t(x | Bh) p_h(h) dh} \int \frac{1}{\sigma(t)} (\beta(t)Bh - BB^\top x) \exp \left(-\frac{\|\beta(t)Bh - x\|_2^2}{2\sigma(t)} \right) p_h(h) dh \\
& \quad - \frac{1}{\int \psi_t(x | Bh) p_h(h) dh} \left(\frac{1}{\sigma(t)} (I_D - BB^\top) x \right) \int \psi_t(x | Bh) p_h(h) dh \\
&= \underbrace{\frac{1}{\int \psi_t(x | Bh) p_h(h) dh} \int \frac{1}{\sigma(t)} (\beta(t)Bh - BB^\top x) \psi_t(x | Bh) p_h(h) dh}_{:=s_+} - \underbrace{\frac{1}{\sigma(t)} (I_D - BB^\top) x}_{:=s_-}.
\end{aligned}$$

To further simplify s_+ , we decompose $\psi_t(x \mid Bh)$ as

$$\begin{aligned}
& \psi_t(x \mid Bh) \\
&= [2\pi h(t)]^{-D/2} \exp \left(-\frac{1}{2\sigma(t)} \|\beta(t)Bh - x\|_2^2 \right) \\
&= [2\pi h(t)]^{-D/2} \exp \left(-\frac{1}{2\sigma(t)} \|\beta(t)Bh - BB^\top x - (I_D - BB^\top)x\|_2^2 \right) \\
&= [2\pi h(t)]^{-D/2} \exp \left(-\frac{1}{2\sigma(t)} \left(\|\beta(t)Bh - BB^\top x\|_2^2 + \|(I_D - BB^\top)x\|_2^2 \right. \right. \\
&\quad \left. \left. - 2(B(\beta(t)h - B^\top x))^\top (I_D - BB^\top)x \right) \right) \\
&= [2\pi h(t)]^{-D/2} \exp \left(-\frac{1}{2\sigma(t)} \left(\|\beta(t)Bh - BB^\top x\|_2^2 + \|(I_D - BB^\top)x\|_2^2 \right) \right) \\
&\quad \text{($B(\beta(t)h - B^\top x)$ is in $\text{Span}(B)$ while $(I_D - BB^\top)x$ is orthogonal to $\text{Span}(B)$)} \\
&= \underbrace{[2\pi h(t)]^{-d_0/2} \exp \left(-\frac{\|\beta(t)h - B^\top x\|_2^2}{2\sigma(t)} \right)}_{:=\psi_t(B^\top x \mid h)} \cdot \underbrace{[2\pi h(t)]^{-(D-d_0)/2} \exp \left(-\frac{\|(I_D - BB^\top)x\|_2^2}{2\sigma(t)} \right)}_{:=\psi_t((I_D - BB^\top)x) \text{ (since B has orthonormal columns)}}
\end{aligned}$$

where both $\psi_t(B^\top x \mid h)$ and $\psi_t((I_D - BB^\top)x)$ are Gaussian.

Plugging $\psi_t(x \mid Bh) = \psi_t(B^\top x \mid h) \psi_t((I_D - BB^\top)x)$ into s_+ , we obtain

$$\begin{aligned}
s_+(x, t) &= C \int \frac{1}{\sigma(t)} (\beta(t)Bh - BB^\top x) \psi_t(B^\top x \mid h) \psi_t((I_D - BB^\top)x) p_h(h) dh \\
&= C \psi_t((I_D - BB^\top)x) \int \frac{1}{\sigma(t)} (\beta(t)Bh - BB^\top x) \psi_t(B^\top x \mid h) p_h(h) dh \\
&= \frac{1}{\int \psi_t(B^\top x \mid h') p_{h'}(h') dh'} \int \frac{1}{\sigma(t)} (\beta(t)Bh - BB^\top x) \psi_t(B^\top x \mid h) p_h(h) dh,
\end{aligned}$$

where $C := [\psi_t((I_D - BB^\top)x) \int \psi_t(B^\top x \mid h') p_{h'}(h') dh']^{-1}$.

Notably, s_+ depends only on the projected data $B^\top x$. Therefore, we are able to replace $s_+(x, t)$ with $s_+(B^\top x, t)$. The benefit is that the dimension d_0 of the first input in $s_+(B^\top x, t)$ is much smaller.

Lastly, by denoting $\bar{h} = B^\top x$ such that $\nabla_{\bar{h}} \psi_t(\bar{h} \mid h) = (\beta(t)h - \bar{h}) \psi_t(B^\top x \mid h) / \sigma(t)$, we arrive

at

$$\begin{aligned}
s_+(B^\top x, t) &= B \int \frac{\nabla_{\bar{h}} \psi_t(\bar{h} \mid h) p_h(h)}{\int \psi_t(\bar{h} \mid h') p_{h'}(h') \mathrm{d}h'} \mathrm{d}h \\
&= B \nabla \log p_t^h(B^\top x). \qquad (p_t^h(\bar{h}) := \int \psi_t(\bar{h} \mid h) p_h(h) \mathrm{d}h)
\end{aligned}$$

This completes the proof. □

D.3 Preliminaries: Strong Exponential Time Hypothesis (SETH) and Tensor Trick

Here we present the ideas we built upon for [Section 4](#).

Strong Exponential Time Hypothesis (SETH). [Impagliazzo and Paturi \[2001\]](#) introduce the Strong Exponential Time Hypothesis (SETH) as a stronger form of the $P \neq NP$ conjecture. It suggests that our current best SAT algorithms are optimal and is a popular conjecture for proving fine-grained lower bounds for a wide variety of algorithmic problems [[Cygan et al., 2016](#), [Williams, 2018](#)].

Hypothesis 1 (SETH). For every $\epsilon > 0$, there is a positive integer $k \geq 3$ such that k -SAT on formulas with n variables cannot be solved in $\mathcal{O}(2^{(1-\epsilon)n})$ time, even by a randomized algorithm.

Tensor Trick for Computing Gradients. The tensor trick [[Diao et al., 2019, 2018](#)] is an instrument to compute complicated gradients in a clean and tractable fashion. We start with some definitions.

Definition D.1 (Vectorization). For any matrix $X \in \mathbb{R}^{L \times d}$, we define $\underline{X} := \text{vec}(X) \in \mathbb{R}^{Ld}$ such that $X_{i,j} = \underline{X}_{(i-1)d+j}$ for all $i \in [L]$ and $j \in [d]$.

Definition D.2 (Matrixization). For any vector $\underline{X} \in \mathbb{R}^{Ld}$, we define $\text{mat}(\underline{X}) = X$ such that $X_{i,j} = \text{mat}(\underline{X})_{i,j} := \underline{X}_{(i-1)d+j}$ for all $i \in [L]$ and $j \in [d]$, namely $\text{mat}(\cdot) = \text{vec}^{-1}(\cdot)$.

Definition D.3 (Kronecker Product). Let $A \in \mathbb{R}^{L_a \times d_a}$ and $B \in \mathbb{R}^{L_b \times d_b}$. We define the Kronecker product of A and B as $A \otimes B \in \mathbb{R}^{L_a L_b \times d_a d_b}$ such that $(A \otimes B)_{(i_a-1)L_b+i_b, (j_a-1)d_b+j_b}$, is equal to $A_{i_a, j_a} B_{i_b, j_b}$ with $i_a \in [L_a], j_a \in [d_a], i_b \in [L_b], j_b \in [d_b]$.

Definition D.4 (Sub-Block of a Tensor). For any $A \in \mathbb{R}^{L_a \times d_a}$ and $B \in \mathbb{R}^{L_b \times d_b}$, let $A := A \otimes B \in \mathbb{R}^{L_a L_b \times d_a d_b}$. For any $\underline{j} \in [L_a]$, we define $A_{\underline{j}} \in \mathbb{R}^{L_b \times d_a d_b}$ be the \underline{j} -th $L_b \times d_a d_b$ sub-block of A .

Lemma D.1 (Tensor Trick [[Diao et al., 2019, 2018](#)]). For any $A \in \mathbb{R}^{L_a \times d_a}$, $B \in \mathbb{R}^{L_b \times d_b}$ and $X \in \mathbb{R}^{d_a \times d_b}$, it holds $\text{vec}(A^\top X B) = (A^\top \otimes B^\top) \underline{X} \in \mathbb{R}^{L_a L_b}$.

To showcase the tensor trick, let's consider a (single data point) attention following [[Gao et al., 2023b,c](#)]. Setting $D := \text{diag}(\exp(X^\top W_K^\top W_Q X) \mathbf{1}_L)$ and $W := W_K W_Q^\top \in \mathbb{R}^{d \times d}$, we have

$$\mathcal{L}_0 := \left\| \underbrace{W_V}_{d \times d} \underbrace{X}_{\mathbb{R}^{d \times L}} \underbrace{D^{-1}}_{\mathbb{R}^{L \times L}} \underbrace{\exp\{X^\top W X\}}_{\mathbb{R}^{L \times L}} - \underbrace{Y}_{\mathbb{R}^{d \times L}} \right\|_2^2. \quad (\text{D.7})$$

Proposition D.1 (Definition 4.7 of [[Gao et al., 2023b](#)]). By [Definition D.3](#) and [Definition D.4](#), we identify $D_{\underline{j}, \underline{j}} := \left\langle \exp(A_{\underline{j}} W), \mathbf{1}_L \right\rangle \in \mathbb{R}$ for all $\underline{j} \in [L]$, with $A := X \otimes X \in$

$\mathbb{R}^{L^2 \times d^2}$ and $\underline{W} \in \mathbb{R}^{d^2}$. Therefore, for each $\underline{j} \in [L]$ and $\underline{i} \in [d]$, it holds $\mathcal{L}_0 = \sum_{\underline{j}=1}^L \sum_{\underline{i}=1}^d \frac{1}{2} \left(\left\langle D_{\underline{j},\underline{j}}^{-1} \exp(\underline{A}_{\underline{j}} \underline{W}), XW_V[\cdot, \underline{i}] \right\rangle - Y_{\underline{j},\underline{i}} \right)^2$.

The elegance of **Proposition D.1** emerges when we vectorize the weights into vectors $\underline{W}, \underline{W}_V$, making the gradient computations (e.g., $\text{d}\mathcal{L}_0/\underline{W}$ and $\text{d}\mathcal{L}_0/\underline{W}_V$) more tractable by avoiding complex matrix or tensor derivatives. This approach systematically simplifies the handling of chain-rule terms in the gradient computation of losses like \mathcal{L}_0 .

E More Background and Auxiliary Lemmas:

Universal Approximation of Transformers via Piecewise Approximation

Here, we review the universal approximation of Transformers following [Yun et al., 2020]. Our goal is to reproduce the results of [Yun et al., 2020] and use or modify them as auxiliary lemmas for proofs of Section 3 (i.e., Appendix F.)

We start with their central result, and the rest of the section aims to prove it.

Lemma E.1 (Universal Approximation of Transformers, Theorem 3 of [Yun et al., 2020]). Let $\epsilon > 0$. For any given compact-supported continuous function $f : \mathbb{R}^{d \times L} \rightarrow \mathbb{R}^{d \times L}$, there exists a Transformer network $f_{\mathcal{T}} \in \mathcal{T}_p^{2,1,4}$ such that we have

$$\left(\int \|f_{\mathcal{T}}(X) - f(X)\|_F^2 dX \right)^{1/2} \leq \epsilon.$$

Proof Overview. We use the following proof strategy:

- **Step 1.** We show that the piecewise-constant function is able to approximate compact-supported continuous function in Appendix E.1.
- **Step 2.** We define modified self-attention and feed-forward layers to construct the modified transformer. We show that the modified transformer is able to approximate piecewise-constant function in Appendix E.2.
- **Step 3.** We show that the modified transformer is able to approximate the normal transformer in Appendix E.3.

Below, we provide details of **Step 1.** in Appendix E.1, **Step 2.** in Appendix E.2 and **Step 3.** in Appendix E.3. Then we give a summary of our results in Appendix E.4.

E.1 Piecewise-constant Function Approximates Compact-Supported Continuous Function

In this subsection, we show that the piecewise-constant function is able to approximate compact-supported continuous function.

We start with the definition of the compact-supported continuous functions of interest.

Assumption E.1. Without loss of generality, we assume that the target function in discussion is supported on $[0, 1]^{d \times L}$. We denote the set of $[0, 1]^{d \times L}$ -supported continuous functions as \mathcal{F} .

We introduce the notion of grid and cube for the compact support $[0, 1]^{d \times L}$.

Definition E.1 (Grid and Cube with Width δ). Given a grid width δ , let $\mathcal{G}_\delta := \{0, \delta, \dots, 1 - \delta\}^{d \times L}$ denote the set of grids within $[0, 1]^{d \times L}$. For a grid point $G = (G_{j \in [d], k \in [L]}) \in \mathcal{G}_\delta$, we denote its associated cube as

$$\mathcal{S}_G := \otimes_{j=1}^d \otimes_{k=1}^L [G_{j,k}, G_{j,k} + \delta) \subset [0, 1]^{d \times L}.$$

We introduce the notion of piecewise-constant function class w.r.t. the $[0, 1]^{d \times L}$ -supported continuous function class \mathcal{F} .

Definition E.2 (Piecewise-Constant Function Class). Let f_δ denote the piecewise constant function of grid width δ , and $\mathbb{1}\{\cdot\}$ denote the indicator function. For each $G \in \mathcal{G}_\delta$, and any matrix $A_G \in \mathbb{R}^{d \times L}$, we define the piecewise-constant function class as

$$\mathcal{F}(\delta) := \left\{ f_\delta : X \rightarrow \sum_{G \in \mathcal{G}_\delta} A_G \cdot \mathbb{1}\{X \in \mathcal{S}_G\}, A_G \in \mathbb{R}^{d \times L} \right\}. \quad (\text{E.1})$$

We recall that for a given sequence-to-sequence function f , we have

$$\|f\|_{L^2} := \left(\int \|f(X)\|_F^2 dX \right)^{1/2}.$$

We approximate the compact-supported function with a piecewise-constant function with the next lemma.

Lemma E.2. (Lemma 8 of [Yun et al., 2020]) For any given $f \in \mathcal{F}$ and $\epsilon/3 > 0$, we can find a $\delta^* > 0$ such that there exists a $f_{\delta^*} \in \mathcal{F}(\delta^*)$ satisfying $\|f - f_{\delta^*}\|_{L^2} \leq \epsilon/3$.

Proof. See [Appendix E.5.2](#) for a detailed proof. □

E.2 Modified Transformer Approximates Piece-Wise Constant Function

In this subsection, we define modified self-attention and feed-forward layers to construct the modified transformers. We use the modified transformers to approximate the piecewise-constant function.

Definition E.3 (Modified Transformer Networks). The modification of transformer networks $\overline{\mathcal{T}}_p^{r,m,l}$ includes two modifications from normal transformer networks $\mathcal{T}_p^{r,m,l}$:

- Modified attention layer: Replace Softmax operator with Hardmax operator $\sigma_H(\cdot)$.
- Modified feed-forward layer: Replace $\text{ReLU}(\cdot)$ with activation function $\zeta \in \Psi$. Here, Ψ denotes the set of all piecewise linear functions with at most three pieces and at least one constant.

We approximate $\mathcal{F}(\delta)$ with this modified transformer networks $\overline{\mathcal{T}}_p^{r,m,l}$ as the following.

Lemma E.3 (Modified from Proposition 4 of [Yun et al., 2020]). For each $f_\delta \in \mathcal{F}(\delta)$, there exists a $f_{\mathcal{T},c} \in \overline{\mathcal{T}}_p^{2,1,1}$ such that $\|f_\delta - f_{\mathcal{T},c}\|_{L^2} = \mathcal{O}(\delta^{d/2})$.

Proof Sketch. Given us δ , we have the grid \mathcal{G}_δ , and the cude \mathcal{S}_G for $G \in \mathcal{G}_\delta$. Our proof follows two steps:

- **Quantization.** For all $X \in \mathbb{R}^{d \times L}$, we quantize it to a finite set:
 - If $X \in \mathcal{S}_G \subset [0, 1]^{d \times L}$, we quantize it to the element $G \in \mathcal{G}_\delta$.
 - If $X \notin [0, 1]^{d \times L}$, we quantize it to an element out of \mathcal{G}_δ .
- **Mapping.** For any $G \in \mathcal{G}_\delta$, we map it to the desired output A_G .

For **Quantization**, We achieve this by a series of modified feed-forward layers. We show this in [Appendix E.2.1](#).

For **Mapping**, we follow two steps:

- For any $G \neq G' \in \mathcal{G}_\delta$, we use a “contextual mapping” $q_c(\cdot)$ (defined as [Definition E.4](#)), which maps all the elements in $q_c(G)$ and $q_c(G')$ to different value. Then we use a series of modified self-attention layers to achieve “contextual mapping.” We show this in [Appendix E.2.2](#).

Definition E.4 (Contextual Mapping). Consider a finite set $\mathcal{G}_\delta \in \mathbb{R}^{d \times L}$. A map $q_c : \mathcal{G}_\delta \rightarrow \mathbb{R}^{1 \times L}$ defines a contextual mapping if the map satisfies the following:

- For any $G \in \mathcal{G}_\delta$, the entries in $q_c(G)$ are all distinct.
 - For any $G \neq G' \in \mathcal{G}_\delta$, all entries of $q_c(G)$ and $q_c(G')$ are distinct.
- For any $G \in \mathcal{G}_\delta$, we use a series of modified feed-forward layers to map $q_c(G)$ to A_G . We show this in [Appendix E.2.3](#).

□

Remark E.1. Our proof differs from [Yun et al., 2020] in one aspect: while Proposition 4 in [Yun et al., 2020] uses a transformer network without positional encoding, we add positional encoding to complete our proof.

E.2.1 Quantization by Modified Feed-forward Layers

We use a series of modified feed-forward layers in $\overline{\mathcal{T}}_p^{r,m,l}$ to quantize an input $X \in \mathbb{R}^{d \times L}$ to an element G in a grid:

$$\{-J, 0, \delta, \dots, 1 - \delta\}^{d \times L},$$

where $J > L > 0$ is a number large enough to be determined later. We achieve this via two steps.

- **Step 1: Map the element out of $[0, 1)$ to $-J$.**

We use e_i to represent the standard unit vector where the i -th element is 1. For the i -th row of X , we define the following feed-forward layer to achieve our aim.

Definition E.5 (Feed-forward Layer 1). The vector e_i acts as the weight parameters, and $\zeta_1(\cdot)$ acts as the activation function in the feed-forward layer.

$$X \rightarrow X + e_i \zeta_1(e_i^\top X), \quad \zeta_1(t) = \begin{cases} -t - J & \text{for } t < 0 \text{ or } t \geq 1, \\ 0 & \text{otherwise.} \end{cases} \quad (\text{E.2})$$

We take $i = 1$ as an example to give the specific calculation. We denote $X = (x_{i,j})_{d \times L}$, then we have

$$\begin{aligned} \text{FF}(X) &= X + \begin{pmatrix} 1 \\ 0 \\ \vdots \\ 0 \end{pmatrix} (\zeta_1(x_{1,1}), \zeta_1(x_{1,2}), \dots, \zeta_1(x_{1,L})) \\ &= X + \begin{pmatrix} \zeta_1(x_{1,1}) & \zeta_1(x_{1,2}) & \dots & \zeta_1(x_{1,L}) \\ 0 & 0 & \dots & 0 \\ \vdots & \vdots & \vdots & \vdots \\ 0 & 0 & \dots & 0 \end{pmatrix}. \end{aligned}$$

In the first row of X , the above layer transforms the element that is out of $[0, 1)$ to $-J$.

We stack the above layers together for $i = 1, 2, \dots, d$. If the element of X is out of $[0, 1)$, the series of layers maps it to J .

- **Step 2: Map the element in $[0, 1)$ to $\{0, \delta, 2\delta, \dots, 1 - \delta\}$.**

For the i -th row of X , we take $k = 0, 1, \dots, 1/\delta - 1$ respectively, and define the following layer.

Definition E.6 (Feed-forward Layer 2). The vector e_i acts as the weight parameters and $\zeta_2(\cdot)$ acts as the activation function in the feed-forward layer.

$$X \rightarrow X + e_i \zeta_2(e_i^\top X - k\delta \mathbf{1}_n^\top), \quad \zeta_2(t) = \begin{cases} 0 & t < 0 \text{ or } t \geq \delta \\ -t & 0 \leq t < \delta. \end{cases} \quad (\text{E.3})$$

We take $i = 1, k = 1$ as an example, and give the specific calculation.

$$\begin{aligned} \text{FF}(X) &= X + \begin{pmatrix} 1 \\ 0 \\ \vdots \\ 0 \end{pmatrix} (\zeta_2(x_{1,1} - \delta) \quad \zeta_2(x_{1,2} - \delta) \quad \cdots \quad \zeta_2(x_{1,L} - \delta)) \\ &= X + \begin{pmatrix} \zeta_2(x_{1,1} - \delta) & \zeta_2(x_{1,2} - \delta) & \cdots & \zeta_2(x_{1,L} - \delta) \\ 0 & 0 & \cdots & 0 \\ \vdots & \vdots & \ddots & \vdots \\ 0 & 0 & \cdots & 0 \end{pmatrix}. \end{aligned}$$

In the first row of X , the above layer transforms the element in $[\delta, 2\delta]$ to δ .

We stack the above layers together for $i = 1, 2, \dots, d$ and $k = 0, 1, \dots, 1/\delta - 1$. If the element of X is in $[k\delta, (k+1)\delta]$, the series layers maps it to $k\delta$.

Combining the above two parts, we achieve our goal with $d/\delta + d$ feed-forward layers. We denote the $d/\delta + d$ series layers as $f_{\mathcal{T},c1}$.

E.2.2 Contextual Mapping by Modified Self-attention Layers

In our attention layers, we use the following positional encoding $E \in \mathbb{R}^{d \times L}$.

$$E = \begin{pmatrix} 0 & 1 & 2 & \cdots & L-1 \\ 0 & 1 & 2 & \cdots & L-1 \\ \vdots & \vdots & \vdots & & \vdots \\ 0 & 1 & 2 & \cdots & L-1 \end{pmatrix}. \quad (\text{E.4})$$

According to [Appendix E.2.1](#), the output of $f_{\mathcal{T},c1}$ is in the grid $\{-J, 0, \delta, \dots, 1 - \delta\}^{d \times L}$. For any X in this grid, the first column of $X + E$ is in

$$\{-J, 0, \delta, \dots, 1 - \delta\}^d,$$

and the second column is in

$$\{-J + 1, 1, 1 + \delta, \dots, 2 - \delta\}^d.$$

For the other columns, the results are similar.

For $i = 0, 1, \dots, L - 1$, we use the following notation:

$$[i : \delta : i + 1 - \delta]_J := \{i - J, i, i + \delta, \dots, i + 1 - \delta\}.$$

The we define the grid \mathcal{G}_δ^+ as the following.

Definition E.7 (Grid \mathcal{G}_δ^+). $X + E$ is in the grid:

$$\mathcal{G}_\delta^+ := [0 : \delta : 1 - \delta]_J^d \times [1 : \delta : 2 - \delta]_J^d \times \cdots \times [L - 1 : \delta : L - \delta]_J^d.$$

Next, we show that the modified attention layer computes contextual mapping (Definition E.4) for \mathcal{G}_δ^+ . For $i = 1, 2, \dots, L - 1$, we use the following notation:

$$[i : \delta : i + 1 - \delta] := \{i, i + \delta, i + 2\delta, \dots, i + 1 - \delta\}.$$

Lemma E.4 (Modified from Lemma 6 of [Yun et al., 2020]). We consider the following subset of \mathcal{G}_δ^+ :

$$\tilde{\mathcal{G}}_\delta := \underbrace{[0 : \delta : 1 - \delta]^d \times [1 : \delta : 2 - \delta]^d \times \cdots \times [L - 1 : \delta : L - \delta]^d}_L.$$

Assume that $L \geq 2$ and $\delta^{-1} \geq 2$. Then, there exist a function $f_{\mathcal{T},c2} : \mathbb{R}^{d \times L} \rightarrow \mathbb{R}^{d \times L}$ composed of $\delta^{-d} + 1$ modified attention layers (Definition E.3), a vector $u \in \mathbb{R}^d$, and two constants $t_l, t_r \in \mathbb{R}$ ($0 < t_l < t_r$), such that $q_c(G) := u^\top f_{\mathcal{T},c2}(G)$, $G \in \mathcal{G}_\delta^+$ satisfies the following properties:

1. For any $G \in \tilde{\mathcal{G}}_\delta$, the entries of $q_c(G)$ are all distinct.
2. For any different $G, G' \in \tilde{\mathcal{G}}_\delta$, all entries of $q_c(G), q_c(G')$ are distinct.
3. For any $G \in \tilde{\mathcal{G}}_\delta$, all the entries of $q_c(G)$ are in $[t_l, t_r]$.
4. For any $G \in \mathcal{G}_\delta^+ \setminus \tilde{\mathcal{G}}_\delta$, all the entries of $q_c(G)$ are outside $[t_l, t_r]$.

Proof. See Appendix E.5.3 for a detailed proof. □

Remark E.2. Our proof differs from [Yun et al., 2020] in one aspect: the original [Yun et al., 2020, Lemma 6] does not include positional encoding (E.4). We add (E.4) to the input of the attention layer.

E.2.3 Map to the Desired Output by Modified Feed-forward Layers

Next, we show that a series of feed-forward layers map the output of modified attention layers $f_{\mathcal{T},c2}$ to the desired output of function f_{δ^*} .

Lemma E.5 (Lemma 7 of [Yun et al., 2020]). There exists a function $f_{\mathcal{T},c3} : \mathbb{R}^{d \times L} \rightarrow \mathbb{R}^{d \times L}$ composed of $\mathcal{O}(L(1/\delta)^{dL}/L!)$ modified feed-forward layers, such that

$$f_{\mathcal{T},c3} \circ f_{\mathcal{T},c2}(G) = \begin{cases} A_G & \text{if } G \in \tilde{\mathcal{G}}_\delta, \\ \mathbf{0}_{d \times L} & \text{if } G \in \mathcal{G}_\delta^+ \setminus \tilde{\mathcal{G}}_\delta. \end{cases}$$

Proof. See [Appendix E.5.4](#) for a detailed proof. \square

From the above conclusions, we have the following lemma for the required number of layers in the modified transformer.

Lemma E.6 ([Yun et al., 2020]). From the proof of [Lemma E.3](#), if we want to achieve a approximation error $\mathcal{O}(\delta^{d/2})$ by the modified transformer, we need $\mathcal{O}(\delta^{-1})$ modified feed-forward layers in $f_{\mathcal{T},c1}$, $\mathcal{O}(\delta^{-d})$ modified self-attention layers in $f_{\mathcal{T},c2}$, and $\mathcal{O}(\delta^{-dL})$ modified feed-forward layers in $f_{\mathcal{T},c3}$.

Proof. By the proof of [Lemma E.3](#), we complete the proof. \square

E.3 Standard Transformers Approximate Modified Transformers

In this subsection, we show that standard neural network layers are able to approximate the modified self-attention layers and the modified feed-forward layers ([Definition E.3](#)). We have the following [Lemma E.7](#).

Lemma E.7 (Lemma 9 of [Yun et al., 2020]). For each $f_{\mathcal{T},c} \in \overline{\mathcal{T}}_p^{2,1,1}$ and any $\epsilon > 0$, there exists $f_{\mathcal{T}} \in \mathcal{T}_p^{2,1,4}$ such that $\|f_{\mathcal{T}} - f_{\mathcal{T},c}\|_{L^2} \leq \epsilon/3$.

Proof. See [Appendix E.5.5](#) for a detailed proof. \square

E.4 All Together: Standard Transformers Approximate Compact-Supported Continuous Functions

We summarize the results of [Lemmas E.2](#), [E.3](#) and [E.7](#), and thus prove [Lemma E.1](#). Furthermore, to achieve the ϵ approximation error in [Lemma E.1](#), we take $\delta = \mathcal{O}(\epsilon^{2/d})$ in [Lemma E.3](#).

E.5 Supplementary Proofs

Here we first present two preliminaries: selective shift operation and bijective column ID mapping in [Appendix E.5.1](#) to proceed with our proof. Then we show the proof of [Lemma E.2](#) in [Appendix E.5.2](#), proof of [Lemma E.4](#) in [Appendix E.5.3](#), proof of [Lemma E.5](#) in [Appendix E.5.4](#), and proof of [Lemma E.7](#) in [Appendix E.5.5](#).

E.5.1 Preliminaries

We give the definition of two preliminaries: selective shift operation and bijective column ID mapping.

Selective Shift Operation. This operation refers to shifting certain entries of the input selectively.

To achieve this, we consider the following function $\xi(\cdot; \cdot) : \mathbb{R}^{d \times L} \rightarrow \mathbb{R}^{d \times L}$.

$$\xi(X; b_Q) = e_1 u^\top X \sigma_H \left[(u^\top X)^\top (u^\top X - b_Q \mathbf{1}_n^\top) \right], \quad (\text{E.5})$$

where $X \in \mathbb{R}^{d \times L}$, $e_1 = (1, 0, 0, \dots, 0)^\top \in \mathbb{R}^d$, $b_Q \in \mathbb{R}$, and $u \in \mathbb{R}^d$ is a vector to be determined.

To see the output, we consider the j -th column of $u^\top X \sigma_H \left[(u^\top X)^\top (u^\top X - b_Q \mathbf{1}_n^\top) \right]$:

- If $u^\top X_{:,j} > b_Q$, it calculates $\arg\max$ of $u^\top X$;
- If $u^\top X_{:,j} < b_Q$, it calculates $\arg\min$ of $u^\top X$.

With e_1 , all rows of $\xi(X; b_Q)$ except the first row are zero. We consider the j -th entry of the first row in $\xi(X; b_Q)$, which is denoted as $\xi(X; b_Q)_{1,j}$. Then for all $j \in [L]$, we have

$$\xi(X; b_Q)_{1,j} = u^\top X \sigma_H \left[(u^\top X)^\top (u^\top X_{:,j} - b_Q) \right] = \begin{cases} \max_k u^\top X_{:,k} & \text{if } u^\top X_{:,j} > b_Q, \\ \min_k u^\top X_{:,k} & \text{if } u^\top X_{:,j} < b_Q. \end{cases}$$

From this observation, we define a function parametrized by b_Q and b'_Q , where $b_Q < b'_Q$.

$$\xi(X; b_Q, b'_Q) := \xi(X; b_Q) - \xi(X; b'_Q). \quad (\text{E.6})$$

Then we have

$$\xi(X; b_Q, b'_Q)_{1,j} = \begin{cases} \max_k u^\top X_{:,k} - \min_k u^\top X_{:,k} & \text{if } b_Q < u^\top X_{:,j} < b'_Q, \\ 0 & \text{others.} \end{cases}$$

We define an attention layer of the form $X \rightarrow X + \xi(X; b_Q, b'_Q)$. For any column $X_{:,j}$, if $b_Q < u^\top X_{:,j} < b'_Q$, its first coordinate $X_{1,j}$ is shifted up by $\max_k u^\top X_{:,k} - \min_k u^\top X_{:,k}$, while all the

other coordinates stay untouched. We call this the selective shift operation, because we can choose b_Q and b'_Q to shift certain entries of the input selectively.

Bijjective Column ID Mapping. We consider the input $G \in \mathcal{G}_\delta^+$ (Definition E.7). We use

$$J = L + 3L\delta^{-dL}, \text{ and } u = (1, \delta^{-1}, \delta^{-2}, \dots, \delta^{-d+1}). \quad (\text{E.7})$$

For any $j \in [L]$, we have the following two conclusions:

- If $G_{i,j} \geq 0$ for all $i \in [d]$, i.e., $G_{:,j} \in [j-1 : \delta : j-\delta]^d$, then we have

$$u^\top G_{:,j} \in [\delta_j : \delta : \delta_j + \delta^{-d+1} - \delta], \text{ where } \delta_j = (j-1) \cdot \left(\frac{\delta - \delta^{-d+1}}{\delta - 1} \right). \quad (\text{E.8})$$

The map $G_{:,j} \rightarrow u^\top G_{:,j}$ from $[j-1 : \delta : j-\delta]^d$ to $[\delta_j : \delta : \delta_j + \delta^{-d+1} - \delta]$ is a bijection.

- If there exists $i \in [d]$ such that $G_{i,j} = -J + j$, then

$$u^\top G_{:,j} \leq -3L\delta^{-dL} + (j-1) \cdot \left(\frac{\delta^{-d+1} - \delta}{1 - \delta} \right) + \delta^{-d+1} < 0. \quad (\text{E.9})$$

We say that $u^\top G_{:,j}$ gives the “column ID” for each possible value of $G_{:,j} \in [j-1 : \delta : j-\delta]^d$.

Remark E.3 (Illustration of Bijection Property). For the bijection property, we give the following illustration. Let $G_{:,j} = (g_{1j}, g_{2j}, \dots, g_{dj})^\top$ and $\bar{G}_{:,j} = (\bar{g}_{1j}, \bar{g}_{2j}, \dots, \bar{g}_{dj})^\top$. If $u^\top G_{:,j} = u^\top \bar{G}_{:,j}$ and $G_{:,j} \neq \bar{G}_{:,j}$, we deduce

$$(g_{1j} - \bar{g}_{1j}) + \delta^{-1}(g_{2j} - \bar{g}_{2j}) + \dots + \delta^{-d+1}(g_{dj} - \bar{g}_{dj}) = 0. \quad (\text{E.10})$$

Because $G_{:,j} \neq \bar{G}_{:,j}$, then there exist a k ($k < d$), such that $g_{kj} \neq \bar{g}_{kj}$ and $g_{ij} = \bar{g}_{ij}$ ($i > k$). We have

$$|\delta^{-k+1}(g_{kj} - \bar{g}_{kj})| \geq \delta^{-k+2}.$$

However,

$$\begin{aligned} & |(g_{1j} - \bar{g}_{1j}) + \dots + \delta^{-k+2}(g_{k-1,j} - \bar{g}_{k-1,j})| \\ & \leq |g_{1j} - \bar{g}_{1j}| + \dots + |\delta^{-k+2}(g_{k-1,j} - \bar{g}_{k-1,j})| \\ & \leq (1 - \delta) + \dots + \delta^{-k+2}(1 - \delta) \\ & < \delta^{-k+2}. \end{aligned}$$

This contradicts with (E.10). Thus we prove the property of bijection.

E.5.2 Proof of Lemma E.2

Proof of Lemma E.2. We restate the proof from [Yun et al., 2020] for completeness.

By the nature of the compact-supported continuous function, f is uniformly continuous.

Because $\|\cdot\|_\infty$ is equivalent to $\|\cdot\|_F$ when the number of entries are finite, we have the following by the definition of uniform continuity.

For any $\epsilon/3 > 0$, there exist a $\delta^* > 0$, such that for any $X, Y \in \mathbb{R}^{d \times L}$, and $\|X - Y\|_\infty < \delta^*$, we have $\|f(X) - f(Y)\|_F < \epsilon/3$.

Then we perform the following steps following Definitions E.1 and E.2:

- We create a grid \mathcal{G}_{δ^*} by choosing grid width δ^* , and cube \mathcal{S}_G with respect to $G \in \mathcal{G}_{\delta^*}$.
- For any grid point $G \in \mathcal{G}_{\delta^*}$, we define $C_G \in \mathcal{S}_G$ to be the center point of the cube \mathcal{S}_G .
- We define a piece-wise constant function $f_{\delta^*}(X) = \sum_{L \in \mathcal{G}_{\delta^*}} f(C_G) \mathbb{1}\{X \in \mathcal{S}_G\}$.

Then for any $X \in \mathcal{S}_G$, we have $\|X - C_G\|_\infty < \delta^*$. According to the uniform continuity, we drive

$$\|f(X) - f_{\delta^*}(X)\|_F = \|f(X) - f(C_G)\|_F < \epsilon/3.$$

This implies that $\|f - f_{\delta^*}\|_{L^2} < \epsilon/3$ and completes the proof. \square

E.5.3 Proof of Lemma E.4

We give the proof of Lemma E.4 by constructing the network to satisfy the requirements.

Proof of Lemma E.4. Recall the selective shift operation in Appendix E.5.1, the overall idea of the construction includes two steps:

- **Step 1:** For each $j \in [L]$, we stack δ^{-d} attention layers. We use the attention layer as

$$\delta^{-d} \xi(\cdot; g - \delta/2, g + \delta/2), \quad (\text{E.11})$$

for $g \in [\delta_j : \delta_j + \delta^{-d+1} - \delta]$ (E.8) in the increasing order. The total number of layers is $L\delta^{-d}$. These layers cast $G \in \tilde{\mathcal{G}}_\delta$ to L different entries required by Property 1 of Lemma E.4.

- **Step 2:** We add an extra single-head attention layer with attention part

$$L\delta^{-(L+1)d-1} \xi(\cdot; 0). \quad (\text{E.12})$$

This layer achieves a global shifting and casts different $G \in \tilde{\mathcal{G}}_\delta$ to unique elements required by properties Property 2 of Lemma E.4.

The two operations together map $\tilde{\mathcal{G}}_\delta$ and $\mathcal{G}_\delta^+ \setminus \tilde{\mathcal{G}}_\delta$ to different sets, as required by properties 3-4 of [Lemma E.4](#). The bounds t_l and t_r are calculated then.

Then, we give detailed proof by showing the impact of the two steps and verifying the four properties of [Lemma E.4](#). We achieve this by making a category division of \mathcal{G}_δ^+ :

- **Category 1:** $G \in \tilde{\mathcal{G}}_\delta$, all entries in the point G are between 0 and $L - \delta$.
- **Category 2:** $G \in \mathcal{G}_\delta^+ \setminus \tilde{\mathcal{G}}_\delta$, the point G has at least one entry that equals to $-J$.

Let $u = (1, \delta^{-1}, \delta^{-2}, \dots, \delta^{-d+1})$, and recall that $\delta_j = (j - 1)(\delta - \delta^{-d+1})/(\delta - 1)$ for any $j \in [L]$ in [\(E.8\)](#).

Category 1. We denote $g_j := u^\top G_{:,j}$, then we have $g_1 < g_2 < \dots < g_L$. The first δ^{-d} layers sweep the set $[\delta_j : \delta : \delta_j + \delta^{-d+1} - \delta], j \in [L]$ and apply selective shift operation on each element in the set. This means that selective shift operation will be applied to g_1 first, then g_2 , and then g_3 , and so on, regardless of the specific values of g_j 's.

- **First Shift Operation.** In the first selective shift operation with g going through $[\delta_1 : \delta : \delta_1 + \delta^{-d+1} - \delta]$, the $(1, 1)$ -th entry of G (e.g., $G_{1,1}$) is shifted by the operation, while the other entries are left untouched. The updated value $\tilde{G}_{1,1}$ is

$$\tilde{G}_{1,1} = G_{1,1} + \delta^{-d} \left[\max_k (u^\top G_{:,k}) - \min_k (u^\top G_{:,k}) \right] = G_{1,1} + \delta^{-d}(g_L - g_1).$$

Therefore, after the operation, the output of the layer is

$$\begin{pmatrix} \tilde{G}_{:,1} & G_{:,2} & \dots & G_{:,L} \end{pmatrix}.$$

We have

$$\begin{aligned} \tilde{g}_1 &:= u^\top \tilde{G}_{:,1} \\ &= \tilde{G}_{1,1} + \sum_{i=2}^d \delta^{-i+1} G_{i,1} \\ &= G_{1,1} + \delta^{-d}(g_L - g_1) + \sum_{i=2}^d \delta^{-i+1} G_{i,1} \\ &= g_1 + \delta^{-d}(g_L - g_1). \end{aligned}$$

Then we deduce $g_L < \tilde{g}_1$, because

$$\begin{aligned}
\tilde{g}_1 &= g_1 + \delta^{-d}(g_L - g_1) \\
&\geq 0 + \delta^{-d} \left[(L-1) \cdot \frac{\delta - \delta^{-d+1}}{\delta - 1} - \delta^{-d+1} + \delta \right] && (\text{By (E.8)}) \\
&= \delta^{-d} \left[(L-1) \frac{\delta}{1-\delta} + \delta + (L-1) \frac{\delta^{-d+1}}{1-\delta} - \delta^{-d+1} \right] \\
&\geq \delta^{-d} \cdot \left((L-1) \frac{\delta}{1-\delta} + \delta \right) \\
&= (L-1) \frac{\delta^{-d+1}}{1-\delta} + \delta^{-d+1} \\
&> g_L. && (\text{By } \delta < 1 \text{ and (E.8)})
\end{aligned}$$

Thus, after updating,

$$\max u^\top \begin{pmatrix} \tilde{G}_{:,1} & G_{:,2} & \cdots & G_{:,L} \end{pmatrix} = \max\{\tilde{g}_1, g_2, \dots, g_L\} = \tilde{g}_1,$$

and the new minimum is g_2 .

- **Second Shift Operation.** In the second selective shift operation with g going through $[\delta_2 : \delta : \delta_2 + \delta^{-d+1} - \delta]$, the $(1, 2)$ -th entry of G (e.g., $G_{1,2}$) is shifted by the operation, while the other entries are left untouched. The updated value $\tilde{G}_{1,2}$ is

$$\begin{aligned}
\tilde{G}_{1,2} &= G_{1,2} + \delta^{-d}(\tilde{g}_1 - g_2) \\
&= G_{1,2} + \delta^{-d}(g_1 - g_2) + \delta^{-2d}(g_L - g_1).
\end{aligned}$$

Therefore, after the operation, the output of the layer is

$$\begin{pmatrix} \tilde{G}_{:,1} & \tilde{G}_{:,2} & \cdots & G_{:,L} \end{pmatrix}.$$

We have

$$\begin{aligned}
\tilde{g}_2 &:= u^\top \tilde{G}_{:,2} \\
&= g_2 + \delta^{-d}(g_1 - g_2) + \delta^{-2d}(g_L - g_1).
\end{aligned}$$

Then we deduce $\tilde{g}_1 < \tilde{g}_2$, because

$$\begin{aligned}
&g_1 + \delta^{-d}(g_L - g_1) < g_2 + \delta^{-d}(g_1 - g_2) + \delta^{-2d}(g_L - g_1) \\
\iff &(\delta^{-d} - 1)(g_2 - g_1) < \delta^{-d}(\delta^{-d} - 1)(g_L - g_1). && (\text{By } \delta^{-d} > 1 \text{ and } g_L > g_2)
\end{aligned}$$

Thus, after updating,

$$\max u^\top \begin{pmatrix} \tilde{G}_{:,1} & \tilde{G}_{:,2} & \cdots & G_{:,L} \end{pmatrix} = \max\{\tilde{g}_1, \tilde{g}_2, \dots, g_L\} = \tilde{g}_2,$$

and the new minimum is g_3 .

- **Repeating The Process.** By repeating this process, we show that the j -th shift operation shifts $G_{1,j}$ by $\delta^{-d}(\tilde{g}_{j-1} - g_j)$, and we have

$$\begin{aligned} \tilde{g}_j &:= u^\top \tilde{G}_{:,j} \\ &= g_j + \sum_{k=1}^{j-1} \delta^{-kd} (g_{j-k} - g_{j-k+1}) + \delta^{-jd} (g_L - g_1). \end{aligned}$$

We deduce $\tilde{g}_{j-1} < \tilde{g}_j$ holds for all $2 \leq j \leq L$, because

$$\begin{aligned} &\tilde{g}_{j-1} < \tilde{g}_j \\ \iff &g_{j-1} + \sum_{k=2}^{j-1} \delta^{-kd+d} (g_{j-k} - g_{j-k+1}) + \delta^{-(j-1)d} (g_L - g_1) \\ &< g_j + \sum_{k=1}^{j-1} \delta^{-kd} (g_{j-k} - g_{j-k+1}) + \delta^{-jd} (g_L - g_1) \\ \iff &\sum_{k=1}^{j-1} \delta^{-kd+d} (\delta^{-d} - 1) (g_{j-k+1} - g_{j-k}) < \delta^{-(j-1)d} (\delta^{-d} - 1) (g_L - g_1), \end{aligned}$$

where the last inequality holds because

$$\begin{aligned} &\sum_{k=1}^{j-1} \delta^{-kd+d} (g_{j-k+1} - g_{j-k}) \\ &< \delta^{-(j-1)d} \sum_{k=1}^{j-1} (g_{j-k+1} - g_{j-k}) \\ &< \delta^{-(j-1)d} (g_L - g_1). \end{aligned}$$

Therefore, after the j -th selective shift operation, \tilde{g}_j is the new maximum among $\{\tilde{g}_1, \dots, \tilde{g}_j, g_{j+1}, \dots, g_L\}$ and g_{j+1} is the new minimum.

- **After L Shift Operations.** After the whole L shift operations, the input G is mapped to a new point \tilde{G} , where $u^\top \tilde{G} = (\tilde{g}_1 \ \tilde{g}_2 \ \dots \ \tilde{g}_L)$ and $\tilde{g}_1 < \tilde{g}_2 < \dots < \tilde{g}_L$. For the lower and upper bound of \tilde{g}_L , we have the following lemma.

Lemma E.8 (Lemma 10 of [Yun et al., 2020]). $\tilde{g}_L = u^\top \tilde{G}_{:,L}$ satisfies the following bounds:

$$\delta^{-(L-1)d+1}(\delta^{-d} - 1) \leq \tilde{g}_L \leq L\delta^{-(L+1)d}.$$

Also, the mapping from $(g_1 \ g_2 \ \cdots \ g_L)$ to \tilde{g}_L is one-to-one mapping.

- **Global Shifting by the Last Layer.** We note that after the above L shift operations, there is another attention layer with attention part $L\delta^{-(L+1)d-1}\xi(\cdot; 0)$. Since $0 < \tilde{g}_1 < \cdots < \tilde{g}_L$, what it does to \tilde{G} is that it adds the following to each entry in the first row of \tilde{G} :

$$L\delta^{-(L+1)d-1} \max_k u^\top \tilde{G}_{:,k} = L\delta^{-(L+1)d-1} \tilde{g}_L.$$

The output of this layer is defined to be the function $f_{\mathcal{T},c2}(G)$.

Now, in summary, for any $G \in \tilde{\mathcal{G}}_\delta$, $i \in [d]$, and $j \in [L]$, we have

$$f_{\mathcal{T},c2}(G)_{i,j} = \begin{cases} G_{1,j} + \delta_j^+ & \text{if } i = 1, \\ G_{i,j} & \text{if } 2 \leq i \leq d, \end{cases}$$

$$\text{where } \delta_j^+ = \sum_{k=1}^{j-1} \delta^{-kd}(g_{j-k} - g_{j-k+1}) + \delta^{-jd}(g_L - g_1) + L\delta^{-(L+1)d-1} \tilde{g}_L.$$

For any $G \in \tilde{\mathcal{G}}_\delta$ and $j \in [L]$,

$$u^\top f_{\mathcal{T},c2}(G)_{:,j} = \tilde{g}_j + L\delta^{-(L+1)d-1} \tilde{g}_L.$$

Next, we check the **Property 1**, **Property 2** and **Property 3** of **Lemma E.4**.

- **Checking Property 1 of Lemma E.4.** Given any $G \in \tilde{\mathcal{G}}_\delta$, we already prove that

$$\tilde{g}_1 < \tilde{g}_2 < \cdots < \tilde{g}_L,$$

so they are all distinct.

- **Checking Property 2 of Lemma E.4.** Note that the upper bound on \tilde{g}_L from **Lemma E.8** also holds for other \tilde{g}_j 's, so for all $j \in [L]$, we have

$$L\delta^{-(L+1)d-1} \tilde{g}_L \leq u^\top f_{\mathcal{T},c2}(G)_{:,j} < L\delta^{-(L+1)d-1} \tilde{g}_L + L\delta^{-(L+1)d}.$$

Now, from **Lemma E.8**, two different $G, G' \in \tilde{\mathcal{G}}_\delta$ map to different \tilde{g}_L and \tilde{g}'_L , and they differ at

least by δ . This means that two intervals

$$\begin{aligned} & [L\delta^{-(L+1)d-1}\tilde{g}_L, L\delta^{-(L+1)d-1}\tilde{g}_L + L\delta^{-(L+1)d}), \\ & [L\delta^{-(L+1)d-1}\tilde{g}'_L, L\delta^{-(L+1)d-1}\tilde{g}'_L + L\delta^{-(L+1)d}), \end{aligned}$$

are guaranteed to be disjoint, so the entries of $u^\top f_{\mathcal{T},c2}(G)$ and $u^\top f_{\mathcal{T},c2}(G')$ are all distinct.

Now, we finish showing that the map $f_{\mathcal{T},c2}(\cdot)$ we constructed using $(1/\delta)^d + 1$ attention layers implements a contextual mapping on $\tilde{\mathcal{G}}_\delta$.

- **Checking Property 3 of Lemma E.4.** With $u^\top f_{\mathcal{T},c2}(G)_{:,j} \in [L\delta^{-(L+1)d-1}\tilde{g}_L, L\delta^{-(L+1)d-1}\tilde{g}_L + L\delta^{-(L+1)d})$ and Lemma E.8, we show that for any $G \in \tilde{\mathcal{G}}_\delta$, we have

$$\begin{aligned} u^\top f_{\mathcal{T},c2}(G)_{:,j} & \geq L\delta^{-2(L+1)d}(\delta^{-d} - 1), \\ u^\top f_{\mathcal{T},c2}(G)_{:,j} & < L^2\delta^{-2(L+1)d-1} + L\delta^{-(L+1)d}. \end{aligned}$$

This proves that all $u^\top f_{\mathcal{T},c2}(L)_{:,j}$ are between t_l and t_r , where

$$\begin{aligned} t_l & = L\delta^{-2(L+1)d}(\delta^{-d} - 1), \\ t_r & = L^2\delta^{-2(L+1)d-1} + L\delta^{-(L+1)d}. \end{aligned}$$

Category 2. Now we check Property 4 of Lemma E.4. For the input points $G \in \mathcal{G}_\delta^+ \setminus \tilde{\mathcal{G}}_\delta$, note that the point G has at least one entry that equals to $-J + k$, $k \in [L-1]$. Let $g_j := u^\top G_{:,j}$, and recall that whenever a column $G_{:,j}$ has an entry that equals to $-J + k$, $k \in [L-1]$, we have $g_j < 0$. Without loss of generality, assume that $g_1 < 0$.

Because the selective shift operation is applied to each element of $[0 : \delta : \delta_L + \delta^{-d+1} - \delta]$, not to negative values, thus we have $\min_k u^\top G_{:,k} = g_1 < 0$, g_1 never gets shifted upwards, and remains as the minimum for the whole time.

- **All g_j 's Are Negative.** When all g_j 's are negative, selective shift operation never shifts the input G , thus $\tilde{G} = G$. Recall that $u^\top \tilde{G}_{:,j} < 0$ for all $j \in [L]$. The last layer with attention part $L\delta^{-(L+1)d-1}\xi(\cdot; 0)$ adds $L\delta^{-(L+1)d-1}\min_k u^\top \tilde{G}_{:,k} < 0$ to each entry in the first row of \tilde{G} , making \tilde{G} remain negative. Therefore, $f_{\mathcal{T},c2}(G)$ satisfies $u^\top f_{\mathcal{T},c2}(G)_{:,j} < 0 < t_l$ for all $j \in [L]$.
- **Not All g_j 's Are Negative.** Now consider the case where at least one g_j is positive. Suppose that there are k positive and satisfies $g_{i_1} < g_{i_2} < \dots < g_{i_k}$. Thus selective shift operation does

not affect g_i , where $i \in [L] \setminus \{i_1, \dots, i_k\}$, but it shifts g_{i_1} by

$$\begin{aligned}
& \delta^{-d}(\max_k u^\top G_{:,k} - \min_k u^\top G_{:,k}) \\
& \geq \delta^{-d}(2L\delta^{-dL} - (L-1)\frac{\delta^{-d+1} - \delta}{1-\delta} - \delta^{-d+1} + (i_k - 1)\frac{\delta^{-d+1} - \delta}{1-\delta}) \quad (\text{By (E.9)}) \\
& = \delta^{-d}(3L\delta^{-dL} - \delta^{-d+1} - (L-i_k)\frac{\delta^{-d+1} - \delta}{1-\delta}) \\
& \geq \delta^{-d} \cdot 2L\delta^{-dL} \quad (\text{By } \delta^{-1} \geq 2) \\
& = 2L\delta^{-(L+1)d}.
\end{aligned}$$

The next shift operations shift g_{i_2}, \dots, g_{i_k} by an even larger amount, so at the end of the first $L(1/\delta)^d$ layers, we have $L\delta^{-(L+1)d} \leq \tilde{g}_{i_1} \leq \dots \leq \tilde{g}_{i_k}$, while $\tilde{g}_j < 0$ for all $j \in [L] \setminus \{i_1, \dots, i_k\}$.

Then, we shift G by the last layer. The last layer with attention part $L\delta^{-(L+1)d-1}\xi(\cdot; 0)$ acts differently for negative and positive \tilde{g}_j 's. (i). For negative \tilde{g}_j 's, it adds the following to $\tilde{g}_j, j \in [L] \setminus \{i_1, \dots, i_k\}$:

$$L\delta^{-(L+1)d-1} \min_k u^\top \tilde{G}_{:,k} = L\delta^{-(L+1)d-1} g_1 < 0.$$

This term pushes them further to the negative side. (ii). For positive \tilde{g}_i 's, it adds

$$L\delta^{-(L+1)d-1} \max_k u^\top \tilde{G}_k = L\delta^{-(L+1)d-1} \tilde{g}_{i_k} \geq 2L^2\delta^{-2(L+1)d-1}.$$

Thus they are all greater than or equal to $2L^2\delta^{-2(L+1)d+1}$.

Note that

$$2L^2\delta^{-2(L+1)d-1} > t_r, \text{ where } t_r = L^2\delta^{-2(L+1)d-1} + L\delta^{-(L+1)d}.$$

Then we have the final output $f_{\mathcal{T},c2}(G)$ satisfies $u^\top f_{\mathcal{T},c2}(G)_{:,j} \notin [t_l, t_r]$, for all $j \in [L]$. This completes the verification of **Property 4** of **Lemma E.4**.

In conclusion, we need $\mathcal{O}(L\delta^{-d})$ layers of modified self-attention layer to obtain our approximation. This completes the proof. \square

E.5.4 Proof of Lemma E.5

Proof of Lemma E.5. We restate the proof from [Yun et al., 2020] for completeness.

Note that $|\mathcal{G}_\delta^+| = (1/\delta + 1)^{dL} < \infty$, so the output of $f_{\mathcal{T},c2}(\mathcal{G}_\delta^+)$ has finite number of distinct real values. Let M be the upper bound of all these possible values. By construction of $f_{\mathcal{T},c2}$, $M > 0$.

Construct the Layers: $f_{\mathcal{T},c3}(f_{\mathcal{T},c2}(G)) = \mathbf{0}_{d \times L}$ if $G \in \mathcal{G}_\delta^+ \setminus \tilde{\mathcal{G}}_\delta$. According to Lemma E.4, for all $j \in [L]$, we have $u^\top f_{\mathcal{T},c2}(G)_{:,j} \in [t_l, t_r]$ if $G \in \tilde{\mathcal{G}}_\delta$, and $u^\top f_{\mathcal{T},c2}(G)_{:,j} \notin [t_l, t_r]$ if $G \in \mathcal{G}_\delta^+ \setminus \tilde{\mathcal{G}}_\delta$. Due to this property, we add the following feed-forward layer:

Definition E.8 (Feed-forward Layer 3). The vectors u and $\mathbf{1}_L$ act as the weight parameters and $\zeta_3(\cdot)$ acts as the activation function in the feed-forward layer.

$$X \rightarrow X - (M + 1)\mathbf{1}_L \zeta_3(u^\top X), \quad \zeta_3(t) = \begin{cases} 0 & \text{if } t \in [t_l, t_r] \\ 1 & \text{if } t \notin [t_l, t_r]. \end{cases} \quad (\text{E.13})$$

- **Case for $G \in \mathcal{G}_\delta^+ \setminus \tilde{\mathcal{G}}_\delta$.** We have $\zeta_3(u^\top f_{\mathcal{T},c2}(G)) = \mathbf{1}_L^\top$, so all the entries of the input are shifted by $-M - 1$, and become strictly negative.
- **Case for $G \in \tilde{\mathcal{G}}_\delta$.** We have $\zeta_3(u^\top f_{\mathcal{T},c2}(G)) = \mathbf{0}_L^\top$, so the output stays the same as the $f_{\mathcal{T},c2}(G)$.

With the input $f_{\mathcal{T},c2}(G)$, if $G \in \tilde{\mathcal{G}}_\delta$, then $\zeta_3(u^\top f_{\mathcal{T},c2}(G)) = \mathbf{0}_L^\top$, so the output stays the same as the input. If $G \in \mathcal{G}_\delta^+ \setminus \tilde{\mathcal{G}}_\delta$, then $\zeta_3(u^\top f_{\mathcal{T},c2}(G)) = \mathbf{1}_L^\top$, so all the entries of the input are shifted by $-M - 1$, and become strictly negative.

Next, we map those negative entries to zero. For $i = 1, 2, \dots, d$, we add the following layer:

Definition E.9 (Feed-forward Layer 4). The vectors u and e_i act as the weight parameters and $\zeta_4(\cdot)$ acts as the activation function in the feed-forward layer.

$$X \rightarrow X + e_i \zeta_4((e_i)^\top X), \quad \zeta_4(t) = \begin{cases} -t & \text{if } t < 0 \\ 0 & \text{if } t \geq 0. \end{cases} \quad (\text{E.14})$$

After these d layers, the output for $G \in \mathcal{G}_\delta^+ \setminus \tilde{\mathcal{G}}_\delta$ is a zero matrix, while the output for $G \in \tilde{\mathcal{G}}_\delta$ remains $f_{\mathcal{T},c2}(G)$.

Construct the Layers: $f_{\mathcal{T},c3}(f_{\mathcal{T},c2}(G)) = A_G$ if $G \in \tilde{\mathcal{G}}_\delta$. Each different G is mapped to L unique numbers $u^\top f_{\mathcal{T},c2}(G)$, which are at least δ apart from each other. We map each unique number to the corresponding output column as follows. We choose one $\bar{G} \in \tilde{\mathcal{G}}_\delta$, for each $u^\top f_{\mathcal{T},c2}(\bar{G})_{:,j}$, $j \in [L]$, we add the following feed-forward layer.

Definition E.10 (Feed-forward Layer 5). The vectors u and e_i act as the weight parameters, and $\zeta_4(\cdot)$ acts as the activation function in the feed-forward layer.

$$X \rightarrow X + ((A_{\bar{G}})_{:,j} - f_{\mathcal{T},c2}(\bar{G})_{:,j}) \zeta_5(u^\top X - u^\top f_{\mathcal{T},c2}(\bar{G})_{:,j} \mathbf{1}_L^\top), \quad (\text{E.15})$$

$$\zeta_5(t) = \begin{cases} 1 & -\delta/2 \leq t < \delta/2, \\ 0 & \text{others.} \end{cases} \quad (\text{E.16})$$

- **Case for $G \in \mathcal{G}_\delta^+ \setminus \tilde{\mathcal{G}}_\delta$.** Recall that the input X of this layer is $f_{\mathcal{T},c2}(G)$. If X is a zero matrix, which is the case for $G \in \mathcal{G}_\delta^+ \setminus \tilde{\mathcal{G}}_\delta$, we have $u^\top X = \mathbf{0}_L^\top$. Then $u^\top X - u^\top f_{\mathcal{T},c2}(\bar{G})_{:,j} \mathbf{1}_L^\top < -t_l \mathbf{1}_L$. Since $t_l > \delta/2$, the output remains the same as X .
- **Case for $G \in \tilde{\mathcal{G}}_\delta$.** Consider the input X is $f_{\mathcal{T},c2}(G)$, where $G \in \tilde{\mathcal{G}}_\delta$ is not equal to \bar{G} . According to **Property 2** of **Lemma E.4**, given a $j \in [L]$, $u^\top f_{\mathcal{T},c2}(G)_{:,k}$, ($k \in [L]$) differs from $u^\top f_{\mathcal{T},c2}(\bar{G})_{:,j}$ by at least δ . Then we have

$$\zeta_5(u^\top f_{\mathcal{T},c2}(G) - u^\top f_{\mathcal{T},c2}(\bar{G})_{:,j} \mathbf{1}_L^\top) = \mathbf{0}_L^\top.$$

Thus the input is left untouched.

If $G = \bar{G}$, then

$$\zeta_5(u^\top f_{\mathcal{T},c2}(G) - u^\top f_{\mathcal{T},c2}(\bar{G})_{:,j} \mathbf{1}_L^\top) = (e_j)^\top.$$

Thus we shift the j -th column of $f_{\mathcal{T},c2}(G)$ to

$$f_{\mathcal{T},c2}(G)_{:,j} + ((A_{\bar{G}})_{:,j} - f_{\mathcal{T},c2}(\bar{G})_{:,j}) = f_{\mathcal{T},c2}(G)_{:,j} + ((A_G)_{:,j} - f_{\mathcal{T},c2}(G)_{:,j}) = (A_G)_{:,j}.$$

In other word, this layer maps the column $f_{\mathcal{T},c2}(G)_{:,j}$ to $(A_G)_{:,j}$, without affecting any other columns.

We defer from above that we need one layer per each unique value of $u^\top f_{\mathcal{T},c2}(G)_{:,j}$ for each $G \in \tilde{\mathcal{G}}_\delta$. Note that there are $\mathcal{O}(\delta^{-dL})$ such numbers, so we use $\mathcal{O}(\delta^{-dL})$ layers to finish our construction. \square

E.5.5 Proof of Lemma E.7

Proof of Lemma E.7. We restate the proof from [Yun et al., 2020] for completeness.

The proof follows two steps: (i) Approximate the modified self-attention layers. (ii) Approximate the modified feed-forward layers.

- **Step 1: Approximate the Modified Self-Attention Layers.**

We achieve this by approximating the Softmax operator σ_S with the Hardmax operator σ_H . Given a matrix $X \in \mathbb{R}^{d \times L}$, we have

$$\sigma_S(\lambda X) \rightarrow \sigma_H(X), \quad \text{as } \lambda \rightarrow \infty.$$

The operator is the only difference between the normal and the modified self-attention layers. We approximate the modified self-attention layer in $\bar{\mathcal{T}}_p^{r,m,l}$ by the normal self-attention layer with the same number of heads r and head size m .

- **Step2: Approximate the Modified Feed-Forward Layers.**

We achieve this by approximating the activation function in Ψ with four ReLU functions. From Definition E.3, we recall that Ψ denotes three-piecewise functions with at least a constant piece. We consider the following $\zeta \in \Psi$:

$$\zeta(x) = \begin{cases} b_1 & \text{if } x < c_1, \\ a_2x + b_2 & \text{if } c_1 \leq x < c_2, \\ a_3x + b_3 & \text{if } c_2 \leq x, \end{cases}$$

where $a_2, a_3, b_1, b_2, b_3, c_1, c_2 \in \mathbb{R}$, and $c_1 < c_2$.

We approximate $\zeta(x)$ by $\tilde{\zeta}(x)$ composed of four ReLU functions:

$$\begin{aligned} \tilde{\zeta}(x) &= b_1 + \frac{a_2c_1 + b_2 - b_1}{\epsilon} \text{ReLU}(x - c_1 + \epsilon) + \left(a_2 - \frac{a_2c_1 + b_2 - b_1}{\epsilon} \right) \text{ReLU}(x - c_1) \\ &\quad + \left(\frac{a_3c_2 + b_3 - a_2(c_2 - \epsilon) - b_2}{\epsilon} - a_2 \right) \text{ReLU}(x - c_2 + \epsilon) \\ &\quad + \left(a_3 - \frac{a_3c_2 + b_3 - a_2(c_2 - \epsilon) - b_2}{\epsilon} \right) \text{ReLU}(x - c_2) \\ &= \begin{cases} b_1 & \text{if } x < c_1 - \epsilon, \\ (a_2c_1 + b_2 - b_1)(x - c_1)/\epsilon + a_2c_1 + b_2 & \text{if } c_1 - \epsilon \leq x < c_1, \\ a_2x + b_2 & \text{if } c_1 \leq x < c_2 - \epsilon, \\ (a_3c_2 + b_3 - a_2(c_2 - \epsilon) - b_2)(x - c_2)/\epsilon + a_3c_2 + b_3 & \text{if } c_2 - \epsilon \leq x < c_2, \\ a_3x + b_3 & \text{if } c_2 \leq x. \end{cases} \end{aligned}$$

As $\epsilon \rightarrow 0$, we approximate $\zeta(x)$ using $\tilde{\zeta}(x)$. The activation function is the only difference between the normal and modified feed-forward layers. We approximate the modified feed-forward layer in $\overline{\mathcal{T}}_p^{r,m,l}$ by the normal one.

Thus, for any $f_{\mathcal{T},c} \in \overline{\mathcal{T}}_p^{2,1,1}$, there exists a function $f_{\mathcal{T}} \in \mathcal{T}_p^{2,1,4}$ to approximate $f_{\mathcal{T},c}$.

This completes the proof. □

F Proofs of Section 3

Our proof is motivated by the approximation and estimation theory of U-Net-based diffusion models in [Chen et al., 2023a]. We use the universal approximation capability Appendix E and the covering number of transformer networks to proceed with our proof. Specifically, we derive the approximation error bound in Appendix F.1 and the corresponding sample complexity bound in Appendix F.2. Then we show that the data distribution generated from the estimated score function converges toward a proximate area of the original one in Appendix F.3.

F.1 Proof of Theorem 3.1

Here we present some auxiliary theoretical results in Appendix F.1.1 to prepare our main proof of Theorem 3.1. Then we derive the approximation error bound of DiTs (i.e., the proof of Theorem 3.1) in Appendix F.1.2.

F.1.1 Auxiliary Lemmas for Theorem 3.1.

We restate some auxiliary lemmas and their proofs here from [Chen et al., 2023a] for later convenience.

Lemma F.1 (Lemma 16 of [Chen et al., 2023a]). Consider a probability density function $p_h(h) = \exp(-C\|h\|_2^2/2)$ for $h \in \mathbb{R}^{d_0}$ and constant $C > 0$. Let $r_h > 0$ be a fixed radius. Then it holds

$$\begin{aligned} \int_{\|h\|_2 > r_h} p_h(h) dh &\leq \frac{2d_0\pi^{d_0/2}}{CT(d_0/2 + 1)} r_h^{d_0-2} \exp(-Cr_h^2/2), \\ \int_{\|h\|_2 > r_h} \|h\|_2^2 p_h(h) dh &\leq \frac{2d_0\pi^{d_0/2}}{CT(d_0/2 + 1)} r_h^{d_0} \exp(-Cr_h^2/2). \end{aligned}$$

Lemma F.2 (Lemma 2 of [Chen et al., 2023a]). Suppose Assumption 2.2 holds and g is defined as:

$$q(\bar{h}, t) = \int \frac{h\psi_t(\bar{h}|h)p_h(h)}{\int \psi_t(\bar{h}|h)p_h(h)dh} dh, \quad \bar{h} = B^\top x.$$

Given $\epsilon > 0$, with $r_h = c \left(\sqrt{d_0 \log(d_0/T_0) + \log(1/\epsilon)} \right)$ for an absolute constant c , it holds

$$\|q(\bar{h}, t) \mathbb{1}_{\{\|\bar{h}\|_2 \geq r_h\}}\|_{L^2(P_t)} \leq \epsilon, \text{ for } t \in [T_0, T].$$

Lemma F.3 (Theorem 1 of [Chen et al., 2023a]). We denote

$$\tau(r_h) = \sup_{t \in [T_0, T]} \sup_{\bar{h} \in [0, r_h]^d} \left\| \frac{\partial}{\partial t} q(\bar{h}, t) \right\|_2.$$

With $q(\bar{h}, t) = \int h \psi_t(\bar{h}|h) p_h(h) / (\int \psi_t(\bar{h}|h) p_h(h) dh) dh$ and p_h satisfies [Assumption 2.2](#), we have a coarse upper bound for $\tau(r_h)$

$$\tau(r_h) = \mathcal{O} \left(\frac{1 + \beta^2(t)}{\beta(t)} \left(L_{s_+} + \frac{1}{\sigma(t)} \right) \sqrt{d_0} r_h \right) = \mathcal{O} \left(e^{T/2} L_{s_+} r_h \sqrt{d_0} \right).$$

Lemma F.4 (Lemma 10 of [\[Chen et al., 2020b\]](#)). For any given $\epsilon > 0$, and L -Lipschitz function g defined on $[0, 1]^{d_0}$, there exists a continuous function \bar{f} constructed by trapezoid function that

$$\|g - \bar{f}\|_\infty \leq \epsilon.$$

Moreover, the Lipschitz continuity of \bar{f} is bounded by

$$|\bar{f}(x) - \bar{f}(y)| \leq 10d_0 L \|x - y\|_2 \quad \text{for any } x, y \in [0, 1]^{d_0}.$$

F.1.2 Main Proof of [Theorem 3.1](#)

Proof of [Theorem 3.1](#). With $\nabla \log p_t^h(\bar{h}) = B^\top s_+(\bar{h}, t)$, we note that in [\(2.4\)](#)

$$q(\bar{h}, t) = \sigma(t) \nabla \log p_t^h(\bar{h}) + B^\top x = \sigma(t) B^\top (s_+(\bar{h}, t) + x). \quad (\text{F.1})$$

We proceed as follows:

- **Step 1.** Approximate $q(\bar{h}, t)$ with a compact-supported continuous function $\bar{f}(\bar{h}, t)$.
- **Step 2.** Approximate $\bar{f}(\bar{h}, t)$ with a Transformer network.

Step 1. Approximate $q(\bar{h}, t)$ with a Compact-supported Continuous Function $\bar{f}(\bar{h}, t)$. Here we partition \mathbb{R}^{d_0} into a compact subset $H_1 := \{\bar{h} | \|\bar{h}\|_2 \leq r_h\}$ and its complement H_2 , where r_h is to be determined later. We approximate $q(\bar{h}, t)$ on the two subsets respectively and then prove \bar{f} 's continuity. Such a step achieves an estimation error of $\sqrt{d_0}\epsilon$ between $q(\bar{h}, t)$ and $\bar{f}(\bar{h}, t)$. We show the main proof here.

- **Approximation on $H_2 \times [T_0, T]$.** For any $\epsilon > 0$, we take $r_h = c(\sqrt{d_0 \log(d_0/T_0) - \log \epsilon})$. We obtain from [Lemma F.2](#) that

$$\|q(\bar{h}, t) \mathbb{1}_{\{\|\bar{h}\|_2 \geq r_h\}}\|_{L^2(P_t)} \leq \epsilon \quad \text{for } t \in [T_0, T].$$

So we set $\bar{f}(\bar{h}, t) = 0$ on $H_2 \times [T_0, T]$.

- **Approximation on $H_1 \times [T_0, T]$.** On $H_1 \times [T_0, T]$, we approximate $q(\bar{h}, t)$ by each coordinate $q_k(\bar{h}, t)$ respectively, where $q(\bar{h}, t) = [q_1(\bar{h}, t), q_2(\bar{h}, t), \dots, q_{d_0}(\bar{h}, t)]$. We firstly rescale the input by $y' = (\bar{h} + r_h \mathbb{1})/2r_h$ and $t' = t/T$, so that the transformed input space is $[0, 1]^{d_0} \times [T_0/T, 1]$. We implement such a transformation by a single feed-forward layer.

By [Assumption 2.3](#), on-support score $s_+(\bar{h}, t)$ is L_{s_+} -Lipschitz in \bar{h} . This implies $q(\bar{h}, t)$ is $(1 + L_{s_+})$ -Lipschitz in \bar{h} . When taking the transformed inputs, $g(y', t') = q(2r_h y' - r_h \mathbf{1}, Tt')$ becomes $2r_h(1 + L_{s_+})$ -Lipschitz in y' ; so is each coordinate $g_k(y', t)$. Here we take $L_h = 1 + L_{s_+}$.

Besides, $g(y', t')$ is $T\tau(r_h)$ -Lipschitz with respect to t , where

$$\tau(r_h) = \sup_{t \in [T_0, T]} \sup_{\bar{h} \in [0, r_h]^d} \left\| \frac{\partial}{\partial t} q(\bar{h}, t) \right\|_2.$$

We have a coarse upper bound for $\tau(r_h)$ in [Lemma F.3](#). We repeat it here for convenience

$$\tau(r_h) = \mathcal{O} \left(\frac{1 + \beta^2(t)}{\beta(t)} \left(L_{s_+} + \frac{1}{\sigma(t)} \right) \sqrt{d_0} r_h \right) = \mathcal{O} \left(e^{T/2} L_{s_+} r_h \sqrt{d_0} \right).$$

In conclusion, each $g_k(y', t)$ is Lipschitz continuous. So we can apply [Lemma F.4](#) to find out $\bar{f}_k(y', t)$ for approximating each coordinate. We concatenate \bar{f}_i 's together and construct $\bar{f} = [\bar{f}_1, \dots, \bar{f}_{d_0}]^\top$. According to the construction in [Lemma F.4](#), for any given ϵ , we achieve

$$\sup_{y', t' \in [0, 1]^d \times [T_0/T, 1]} \left\| \bar{f}(y', t') - g(y', t') \right\|_\infty \leq \epsilon,$$

Considering the input rescaling (i.e., $\bar{h} \rightarrow y'$ and $t \rightarrow t'$), we obtain:

- The constructed function is Lipschitz continuous in \bar{h} , i.e., for any $\bar{h}_1, \bar{h}_2 \in H_1$ and $t \in [T_0, T]$, it holds

$$\left\| \bar{f}(\bar{h}_1, t) - \bar{f}(\bar{h}_2, t) \right\|_\infty \leq 10d_0 L_h \left\| \bar{h}_1 - \bar{h}_2 \right\|_2. \quad (\text{F.2})$$

- The function is also Lipschitz in t , i.e., for any $t_1, t_2 \in [T_0, T]$ and $\left\| \bar{h} \right\|_2 \leq r_h$, it holds

$$\left\| \bar{f}(\bar{h}, t_1) - \bar{f}(\bar{h}, t_2) \right\|_\infty \leq 10\tau(r_h) \left\| t_1 - t_2 \right\|_2.$$

Due to the fact that the construction of $\bar{f}(\bar{h}, t)$ is based on trapezoid function, we have $\bar{f}(\bar{h}, t) = 0$ for $\left\| \bar{h} \right\|_2 = r_h, \forall t \in [T_0, T]$. So the two parts of $\bar{f}(\bar{h}, t)$ can be joined together. To be more specific, the above Lipschitz continuity in \bar{h} extends to the whole \mathbb{R}^{d_0} .

- **Approximation Error Analysis under L^2 Norm.** The L^2 approximation error of \bar{f} can be decomposed into two terms:

$$\left\| q(\bar{h}, t) - \bar{f}(\bar{h}, t) \right\|_{L^2(P_t^h)} = \left\| (q(\bar{h}, t) - \bar{f}(\bar{h}, t)) \mathbf{1}_{\{\left\| \bar{h} \right\|_2 < r_h\}} \right\|_{L^2(P_t^h)} + \left\| q(\bar{h}, t) \mathbf{1}_{\{\left\| \bar{h} \right\|_2 > r_h\}} \right\|_{L^2(P_t^h)}.$$

The second term on the right-hand side above has already been bounded with the selection of

r_h :

$$\|g(\bar{h}, t) \mathbb{1}\{\|\bar{h}\|_2 > r_h\}\|_{L^2(P_t^h)} \leq \epsilon.$$

The first term is bounded by:

$$\|(q(\bar{h}, t) - \bar{f}(\bar{h}, t)) \mathbb{1}\{\|\bar{h}\|_2 < r_h\}\|_{L^2(P_t^h)} \leq \sqrt{d_0} \sup_{y', t' \in [0, 1]^d \times [T_0/T, 1]} \|\bar{f}(y', t') - g(y', t')\|_\infty \leq \sqrt{d_0} \epsilon.$$

So we obtain

$$\|q(\bar{h}, t) - \bar{f}(\bar{h}, t)\|_{L^2(P_t^h)} \leq (\sqrt{d_0} + 1) \epsilon.$$

If we substitute ϵ with $\epsilon/2$, we obtain that the approximation error of $\bar{f}(\bar{h}, t)$ is $\sqrt{d_0} \epsilon$.

Step 2. Approximate $\bar{f}(\bar{h}, t)$ by a Transformer. This step is based on the universal approximation of transformers for the compact-supported continuous function in [Lemma E.1](#). Following [\[Peebles and Xie, 2023\]](#), DiT uses time point t to calculate the scale and shift value in the Transformer backbone, and it transforms an input picture into a sequential version. We ignore time point t in the notation of the Transformer network in DiT. Recall that the reshape layer $R(\cdot)$ in [Definition 3.1](#), we consider use $f(\cdot) := R^{-1} \circ f_{\mathcal{T}} \circ R(\cdot)$ to approximate $\bar{f}_t(\cdot) := \bar{f}(\cdot, t)$, where $f_{\mathcal{T}} \in \mathcal{T}_p^{2,1,4}$.

- **Overall Approximation Error.** With [Lemma E.1](#), we approximate $\bar{f}_t(\cdot)$ with $\hat{f}(\cdot) := R^{-1} \circ \hat{f}_{\mathcal{T}} \circ R(\cdot)$, and denote

$$H = R(\bar{h}).$$

We have

$$\begin{aligned} \|\bar{f}_t(\bar{h}) - \hat{f}(\bar{h})\|_{L^2(P_t^h)} &= \left(\int_{P_t^h} \|\bar{f}_t(\bar{h}) - \hat{f}(\bar{h})\|_2^2 dh \right)^{1/2} \\ &= \left(\int_{P_t^h} \|R \circ \bar{f}_t \circ R^{-1}(H) - R \circ \hat{f} \circ R^{-1}(H)\|_F^2 dh \right)^{1/2} \\ &= \left(\int_{P_t^h} \|R \circ \bar{f}_t \circ R^{-1}(H) - \hat{f}_{\mathcal{T}}(H)\|_F^2 dh \right)^{1/2} \\ &\leq \epsilon. \end{aligned} \tag{F.3}$$

Along with Step 1, we obtain

$$\|q(\bar{h}, t) - \hat{f}(\bar{h})\|_{L^2(P_t^h)} \leq \|q(\bar{h}, t) - \bar{f}(\bar{h}, t)\|_{L^2(P_t^h)} + \|\bar{f}(\bar{h}, t) - \hat{f}(\bar{h})\|_{L^2(P_t^h)} \leq (1 + \sqrt{d_0}) \epsilon.$$

The constructed approximator to $\nabla \log p_t(x)$ is $s_{\widehat{W}} = (B\widehat{f}(B^\top x, t) - x)/\sigma(t)$, whose approximation error is

$$\|\nabla \log p_t(\cdot) - s_{\widehat{W}}(\cdot, t)\|_{L^2(P_t)} \leq \frac{1 + \sqrt{d_0}}{\sigma(t)} \epsilon, \quad \forall t \in [T_0, T].$$

- **Settling-down of Hyperparameters.** We settle down the hyperparameters to configure our network here. We refer to [Appendix E.2](#) for some of the following calculations.

1. Model Architecture Depth K .

We see from [Lemma E.6](#) that $K = \mathcal{O}((1/\delta)^{dL})$. To achieve ϵ -error approximation, we set $\delta = \mathcal{O}(\epsilon^{2/d})$ according to [Lemma E.3](#). Thus we obtain

$$K = \mathcal{O}(\epsilon^{-2L}). \quad (\text{F.4})$$

- ### 2. Lipchitz Upperbound for Transformer: $L_{\mathcal{T}}$.
- We denote $\bar{f}_{t,R}(\cdot) = R \circ \bar{f}_t \circ R^{-1}(\cdot)$. We get the Lipshitz upper bound for $\widehat{f}_{\mathcal{T}} \in \mathcal{T}_p^{2,1,4}$ in the following way

$$\begin{aligned} \|\widehat{f}_{\mathcal{T}}(H_1) - \widehat{f}_{\mathcal{T}}(H_2)\|_F &\leq \|\widehat{f}_{\mathcal{T}}(H_1) - \bar{f}_{t,R}(H_1)\|_F + \|\bar{f}_{t,R}(H_1) - \bar{f}_{t,R}(H_2)\|_F \\ &\quad + \|\bar{f}_{t,R}(H_2) - \widehat{f}_{\mathcal{T}}(H_2)\|_F \\ &\leq 2\epsilon + \|\bar{f}_{t,R}(H_1) - \bar{f}_{t,R}(H_2)\|_F \quad (\text{By (F.3)}) \\ &\leq 2\epsilon + 10d_0L_{s_+}\|H_1 - H_2\|_F. \quad (\text{By (F.2)}) \end{aligned}$$

Then we get

$$L_{\mathcal{T}} = \mathcal{O}(d_0L_{s_+}). \quad (\text{F.5})$$

3. Model Output Bound for $\mathcal{S}_{\mathcal{T}_p^{2,1,4}}$.

For the output of the constructed transformer $\widehat{f}_{\mathcal{T}}(\cdot)$, according to [Lemma E.5](#), we have $\widehat{f}_{\mathcal{T}}(O) = O$, with $O = \mathbf{0}_{d \times L}$. Thus with the Lipschitz upperbound $\mathcal{O}(d_0L_{s_+})$, we have $\|\widehat{f}_{\mathcal{T}}(H)\|_F = \mathcal{O}(d_0L_{s_+}r_h)$, where $\|H\|_F \leq r_h$. With $r_h = c(\sqrt{d_0 \log(d_0/T_0) + \log(1/\epsilon)})$, we obtain

$$C_{\mathcal{T}} = \mathcal{O}\left(d_0L_{s_+} \cdot \sqrt{d_0 \log(d_0/T_0) + \log(1/\epsilon)}\right). \quad (\text{F.6})$$

4. Model Parameters Bound: $C_{OV}^{2,\infty}, C_{OV}, C_{KQ}^{2,\infty}, C_{KQ}, C_E$.

By definition, we have:

$$\|(W_{OV}^i)^\top\|_{2,\infty} \leq C_{OV}^{2,\infty}, \quad \|(W_{OV}^i)^\top\|_2 \leq C_{OV}, \quad \|W_{KQ}^i\|_{2,\infty} \leq C_{KQ}^{2,\infty}, \quad \|W_{KQ}^i\|_2 \leq C_{KQ},$$

where $i = 1, 2$. For simplicity, we omit i hereafter, which does not affect our discussion.

Recall that $\|Z\|_{2,\infty}$ denotes the $2, \infty$ -norm where the 2-norm is over columns and ∞ -norm is over rows. By the construction of modified attention layers (E.11) and (E.12) in Appendix E.5.3, we consider W_{OV} with the largest norm, i.e.,

$$W_{OV} = L\delta^{-(L+1)d-1} \cdot \begin{pmatrix} 1 & \delta^{-1} & \dots & \delta^{-d+1} \\ 0 & 0 & \dots & 0 \\ \vdots & \vdots & \dots & \vdots \\ 0 & 0 & \dots & 0 \end{pmatrix}.$$

We give the following upper bounds

$$\|W_{OV}^\top\|_{2,\infty} = Ld\delta^{-(L+2)d} = \mathcal{O}(\delta^{-Ld}), \quad (\text{F.7})$$

$$\|W_{OV}^\top\|_2 = \sup_{\|x\|_2=1} \|W_{OV}^\top x\|_2 = L\delta^{-(L+1)d-1} \cdot \sqrt{\sum_{i=0}^{d-1} \delta^{-2i}} = \mathcal{O}(\delta^{-Ld}). \quad (\text{F.8})$$

By (E.11) and (E.12) in Appendix E.5.3 and approximation by self-attention layers in Appendix E.5.5, we consider W_{KQ} with the largest norm, i.e.,

$$W_{KQ} := \begin{pmatrix} 1 \\ \delta^{-1} \\ \vdots \\ \delta^{-d+1} \end{pmatrix} (1, \delta^{-1}, \dots, \delta^{-d+1}) = \begin{pmatrix} 1 & \delta^{-1} & \dots & \delta^{-d+1} \\ \delta^{-1} & \delta^{-2} & \dots & \delta^{-d} \\ \vdots & \vdots & \dots & \vdots \\ \delta^{-d+1} & \delta^{-d} & \dots & \delta^{-2d+2} \end{pmatrix}.$$

So we have

$$\|W_{KQ}\|_{2,\infty} = \sqrt{\sum_{i=0}^{d-1} \delta^{-2i-2d+2}} = \mathcal{O}(\delta^{-2d}), \quad (\text{F.9})$$

$$\|W_{KQ}\|_2 = \sup_{\|x\|_2=1} \|W_{KQ}x\|_2 = \delta^{-2d+2} = \mathcal{O}(\delta^{-2d}). \quad (\text{F.10})$$

We substitute δ with $\mathcal{O}(\epsilon^{2/d})$ (according to Appendix E.4) and get:

$$\begin{aligned} C_{OV}^{2,\infty} &= (1/\epsilon)^{\mathcal{O}(1)}, \\ C_{OV} &= (1/\epsilon)^{\mathcal{O}(1)}, \\ C_{KQ}^{2,\infty} &= (1/\epsilon)^{\mathcal{O}(1)}, \\ C_{KQ} &= (1/\epsilon)^{\mathcal{O}(1)}. \end{aligned}$$

From the construction of positional encoder (E.4) in Appendix E.2, we have

$$E = \begin{pmatrix} 0 & 1 & \cdots & L-1 \\ 0 & 1 & \cdots & L-1 \\ \vdots & \vdots & \vdots & \vdots \\ \vdots & \vdots & \vdots & \vdots \\ 0 & 1 & \cdots & L-1 \end{pmatrix}.$$

We deduce

$$\|E^\top\|_{2,\infty} = \sqrt{L}(L-1) = \mathcal{O}(L^{3/2}).$$

Thus we have

$$C_E = \mathcal{O}(L^{3/2}). \quad (\text{F.11})$$

5. Parameters Bound in Feed Forward Layers: $C_F^{2,\infty}, C_F$.

Recall the construction of modified feed-forward layers in the proof of Lemma E.4, including Definitions E.5, E.6 and E.8 to E.10. With the approximation by normal feed-forward layers in Appendix E.5.5, we consider the weight parameters with the largest norm in the feed-forward layers. i.e.,

$$W_1 := \begin{pmatrix} 1 \\ 1 \\ 1 \\ 1 \end{pmatrix} (1, \delta^{-1}, \dots, \delta^{-d+1}) = \begin{pmatrix} 1 & \delta^{-1} & \cdots & \delta^{-d+1} \\ 1 & \delta^{-1} & \cdots & \delta^{-d+1} \\ 1 & \delta^{-1} & \cdots & \delta^{-d+1} \\ 1 & \delta^{-1} & \cdots & \delta^{-d+1} \end{pmatrix} \in \mathbb{R}^{4 \times d}.$$

Then we have

$$\begin{aligned} C_F^{2,\infty} &= \mathcal{O} \left(\sqrt{\sum_{i=0}^{d-1} \delta^{-2i}} \right) = \mathcal{O}(\delta^{-d}) \\ &= (1/\epsilon)^{\mathcal{O}(1)}. \end{aligned} \quad (\text{By setting } \delta = \mathcal{O}(\epsilon^{2/d}) \text{ according to Appendix E.4}) \quad (\text{F.12})$$

and

$$\begin{aligned} C_F &= \sup_{\|x\|_2=1} \|W_1 x\|_2 = \mathcal{O}(\delta^{-d}) \\ &= (1/\epsilon)^{\mathcal{O}(1)}. \end{aligned} \quad (\text{By setting } \delta = \mathcal{O}(\epsilon^{2/d}) \text{ according to Appendix E.4}) \quad (\text{F.13})$$

This completes the proof. \square

F.2 Proof of Corollary 3.1.1

Here we present the auxiliary theoretical results about the covering number of transformer networks in Appendix F.2.1 to prepare our main proof of Corollary 3.1.1. The results is based on the Theorem A.17 of [Edelman et al., 2022]. Then we derive the sample complexity bound of DiTs (i.e., the proof of Corollary 3.1.1) in Appendix F.2.

F.2.1 Auxiliary Lemmas for Corollary 3.1.1

Lemma F.5 (Lemma 15 of [Chen et al., 2023a]). Let \mathcal{G} be a bounded function class, i.e., there exists a constant b such that any $g \in \mathcal{G} : \mathbb{R}^{d_0} \mapsto [0, b]$. Let $z_1, z_2, \dots, z_n \in \mathbb{R}^{d_0}$ be i.i.d. random variables. For any $\delta \in (0, 1)$, $a \leq 1$, and $c > 0$, we have

$$P \left(\sup_{g \in \mathcal{G}} \frac{1}{n} \sum_{i=1}^n g(z_i) - (1+a)\mathbb{E}[g(z)] > \frac{(1+3/a)B}{3n} \log \frac{\mathcal{N}(c, \mathcal{G}, \|\cdot\|_\infty)}{\delta} + (2+a)c \right) \leq \delta,$$

$$P \left(\sup_{g \in \mathcal{G}} \mathbb{E}[g(z)] - \frac{1+a}{n} \sum_{i=1}^n g(z_i) > \frac{(1+6/a)B}{3n} \log \frac{\mathcal{N}(c, \mathcal{G}, \|\cdot\|_\infty)}{\delta} + (2+a)c \right) \leq \delta.$$

Now, we give the definition of covering number as follows.

Definition F.1 (Covering Number). Given a function class \mathcal{F} and a data distribution P . Sample n data points $\{X_i\}_{i=1}^n$ from P , then the covering number $\mathcal{N}(\epsilon, \mathcal{F}, \{X_i\}_{i=1}^n, \|\cdot\|)$ is the smallest size of a collection (a cover) $\mathcal{C} \in \mathcal{F}$ such that for any $f \in \mathcal{F}$, there exist $\hat{f} \in \mathcal{C}$ satisfying

$$\max_i \left\| f(X_i) - \hat{f}(X_i) \right\| \leq \epsilon.$$

Further, we define the covering number with respect to the data distribution as

$$\mathcal{N}(\epsilon, \mathcal{F}, \|\cdot\|) = \sup_{\{X_i\}_{i=1}^n \sim P} \mathcal{N}(\epsilon, \mathcal{F}, \{X_i\}_{i=1}^n, \|\cdot\|).$$

Then we give the covering number of the transformer networks.

Lemma F.6 (Modified from Theorem A.17 of [Edelman et al., 2022]). Let $\mathcal{T}_p^{r,m,l}(K, C_{\mathcal{T}}, C_{OV}^{2,\infty}, C_{OV}, C_{KQ}^{2,\infty}, C_{KQ}, C_F^{2,\infty}, C_F, C_E, L_{\mathcal{T}})$ represent the class of functions of K -layer transformer blocks satisfying the norm bound for matrix and Lipschitz property for feed-forward layers. Then for all data point $\|X\|_{2,\infty} \leq C_X$ we have

$$\log \mathcal{N}(\epsilon_c, \mathcal{T}_p^{r,m,l}(K, C_{\mathcal{T}}, C_{OV}^{2,\infty}, C_{OV}, C_{KQ}^{2,\infty}, C_{KQ}, C_F^{2,\infty}, C_F, C_E, L_{\mathcal{T}}), \|\cdot\|_2)$$

$$\leq \frac{\log(nL)}{\epsilon_c^2} \cdot \left(\sum_{i=1}^K \alpha^{\frac{2}{3}} \left(d^{\frac{2}{3}} (C_F^{2,\infty})^{\frac{4}{3}} + d^{\frac{2}{3}} (2(C_F)^2 C_{OV} C_{KQ}^{2,\infty})^{\frac{2}{3}} + \tau m^{\frac{2}{3}} ((C_F)^2 C_{OV}^{2,\infty})^{\frac{2}{3}} \right) \right)^3,$$

where $\alpha := \prod_{j < i} (C_F)^2 C_{OV} (1 + 4C_{KQ}) (C_X + C_E)$.

Remark F.1. We modify [Edelman et al., 2022, Theorem A.17] in seven aspects:

1. We do not consider the last linear layer in the model: converting each column vector of the Transformer output to a scalar. Therefore, we ignore the item related to the last linear layer in [Edelman et al., 2022, Theorem A.17].
2. We do not consider the normalization layer in our model. Because the normalization layer in the original proof only applies $\|\prod_{\text{norm}}(X_1) - \prod_{\text{norm}}(X_2)\|_{2,\infty} \leq \|X_1 - X_2\|_{2,\infty}$, ignoring this layer does not change the result.
3. Our activation function is ReLU, we replace the Lipschitz upperbound of activate function by 1.
4. We consider the positional encoding (E.4) in our work, we need to replace the upperbound C_X for the inputs with the upperbound $C_X + C_E$. Besides, for multi-layer Transformer, the original conclusion in [Edelman et al., 2022, Theorem A.17] considers the upperbound for the $2, \infty$ -norm of inputs is 1, we add the upperbound for the inputs in Lemma F.6.
5. We use (2.7) as the feed forward layer, including two linear layers and a residual layer. Thus, in Lemma F.6, we replace the original upperbound for the norm of weight matrix with the upperbound for the norm of $I_d + W_2 W_1$. In the following, we use \mathcal{O} to estimate the log-covering number, thus we ignore the item for I_d here for convenience. This is the same for the self-attention layer.
6. We use multi-head attention, we add the number of heads τ in our result, similar to [Edelman et al., 2022, Theorem A.12].
7. In our work, we use Transformer $\mathcal{T}_p^{2,1,4}$, i.e., $\tau = 2, m = 1$.

F.2.2 Proof of Corollary 3.1.1

Proof of Corollary 3.1.1. Our proof is built on [Chen et al., 2023a, Appendix B.2]. Firstly, for one data sample, we define the empirical score matching loss objective (2.1) as follows

$$\ell(x; s_{\widehat{W}}) = \frac{1}{T - T_0} \int_{T_0}^T \mathbb{E}_{x_t|x_0=x} [\|\nabla_{x_t} \log \psi_t(x_t|x_0) - s_{\widehat{W}}(x_t, t)\|_2^2] dt.$$

Then we define $\mathcal{L}(s_{\widehat{W}}) = \mathbb{E}_{x \sim P_0} [\ell(x; s_{\widehat{W}})]$.

Following [Chen et al., 2023a, Appendix B.2], for any $a \in (0, 1)$, we have

$$\mathcal{L}(s_{\widehat{W}}) \leq \underbrace{\mathcal{L}^{\text{trunc}}(s_{\widehat{W}}) - (1+a)\widehat{\mathcal{L}}^{\text{trunc}}(s_{\widehat{W}})}_{(I)} + \underbrace{\mathcal{L}(s_{\widehat{W}}) - \mathcal{L}^{\text{trunc}}(s_{\widehat{W}})}_{(II)} + (1+a) \underbrace{\inf_{s_W \in \mathcal{S}_{\text{NN}}} \widehat{\mathcal{L}}(s_W)}_{(III)}.$$

where

$$\mathcal{L}^{\text{trunc}}(s_{\widehat{W}}) := \mathbb{E}_{x \sim P_0} [\ell^{\text{trunc}}(x; s_{\widehat{W}})] = \mathbb{E}_{x \sim P_0} [\ell(x; s_{\widehat{W}}) \mathbb{1}\{\|x\|_2 \leq r_x\}], \quad r_x > B.$$

We denote

$$\eta := 4C_{\mathcal{T}}(C_{\mathcal{T}} + r_x)(r_x/D)^{D-2} \exp(-r_x^2/\sigma(t))/(T_0(T - T_0)),$$

$$r_x := \mathcal{O}\left(\sqrt{d_0 \log d_0 + \log C_{\mathcal{T}} + \log(n/\bar{\delta})}\right).$$

For any $\bar{\delta} > 0$, following [Chen et al., 2023a, Appendix B.2], we have the following for term (I) with probability $1 - \bar{\delta}$,

$$(I) = \mathcal{O}\left(\frac{(1 + 3/a)(C_{\mathcal{T}}^2 + r_x^2)}{nT_0(T - T_0)} \log \frac{\mathcal{N}\left(\frac{(T-T_0)(\iota-\eta)}{(C_{\mathcal{T}}+r_x)\log(T/T_0)}, \mathcal{S}_{\mathcal{T}_p^{2,1,4}}, \|\cdot\|_2\right)}{\bar{\delta}} + (2 + a)c\right).$$

where $c \leq 0$ is a constant, and $\iota > 0$ will be determined later.

We set $\iota = 1/(n^{1/4}T_0(T - T_0))$, then we have

$$(I) = \mathcal{O}\left(\frac{(1 + 3/a)(C_{\mathcal{T}}^2 + r_x^2)}{nT_0(T - T_0)} \log \frac{\mathcal{N}\left((n(C_{\mathcal{T}} + r_x)T_0 \log(T/T_0))^{-1}, \mathcal{S}_{\mathcal{T}_p^{2,1,4}}, \|\cdot\|_2\right)}{\bar{\delta}} + \frac{1}{n}\right),$$

with probability $1 - \bar{\delta}$.

Following the upper bound of the other two terms and the proof details in [Chen et al., 2023a, Appendix B.2], we have

$$\begin{aligned} & \frac{1}{T - T_0} \int_{T_0}^T \|s_{\widehat{W}}(\cdot, t) - \nabla \log p_t(\cdot)\|_{L^2(P_t)}^2 dt \\ &= \mathcal{O}\left(\frac{(C_{\mathcal{T}}^2 + r_x^2)}{\epsilon^2 n T_0(T - T_0)} \log \frac{\mathcal{N}\left((n(C_{\mathcal{T}} + r_x)T_0 \log(T/T_0))^{-1}, \mathcal{S}_{\mathcal{T}_p^{2,1,4}}, \|\cdot\|_2\right)}{\bar{\delta}} + \frac{1}{n} + \frac{d_0^2}{T_0(T - T_0)} \epsilon^2\right), \end{aligned} \tag{F.14}$$

with probability $1 - 3\bar{\delta}$.

Covering Number of $\mathcal{S}_{\mathcal{T}_p^{2,1,4}}$. The next step is to calculate the covering number of $\mathcal{S}_{\mathcal{T}_p^{2,1,4}}$. $\mathcal{S}_{\mathcal{T}_p^{2,1,4}}$ consists of two components: (i) Matrix W_B with orthonormal columns; (ii) Network

function $f_{\mathcal{T}}$. Suppose we have W_{B1}, W_{B2} and f_1, f_2 such that $\|W_{B1} - W_{B2}\|_F \leq \delta_1$ and $\sup_{\|x\|_2 \leq 3r_x + \sqrt{D \log D}, t \in [T_0, T]} \|f_1(x, t) - f_2(x, t)\|_2 \leq \delta_2$, where $f_1 = R^{-1} \circ f_{\mathcal{T}1} \circ R, f_2 = R^{-1} \circ f_{\mathcal{T}2} \circ R$. Then we evaluate

$$\begin{aligned}
& \sup_{\|x\|_2 \leq 3r_x + \sqrt{D \log D}, t \in [T_0, T]} \|s_{W_{B1}, f_{\mathcal{T}1}}(x, t) - s_{W_{B2}, f_{\mathcal{T}2}}(x, t)\|_2 \\
&= \frac{1}{\sigma(t)} \sup_{\|x\|_2 \leq 3r_x + \sqrt{D \log D}, t \in [T_0, T]} \|W_{B1} f_1(W_{B1}^\top x, t) - W_{B2} f_2(W_{B2}^\top x, t)\|_2 \\
&\leq \frac{1}{\sigma(t)} \sup_{\|x\|_2 \leq 3r_x + \sqrt{D \log D}, t \in [T_0, T]} \left(\|W_{B1} f_1(W_{B1}^\top x, t) - W_{B1} f_1(W_{B2}^\top x, t)\|_2 \right. \\
&\quad \left. + \|W_{B1} f_1(W_{B2}^\top x, t) - W_{B1} f_2(W_{B2}^\top x, t)\|_2 + \|W_{B1} f_2(W_{B2}^\top x, t) - W_{B2} f_2(W_{B2}^\top x, t)\|_2 \right) \\
&\leq \frac{1}{\sigma(t)} \left(L_{\mathcal{T}} \delta_1 \sqrt{d_0} (3r_x + \sqrt{D \log D}) + \delta_2 + \delta_1 K \right), \tag{F.15}
\end{aligned}$$

where $L_{\mathcal{T}}$ upper bounds the Lipschitz constant of $f_{\mathcal{T}}$.

For set $\{W_B \in \mathbb{R}^{D \times d_0} : \|W_B\|_2 \leq 1\}$, its δ_1 -covering number is $(1 + 2\sqrt{d_0}/\delta_1)^{D d_0}$ ([Chen et al., 2020a, Lemma 8]). The δ_2 -covering number of f needs further discussion as there is a reshaping process in our network. For the input reshaped from $\bar{h} \in \mathbb{R}^{d_0}$ to $H \in \mathbb{R}^{d \times L}$, we have

$$\|\bar{h}\|_2 \leq r_x \iff \|H\|_F \leq r_x,$$

$$\sup_{\|\bar{h}\|_2 \leq 3r_x + \sqrt{D \log D}, t \in [T_0, T]} \|f_1(\bar{h}, t) - f_2(\bar{h}, t)\|_2 \leq \delta_2,$$

and

$$\iff \sup_{\|H\|_F \leq 3r_x + \sqrt{D \log D}, t \in [T_0, T]} \|f_{\mathcal{T}1}(H) - f_{\mathcal{T}2}(H)\|_2 \leq \delta_2.$$

Thus we can follow the covering number property for sequence-to-sequence transformer $\mathcal{T}_p^{2,1,4}$, i.e., Lemma F.6 and get the following δ_2 -covering number

$$\frac{\log(nL)}{\delta_2^2} \cdot \left(\sum_{i=1}^K \alpha_i^{\frac{2}{3}} \left(d^{\frac{2}{3}} (C_F^{2,\infty})^{\frac{4}{3}} + d^{\frac{2}{3}} (2(C_F)^2 C_{OV} C_{KQ}^{2,\infty})^{\frac{2}{3}} + \tau m^{\frac{2}{3}} ((C_F)^2 C_{OV}^{2,\infty})^{\frac{2}{3}} \right) \right)^3,$$

where

$$\alpha_i := \prod_{j < i} (C_F)^2 C_{OV} (1 + 4C_{KQ})(C_X + C_E).$$

According to the (F.4), (F.5), (F.7), (F.8), (F.9), (F.10), (F.12), (F.13), (F.11) and (F.6) in Appendix F.1.2, we derive the following with $\delta = \mathcal{O}(\epsilon^{2/d})$ (Appendix E.4) and $d = 4$ (Theorem 3.1):

$$\begin{aligned} K &= \mathcal{O}(\epsilon^{-2L}), L_{\mathcal{T}} = \mathcal{O}(d_0 L_{s_+}), C_{OV}^{2,\infty} = \mathcal{O}(d\epsilon^{-4L}), C_{OV} = \mathcal{O}(\epsilon^{-4L}), \\ C_{KQ}^{2,\infty} &= \mathcal{O}(\epsilon^{-4}), C_{KQ} = \mathcal{O}(\epsilon^{-4}), C_F^{2,\infty} = \mathcal{O}(\epsilon^{-4}), C_F = \mathcal{O}(\epsilon^{-2}), C_E = \mathcal{O}(L^{3/2}), \\ C_{\mathcal{T}} &= \mathcal{O}\left(d_0 L_{s_+} \cdot \sqrt{d_0 \log(d_0/T_0) + \log(1/\epsilon)}\right), r_x = \mathcal{O}\left(\sqrt{d_0 \log d_0 + \log C_{\mathcal{T}} + \log(n/\bar{\delta})}\right). \end{aligned} \quad (\text{F.16})$$

We consider that each elements of the input data are within $[0, 1]$ as shown in Appendix E.

Recall that $\iota = 1/(n^{1/4}T_0(T - T_0))$, then we get the log-covering number of $\mathcal{T}_p^{2,1,4}$,

$$\begin{aligned} \log \mathcal{N}(\iota, \mathcal{T}_p^{2,1,4}, \|\cdot\|_2) &= \mathcal{O}\left(\frac{\epsilon^{-8K} \cdot L^K d^2 \log(nL)}{\iota}\right) \\ &= \mathcal{O}(1) \cdot \left(\frac{2^{8K \log(L/\epsilon)} d^2 \log(nL)}{\iota}\right). \end{aligned}$$

Following [Chen et al., 2023a, Appendix B.2], then the log-covering number of $\mathcal{S}_{\mathcal{T}_p^{2,1,4}}$ is

$$\begin{aligned} &\log \mathcal{N}\left(\iota, \mathcal{S}_{\mathcal{T}_p^{2,1,4}}, \|\cdot\|_2\right) \\ &= \mathcal{O}\left(2Dd_0 \cdot \log\left(1 + \frac{6C_{\mathcal{T}}L_{\mathcal{T}}\sqrt{d_0}(3r_x + \sqrt{D \log D})}{T_0\iota}\right) + \frac{2^{8K \log(L/\epsilon)} d^2 \log(nL)}{T_0^2 \iota^2}\right) \quad (\text{By (F.15)}) \\ &= \mathcal{O}\left(n^{1/2} 2^{8(1/\epsilon)^L \log(L/\epsilon)} D d^2 d_0^6 L_{s_+}^2 (T - T_0)^2 \cdot \log(nL)\right) \quad (\text{By (F.16)}) \\ &= \mathcal{O}\left(n^{1/2} 2^{(1/\epsilon)^{2L}} D d^2 d_0^6 L_{s_+}^2 (T - T_0)^2 \cdot \log(nL)\right) \quad (\text{By } (1/\epsilon)^L \geq 8 \log(L/\epsilon)) \\ &= \tilde{\mathcal{O}}\left(n^{1/2} 2^{(1/\epsilon)^{2L}} D d^2 d_0^6 L_{s_+}^2 (T - T_0)^2\right) \quad (\text{By ignoring the log factors}) \\ &= \tilde{\mathcal{O}}\left(n^{1/2} 2^{(1/\epsilon)^{2L}} D d^2 d_0^6 L_{s_+}^2 T^2\right). \end{aligned}$$

Substituting the log-covering number into (F.14), we have

$$\begin{aligned} &\frac{1}{T - T_0} \int_{T_0}^T \|s_{\widehat{W}}(\cdot, t) - \nabla \log p_t(\cdot)\|_{L^2(P_t)}^2 dt \\ &= \mathcal{O}\left(\frac{C_{\mathcal{T}}^2 + r_x^2}{\epsilon^2 n T_0 (T - T_0)} (\log(\mathcal{N}) + \log(1/\bar{\delta})) + \frac{d_0^2}{T_0 (T - T_0)} \epsilon^2 + \frac{1}{n}\right) \\ &= \mathcal{O}\left(\underbrace{\frac{C_{\mathcal{T}}^2 + r_x^2}{\epsilon^2 n T_0 T} (\log(\mathcal{N}) + \log(1/\bar{\delta}))}_{\text{1st term}} + \underbrace{\frac{d_0^2}{T_0 T} \epsilon^2 + \frac{1}{n}}_{\text{2nd term}}\right). \end{aligned} \quad (\text{F.17})$$

Recall the following parameters,

- $C_{\mathcal{T}}^2 = \mathcal{O}(d_0^2 L_{s+}^2 d_0 \log(d_0/T_0) + \log(1/\epsilon))$
- $r_x^2 = \mathcal{O}(d_0 \log d_0 + \log C_{\mathcal{T}} + \log(n/\bar{\delta}))$
- $\bar{\delta}$: probability error
- ϵ : approximation error
- n : sample size
- $T_0 < T/2$
- $D, d, d_0 > 1$: feature dimension
- $L > 1$: sequence length
- $d_0 = L \cdot d$
- L_{s+} : Lipschitz coefficient

Ignoring the log factors, and $\text{poly}(D, d, d_0, L_{s+})$, the first term in (F.17) becomes

$$\frac{1}{n^{1/2}} \cdot \frac{T}{T_0} \cdot 2^{(1/\epsilon)^{2L}}.$$

The second term simplifies to

$$\frac{1}{T_0 T} \epsilon^2.$$

Thus, the final bound is

$$\tilde{O}\left(\frac{1}{n^{1/2}} \frac{T}{T_0} \cdot 2^{(1/\epsilon)^{2L}} + \frac{1}{T_0 T} \epsilon^2 + \frac{1}{n}\right).$$

Thus, we complete the proof of **Corollary 3.1.1**. □

F.3 Proof of Corollary 3.1.2

Our proof is built on [Chen et al., 2023a, Appendix C]. The main difference between our work and [Chen et al., 2023a] is our score estimation error from Corollary 3.1.1. Consequently, only the subspace error and the total variation distance differ from [Chen et al., 2023a, Theorem 3].

Proof Sketch of (i). We show that if the orthogonal score increases significantly, the mismatch between the column span of B and W_B will be greatly amplified. Therefore, an accurate score network estimator forces B and W_B to align with each other.

Proof Sketch of (ii). We conduct the proof via 2 steps:

- **Step 1: Total Variation Distance Bound.** We obtain the discrete result from the continuous-time generated distribution \hat{P}_{T_0} by adding discretization error [Chen et al., 2023a, Lemma 4]. It suffices to bound the divergence between the following two stochastic processes:

- For the ground-truth backward process, consider $h_t^\leftarrow = B^\top y_t$ and the following SDE:

$$dh_t^\leftarrow = \left[\frac{1}{2} h_t^\leftarrow + \nabla \log p^h T - t(h_t^\leftarrow) \right] dt + d\bar{B}_t^h.$$

Denote the marginal distribution of the ground-truth process as $P_{T_0}^h$.

- For the learned process, consider $\tilde{h}_t^{\leftarrow, r}$ and the following SDE:

$$d\tilde{h}_t^{\leftarrow, r} = \left[\frac{1}{2} \tilde{h}_t^{\leftarrow, r} + \tilde{s}_{f,U}^h(\tilde{h}_t^{\leftarrow, r}, T - t) \right] dt + d\bar{B}_t^h,$$

where $\tilde{s}_{f,U}^h(z, t) := [U^\top f(Uz, t) - z]/\sigma(t)$ and U is an orthogonal matrix. Following the notation in [Chen et al., 2023a], we use $(W_B U)^\top \hat{P}_{T_0}$ to denote the marginal distribution of \hat{P}_{T_0} . We first calculate the latent score matching error, i.e., the error between $\nabla \log p_t^h(h)$ and $\tilde{s}_{U,f}^h(h, t)$. Then, we adopt Girsanov's Theorem [Chen et al., 2023b] and bound the difference in the KL divergence of the above two processes to derive the score-matching error bound.

- **Step 2: Wasserstein-2 Distance Bound.** We use the same technique as [Chen et al., 2023a, Theorem 3].

Proof Sketch of (iii). We derive item (iii) by solving the orthogonal backward process of the diffusion model.

Next, we present the auxiliary theoretical results in Appendix F.3.1 to prepare our main proof of Corollary 3.1.2. Then we give a detailed proof of Corollary 3.1.2 in Appendix F.3.2.

F.3.1 Auxiliary Lemmas

Here we include a few auxiliary lemmas from [Chen et al., 2023a] without proofs. Recall the definition of Lipschitz norm: for a given function f , $\|f(\cdot)\|_{Lip} = \sup_{x \neq y} (\|f(x) - f(y)\|_2 / \|x - y\|_2)$.

Lemma F.7 (Lemma 3 of [Chen et al., 2023a]). Assume that the following holds

$$\mathbb{E}_{h \sim P_h} \|\nabla \log p_h(h)\|_2^2 \leq C_{sh}, \quad \lambda_{\min} \mathbb{E}_{h \sim P_h} [hh^\top] \geq c_0, \quad \mathbb{E}_{h \sim P_h} \|h\|_2^2 \leq C_h,$$

where λ_{\min} denotes the smallest eigenvalue. We denote

$$\bar{\mathbb{E}}[\phi(\cdot, t)] = \int_{T_0}^T \frac{1}{\sigma^2(t)} \mathbb{E}_{x \sim P_t} [\phi(\cdot, t)] dt.$$

We set $T_0 \leq \min\{2 \log(d_0/C_{sh}), 1, 2 \log(c_0), c_0\}$ and $T \geq \max\{2 \log(C_h/d_0), 1\}$. Suppose we have

$$\bar{\mathbb{E}} \|W_B f(W_B^\top x, t) - Bq(B^\top x, t)\|_2^2 \leq \epsilon.$$

Then we have

$$\|W_B W_B^\top - B B^\top\|_F^2 = \mathcal{O}(\epsilon T_0 / c_0),$$

and there exists an orthogonormal matrix $U \in \mathbb{R}^{d_0 \times d_0}$, such that:

$$\begin{aligned} & \bar{\mathbb{E}} \|U^\top f(Uh, t) - q(h, t)\|_2^2 \\ &= \epsilon \cdot \mathcal{O} \left(1 + \frac{T_0}{c_0} \left[(T - \log T_0) d_0 \cdot \max_t \|f(\cdot, t)\|_{Lip}^2 + C_s h \right] + \frac{\max_t \|f(\cdot, t)\|_{Lip}^2 \cdot C_h}{c_0} \right). \end{aligned}$$

Lemma F.8 (Lemma 4 of [Chen et al., 2023a]). Assume that P_h is sub-Gaussian, $f(h, t)$ and $\nabla \log p_t^h(h)$ are Lipschitz in both h and t . Assume we have the latent score matching error bound

$$\int_{T_0}^T \mathbb{E}_{h \sim P_t^h} \|\tilde{s}_{U,f}^h(h_t, t) - \nabla \log p_t^h(h_t)\|_2^2 dt \leq \epsilon_{\text{latent}} (T - T_0).$$

Then we have the following latent distribution estimation error for the undiscretized backward SDE

$$\text{TV} \left(P_{T_0}^h, \hat{P}_{T_0}^h \right) \lesssim \sqrt{\epsilon_{\text{latent}} (T - T_0)} + \sqrt{\text{KL}(P_h \| N(0, I_{d_0}))} \cdot \exp(-T).$$

Furthermore, we have the following latent distribution estimation error for the discretized backward SDE

$$\text{TV} \left(P_{T_0}^h, \hat{P}_{T_0}^{h, \text{dis}} \right) \lesssim \sqrt{\epsilon_{\text{latent}} (T - T_0)} + \sqrt{\text{KL}(P_h \| N(0, I_{d_0}))} \cdot \exp(-T) + \sqrt{\epsilon_{\text{dis}} (T - T_0)},$$

where

$$\begin{aligned} \epsilon_{\text{dis}} = & \left(\frac{\max_h \|f(h, \cdot)\|_{\text{Lip}}}{\sigma(T_0)} + \frac{\max_{h,t} \|f(h, t)\|_2}{T_0^2} \right)^2 \eta^2 \\ & + \left(\frac{\max_t \|f(\cdot, t)\|_{\text{Lip}}}{\sigma(T_0)} \right)^2 \eta^2 \max \{ \mathbb{E} \|h_0\|^2, d_0 \} + \eta d_0, \end{aligned}$$

and η is the step size in the backward process.

Lemma F.9 (Lemma 6 of [Chen et al., 2023a]). Consider the following discretized SDE with step size μ satisfying $T - T_0 = K_T \mu$

$$dy_t = \left[\frac{1}{2} - \frac{1}{\sigma(T - k\mu)} \right] y_{k\mu} dt + dB_t, \text{ for } t \in [k\mu, (k+1)\mu),$$

where $Y_0 \sim N(0, I)$. Then when $T > 1$ and $T_0 + \mu \leq 1$, we have $Y_{T-T_0} \sim N(0, \sigma^2 I)$ with $\sigma^2 \leq e(T_0 + \mu)$.

Lemma F.10 (Lemma 10 in [Chen et al., 2023a]). Assume that $\nabla \log p_h(h)$ is L_h -Lipschitz. Then we have $\mathbb{E}_{h \sim P_h} \|\nabla \log p_h(h)\|_2^2 \leq d_0 L_h$.

F.3.2 Main Proof of Corollary 3.1.2

Proof. Recall

$$\xi(n, \epsilon, L) := \frac{1}{n^{1/2}} \frac{T}{T_0} \cdot 2^{(1/\epsilon)^{2L}} + \frac{1}{T_0 T} \epsilon^2 + \frac{1}{n}.$$

- **Proof of (i).** With Lemma F.7, we replace ϵ to be $\epsilon(T - T_0)$ and we set $C_{sh} = L_h d_0$ by Lemma F.10, we have

$$\|W_B W_B^\top - B B^\top\|_F^2 = \mathcal{O} \left(\frac{T_0 \xi(n, \epsilon, L)}{c_0} \right).$$

We substitute the score estimation error in Corollary 3.1.1 and $T = \mathcal{O}(\log n)$ into the bound above, we deduce

$$\|W_B W_B^\top - B B^\top\|_F^2 = \tilde{\mathcal{O}} \left(\frac{1}{c_0} n^{-\zeta(n)} \cdot \log^3 n \right),$$

where $\zeta(n) = 1/2 - 9L^{2L} \cdot n^{(2L^{2L+1}/(37L \cdot \log n))} / (37 \log n)$.

We note that $\log n$ is great enough to make T satisfies $T \geq \max\{\log(C_h/d_0 + 1), 1\}$ where $C_h \geq \mathbb{E}_{h \sim P_h} \|h\|_2^2$.

- **Proof of (ii).** [Lemma F.7](#) and [Lemma F.10](#) imply that

$$\mathbb{E} \|U^\top f(Uh, t) - q(h, t)\|_2^2 = \mathcal{O}(\epsilon_{\text{latent}}(T - T_0)),$$

where

$$\epsilon_{\text{latent}} = \epsilon \cdot \mathcal{O} \left(\frac{T_0}{c_0} [(T - \log T_0)d_0 \cdot L_{s+}^2 + d_0 L_h] + \frac{L_{s+}^2 \cdot C_h}{c_0} \right).$$

Through the algebra calculation, we get

$$\begin{aligned} \mathbb{E} \|U^\top f(Uh, t) - q(h, t)\|_2^2 &= \int_{T_0}^T \mathbb{E}_{h \sim P_t^h} \left\| \frac{U^\top f(Uh, t) - h}{\sigma(t)} - \nabla \log p_t^h(h) \right\|_2^2 dt \\ &\leq \epsilon_{\text{latent}}(T - T_0). \end{aligned}$$

With ϵ_{latent} and [Lemma F.8](#), we obtain

$$\begin{aligned} &\text{TV}(P_{T_0}^h, (W_B U)_\#^\top \hat{P}_{T_0}^{\text{dis}}) \\ &\lesssim \sqrt{\epsilon_{\text{latent}}(T - T_0)} + \sqrt{\text{KL}(P_h \| N(0, I_{d_0}))} \exp(-T) + \sqrt{\epsilon_{\text{dis}}(T - T_0)} \\ &= \tilde{\mathcal{O}} \left(\frac{1}{\sqrt{c_0}} \sqrt{\xi(n, \epsilon, L)} + \frac{1}{n} + \mu \frac{\sqrt{d_0^2 \log d_0}}{T_0^2} + \sqrt{\mu} \sqrt{d_0} \right). \end{aligned}$$

As we choose time step $\mu = \mathcal{O}(\xi(n, \epsilon, L) \cdot T_0^2 / d_0 \sqrt{\log d_0})$, we obtain

$$\text{TV}(P_{T_0}^h, (W_B U)_\#^\top \hat{P}_{T_0}^{\text{dis}}) = \tilde{\mathcal{O}} \left(\sqrt{\xi(n, \epsilon, L)} \right).$$

By definition, $\hat{P}_{T_0}^{h, \text{dis}} = (UW_B)_\#^\top \hat{P}_{T_0}^{\text{dis}}$. This completes the proof of the total variation distance in [\(3.2\)](#).

For Wasserstein-2 distance $W_2(P_{T_0}^h, P_h)$, we bound it by using the same technique as [[Chen et al., 2023b](#), Lemma 16]. Specifically, our proof only requires a finite second moment of P_h verified in [Assumption 2.2](#). As a result, we have

$$W_2(P_{T_0}^h, P_h) = \mathcal{O} \left(\sqrt{d_0 T_0} \right).$$

- **Proof of (iii).** We apply [Lemma F.9](#) due to our score decomposition. With the marginal distribution at time $T - T_0$ and observing $\mu \ll T_0$, we obtain the last property.

This completes the proof. □

G Proofs of Section 4

Our proofs are motivated by the observation of low-rank gradient decomposition in transformer-like models [Alman and Song, 2024a, Gu et al., 2024]. With our simplifications and observations made in Section 4, we utilize the fine-grained complexity results of transformer and attention [Hu et al., 2024c, Alman and Song, 2024b, 2023] and tensor trick (Lemma D.1 and [Diao et al., 2019, 2018]) to proceed our proofs. Specifically, we approximate DiT training gradients with a series of low-rank approximations in Appendices G.1.1 to G.1.3, and carefully match the multiplication dimensions so that the computation of $\frac{dg_2}{dW}$ forms a chained low-rank approximation in Appendix G.2.

G.1 Auxiliary Theoretical Results for Theorem 4.1

Here we present some auxiliary theoretical results to prepare our main proof of the Existence of almost-linear Time Algorithms for ADITGC Theorem 4.1.

G.1.1 Low-Rank Decomposition of DiT Gradients

We start by some definitions. Recall that $W \in \mathbb{R}^{d \times d}$ and $\underline{W} \in \mathbb{R}^{d^2}$ denotes the vectorization of $W \in \mathbb{R}^{d \times d}$ following Definition D.1.

Definition G.1. Let $A_1, A_2 \in \mathbb{R}^{d \times L}$ be two matrices. Suppose $A = A_1^\top \otimes A_2^\top \in \mathbb{R}^{L^2 \times d^2}$. Define $A_{j_0} \in \mathbb{R}^{L \times d^2}$ as an $L \times d^2$ sub-block of A . There are L such sub-blocks in total. For each $j_0 \in [L]$, define the function $u(\underline{W})_{j_0} : \mathbb{R}^{d^2} \rightarrow \mathbb{R}^L$ by $u(\underline{W})_{j_0} := \exp(A_{j_0} \underline{W}) \in \mathbb{R}^L$.

Definition G.2. Let $A_1, A_2 \in \mathbb{R}^{d \times L}$ be two matrices. Suppose $A = A_1^\top \otimes A_2^\top \in \mathbb{R}^{L^2 \times d^2}$. Define $A_{j_0} \in \mathbb{R}^{L \times d^2}$ as an $L \times d^2$ sub-block of A . There are L such sub-blocks in total. For every index $j_0 \in [L]$, consider the function $\alpha(\underline{W})_{j_0} : \mathbb{R}^{d^2} \rightarrow \mathbb{R}$ defined by $\alpha(\underline{W})_{j_0} := \underbrace{\langle \exp(A_{j_0} \underline{W}), \mathbf{1}_L \rangle}_{L \times 1}$.

Definition G.3. Suppose that $\alpha(\underline{W})_{j_0} \in \mathbb{R}$ and $u(\underline{W})_{j_0} \in \mathbb{R}^L$ are defined as in Definitions G.1 and G.2, respectively. For a fixed $j_0 \in [L]$, consider the function $f(\underline{W})_{j_0} : \mathbb{R}^{d^2} \rightarrow \mathbb{R}^L$ defined by

$$f(\underline{W})_{j_0} := \underbrace{\alpha(\underline{W})_{j_0}^{-1}}_{\text{scalar}} \underbrace{u(\underline{W})_{j_0}}_{L \times 1}.$$

Define $f(\underline{W}) \in \mathbb{R}^{L \times L}$ as the matrix where the j_0 -th row is $(f(\underline{W})_{j_0})^\top$.

Definition G.4. For every $i_0 \in [d]$, define the function $h(\underline{W}_{OV})_{i_0} : \mathbb{R}^{d^2} \rightarrow \mathbb{R}^L$ by

$$h(\underline{W}_{OV})_{i_0} := \underbrace{A_3^\top}_{L \times d} \underbrace{(W_{OV}^\top)_{*, i_0}}_{d \times 1}.$$

Here, $W_{OV} \in \mathbb{R}^{d \times d}$ denotes the matrix representation of $\underline{W}_{OV} \in \mathbb{R}^{d^2}$, and $(W_{OV})_{*,i_0}^\top$ represents the i_0 -th column of W_{OV}^\top . Define $h(\underline{W}_{OV}) \in \mathbb{R}^{L \times d}$ as the matrix where the i_0 -th column is $h(W_{OV})_{i_0}$.

Definition G.5. For each $j_0 \in [L]$, we denote $f(W)_{j_0} \in \mathbb{R}^L$ as the normalized vector defined by [Definition G.3](#). For each $i_0 \in [d]$, $h(W_{OV})_{i_0}$ is defined as per [Definition G.4](#). For every pair $(j_0, i_0) \in [L] \times [d]$, define the function $c(\underline{W})_{j_0, i_0} : \mathbb{R}^{d^2} \times \mathbb{R}^{d^2} \rightarrow \mathbb{R}$ by

$$c(W)_{j_0, i_0} := \langle f(W)_{j_0}, h(W_{OV})_{i_0} \rangle - Y_{j_0, i_0}^\top,$$

where $(W_{OV})_{j_0, i_0}$ is the element at the (j_0, i_0) position of the matrix $W_{OV} \in \mathbb{R}^{L \times d}$. $c(\cdot)$ has matrix form

$$\underbrace{c(W)}_{L \times d} = \underbrace{f(W)}_{L \times L} \underbrace{h(W_{OV})}_{L \times d} - \underbrace{Y^\top}_{L \times d}.$$

With the tensor trick ([Appendix D.3](#)), we compute the gradient $\frac{dg_2}{dW}$ of the DiT loss as follows:

$$\frac{dg_2}{dW} = \frac{d}{dW} \left[\frac{1}{2} \sum_{j_0=1}^L \sum_{i_0=1}^d c_{j_0, i_0}^2(W) \right]. \quad (\text{G.1})$$

([G.1](#)) presents a neat decomposition of $\frac{dg_2}{dW}$. Each term is easy enough to handle. Thus, we arrive at the following lemma. Let $Z[i, \cdot]$ and $Z[\cdot, j]$ be the i -th row and j -th column of matrix Z .

Lemma G.1 (Low-Rank Decomposition of DiT Gradient). Let matrix $A_1, A_2, A_3, W, W_{OV}, Y$ and loss function \mathcal{L} follow [Definition 4.1](#), and $A := A_1^\top \otimes A_2^\top$. It holds

$$\frac{dg_2}{dW} = \sum_{j_0=1}^L \sum_{i_0=1}^d c(W)_{j_0, i_0} A_{j_0}^\top \underbrace{\left(\overbrace{\text{diag}(f(W)_j)}^{(II)} - \overbrace{f(W)_{j_0} f(W)_{j_0}^\top}^{(III)} \right)}_{(I)} h(W_{OV})_{i_0}. \quad (\text{G.2})$$

Proof. Let $Z[i, \cdot]$ and $Z[\cdot, j]$ be the i -th row and j -th column of matrix Z .

With DiT loss [Definition 4.1](#), we have

$$\begin{aligned}
\frac{dg_2}{d\underline{W}} &= \frac{1}{2} \sum_{j_0=1}^L \sum_{i=1}^d \frac{d}{d\underline{W}} c_{j_0, i_0}^2(\underline{W}) \\
&= \sum_{j_0=1}^L \sum_{i=1}^d \frac{d}{d\underline{W}} c_{j_0, i_0}^2 c(\underline{W})_{j_0, i_0} \cdot \frac{dc(\underline{W})_{j_0, i_0}}{d\underline{W}_{i_0}} \\
&= \sum_{j_0=1}^L \sum_{i=1}^d \frac{d}{d\underline{W}} c_{j_0, i_0}^2 c(\underline{W})_{j_0, i_0} \cdot \frac{d \langle f(\underline{W})_{j_0}, h(\underline{W}_{OV})_{i_0} \rangle}{d\underline{W}_{i_0}} && \text{(By [Definition G.5](#))} \\
&= \sum_{j_0=1}^L \sum_{i=1}^d \frac{d}{d\underline{W}} c_{j_0, i_0}^2 c(\underline{W})_{j_0, i_0} \cdot \left\langle \frac{df(\underline{W})_{j_0}}{d\underline{W}_i}, h(\underline{W}_{OV})_{i_0} \right\rangle \\
&= \sum_{j_0=1}^L \sum_{i=1}^d \frac{d}{d\underline{W}} c_{j_0, i_0}^2 c(\underline{W})_{j_0, i_0} \cdot \left\langle \frac{d\alpha^{-1}(\underline{W})_{j_0} u(\underline{W})_{j_0}}{d\underline{W}_i}, h(\underline{W}_{OV})_{i_0} \right\rangle && \text{(By [Definition G.3](#))} \\
&= \sum_{j_0=1}^L \sum_{i=1}^d \frac{d}{d\underline{W}} c_{j_0, i_0}^2 c(\underline{W})_{j_0, i_0} \cdot \left\langle \alpha(\underline{W})_{j_0}^{-1} \cdot \frac{du(\underline{W})_{j_0}}{d\underline{W}_{i_0}} + \frac{d\alpha(\underline{W})_{j_0}^{-1}}{d\underline{W}_{i_0}} \cdot u(\underline{W})_{j_0}, h(\underline{W}_{OV})_{i_0} \right\rangle \\
&= \sum_{j_0=1}^L \sum_{i=1}^d \frac{d}{d\underline{W}} c_{j_0, i_0}^2 c(\underline{W})_{j_0, i_0} \cdot \left\langle \alpha(\underline{W})_{j_0}^{-1} \cdot \frac{du(\underline{W})_{j_0}}{d\underline{W}_{i_0}} - \alpha(\underline{W})_{j_0}^{-2} \frac{d\alpha(\underline{W})_{j_0}}{d\underline{W}_{i_0}} \cdot u(\underline{W})_{j_0}, h(\underline{W}_{OV})_{i_0} \right\rangle. \\
&&& \text{(By chain rule)}
\end{aligned}$$

For each $j_0 \in [L]$, we have

$$\frac{d(A_{j_0} \underline{W})}{d\underline{W}_{i_0}} = A_{j_0} \cdot \frac{d\underline{W}}{d\underline{W}_{i_0}} = (A_{j_0})[\cdot, i].$$

Therefore, for each $j_0 \in [L]$, we have

$$\begin{aligned}
\frac{du(\underline{W})_{j_0}}{d\underline{W}_{i_0}} &= \frac{d \exp(A_{j_0} \underline{W})}{d\underline{W}_{i_0}} && \text{(By [Definition G.1](#))} \\
&= \exp(A_{j_0} \underline{W}) \odot \frac{dA_{j_0} \underline{W}}{d\underline{W}_{i_0}} && \text{(By entry-wise product rule)} \\
&= A_{j_0}[\cdot, i] \odot u(\underline{W})_{j_0}. && \text{(By [Definition G.1](#) again)}
\end{aligned}$$

Similarly,

$$\begin{aligned}
\frac{d\alpha(\underline{W})_{j_0}}{d\underline{W}_{i_0}} &= \frac{d \langle u(\underline{W})_{j_0}, \mathbf{1}_L \rangle}{d\underline{W}_{i_0}} && \text{(By Definition G.2)} \\
&= \langle \mathbf{A}_{j_0}[\cdot, i] \odot u(\underline{W})_{j_0}, \mathbf{1}_L \rangle && \text{(By entry-wise product rule)} \\
&= \langle \mathbf{A}_{j_0}[\cdot, i], u(\underline{W})_{j_0} \rangle. && \text{(By Definition G.1 again)}
\end{aligned}$$

Putting all together, we have

$$\begin{aligned}
&\frac{dg_2(\underline{W})_{j_0, i_0}}{d\underline{W}_{i_0}} \\
&= [\langle h(\underline{W}_{OV})_{i_0}, \mathbf{A}_{j_0}[\cdot, i] \odot f(\underline{W})_{j_0} \rangle - \langle h(\underline{W}_{OV})_{i_0}, f(\underline{W})_{j_0} \rangle \cdot \langle \mathbf{A}_{j_0}[\cdot, i], f(\underline{W})_{j_0} \rangle] \cdot c(\underline{W})_{j_0, i_0},
\end{aligned}$$

where

$$\begin{aligned}
&\langle h(\underline{W}_{OV})_{i_0}, \mathbf{A}_{j_0}[\cdot, i] \odot f(\underline{W})_{j_0} \rangle - \langle h(\underline{W}_{OV})_{i_0}, f(\underline{W})_{j_0} \rangle \cdot \langle \mathbf{A}_{j_0}[\cdot, i], f(\underline{W})_{j_0} \rangle \\
&= \mathbf{A}_{j_0}^\top (\text{diag}(f(\underline{W})_{j_0}) - f(\underline{W})_{j_0} f(\underline{W})_{j_0}^\top) h(\underline{W}_{OV})_{i_0}.
\end{aligned}$$

This completes the proof. \square

Observe (G.2) carefully. We see that (I) is diagonal and (II) is low-rank. This provides a hint for algorithmic speedup through low-rank approximation: If we approximate the other parts with low-rank approximation and carefully match the multiplication dimensions, we might formulate the computation of $\frac{dg_2}{d\underline{W}}$ as a chained low-rank approximation.

Surprisingly, such an approach makes computing (G.2) as fast as in almost-linear time. To proceed, we further decompose (G.2) according to the chain-rule in the next lemma, and then conduct the approximation term-by-term.

To facilitate our proof, it's convenient to introduce the following notations.

Definition G.6 ($q(\cdot)$). Define $c(\underline{W}) \in \mathbb{R}^{L \times d}$ as specified in Definition G.5 and $h(\underline{W}_{OV}) \in \mathbb{R}^{L \times d}$ as described in Definition G.4. Define $q(\underline{W}) \in \mathbb{R}^{L \times L}$ by

$$q(\underline{W}) := \underbrace{c(\underline{W})}_{L \times d} \underbrace{h(\underline{W}_{OV})^\top}_{d \times L}.$$

In addition, $q(\underline{W})_{j_0}^\top$ denotes the j_0 -th row of $q(\underline{W})$, transposed, making it an $L \times 1$ vector.

Definition G.7 ($p(\cdot), p_1(\cdot), p_2(\cdot)$). For each index $j_0 \in [L]$, we define $p(\underline{W})_{j_0} \in \mathbb{R}^n$ as follows:

$$p(\underline{W})_{j_0} := (\text{diag}(f(\underline{W})_{j_0}) - f(\underline{W})_{j_0} f(\underline{W})_{j_0}^\top) q(\underline{W})_{j_0}.$$

We define $p(W) \in \mathbb{R}^{L \times L}$ such that $p(W)_{j_0}^\top$ forms the j_0 -th row of $p(W)$. In addition, for every index $j_0 \in [L]$, we define $p_1(W)_{j_0}, p_2(W)_{j_0} \in \mathbb{R}^L$ as

$$p_1(W)_{j_0} := \text{diag}\left(f(W)_{j_0}\right) q(W)_{j_0}, \quad p_2(W)_{j_0} := f(W)_{j_0} f(W)_{j_0}^\top q(W)_{j_0},$$

such that $p(W) = p_1(W) - p_2(W)$.

$p(\cdot)$ allows us to express $\frac{dg_2}{dW}$ in a neat form:

Lemma G.2. Define the functions $f(W) \in \mathbb{R}^{L \times L}$, $c(W) \in \mathbb{R}^{d \times L}$, $h(W_{OV}) \in \mathbb{R}^{d \times L}$, $q(W) \in \mathbb{R}^{L \times L}$, and $p(W) \in \mathbb{R}^{L \times L}$ as specified in **Definitions G.3 to G.7**, respectively. Let $A_1, A_2 \in \mathbb{R}^{d \times L}$ be two given matrices, and define $A = A_1^\top \otimes A_2^\top$. Define g_2 according to **(O1)**, and let $g_2(W)_{j_0, i_0}$ be as described in **(G.1)**. It holds

$$\frac{dg_2}{dW} = \text{vec}\left(A_1 p(W) A_2^\top\right). \quad (\text{G.3})$$

Proof. By definitions, **(G.1)** gives

$$\begin{aligned} & \frac{d(g_2)_{j_0, i_0}}{dW_{i_0}} \\ &= c_{j_0, i_0} \cdot \left(\underbrace{\langle f(W)_{j_0} \odot A_{j_0, i_0}, h(W_{OV})_{i_0} \rangle}_{= A_{j_0, i}^\top \text{diag}(f(W)_{j_0}) h(W_{OV})_{i_0}} - \underbrace{\langle f(W)_{j_0}, h(W_{OV})_{i_0} \rangle \cdot \langle f(W)_{j_0}, A_{j_0, i_0} \rangle}_{= A_{j_0, i}^\top f(W)_{j_0} f(W)_{j_0}^\top h(W_{OV})_{i_0}} \right). \end{aligned} \quad (\text{G.4})$$

(By $\langle a \odot b, c \rangle = a^\top \text{diag}(b)c$ for $a, b, c \in \mathbb{R}^L$)

Therefore, **(G.4)** becomes

$$\begin{aligned} \frac{d(g_2)_{j_0, i_0}}{dW_{i_0}} &= c_{j_0, i_0} \cdot (A_{j_0, i}^\top \text{diag}(f(W)_{j_0}) h(W_{OV})_{i_0} - A_{j_0, i}^\top f(W)_{j_0} f(W)_{j_0}^\top h(W_{OV})_{i_0}) \\ &= c_{j_0, i_0} \cdot A_{j_0, i}^\top (\text{diag}(f(W)_{j_0}) - f(W)_{j_0} f(W)_{j_0}^\top) h(W_{OV})_{i_0}. \end{aligned} \quad (\text{G.5})$$

Then, by definitions of $q(\cdot), p(\cdot)$, we complete the proof. \square

G.1.2 Low-Rank Approximations of Building Blocks I

The definitions of p , p_1 , p_2 , and **Lemma G.2** show that the DiT training gradient $\frac{dg_2}{dW}$ involves entry-wise products of f , q , and c . Therefore, if we approximate these with inner-dimension-matched low-rank approximations, computing $\frac{dg_2}{dW}$ itself becomes a low-rank approximation. In the following sections, we present low-rank approximations for f , q , and c .

Lemma G.3 (Approximate $f(\cdot)$, Modified from [Alman and Song, 2023]). Let $\Gamma = o(\sqrt{\log L})$ and $k_1 = L^{o(1)}$. Let $A_1, A_2 \in \mathbb{R}^{d \times L}$, $W \in \mathbb{R}^{d \times d}$ and $f(W) = D^{-1} \exp(A_1^\top X A_2)$ with $D = \text{diag}(\exp(A_1^\top W A_2) \mathbf{1}_L)$ follows **Definitions G.1 to G.3** and **G.5**. If $\max(\|A_1^\top W\|_{\max} \leq \Gamma, \|A_2\|_{\max}) \leq \Gamma$, then there exist two matrices $U_1, V_1 \in \mathbb{R}^{L \times k_1}$ such that $\|U_1 V_1^\top - f(W)\|_{\max} \leq \epsilon/\text{poly}(L)$. In addition, it takes $L^{1+o(1)}$ time to construct U_1 and V_1 .

Proof. By [Alman and Song, 2023, Theorem 3], we complete the proof. \square

Lemma G.4 (Approximate $c(\cdot)$). Assume all numerical values are in $O(\log L)$ bits. Let $d = O(\log L)$ and $c(W) \in \mathbb{R}^{L \times d}$ follows **Definition G.5**. There exist two matrices $U_1, V_1 \in \mathbb{R}^{L \times k_1}$ such that $\|U_1 V_1^\top h(W_{OV}) - Y^\top - c(W)\|_{\max} \leq \epsilon/\text{poly}(L)$.

Proof of Lemma G.4.

$$\begin{aligned} \|U_1 V_1^\top h(W_{OV}) - Y^\top - c(W)\|_{\max} &= \|U_1 V_1^\top h(W_{OV}) - Y^\top - (f(W)h(W_{OV}) - Y^\top)\|_{\max} \\ &\quad \text{(By Definition G.5)} \\ &= \|[U_1 V_1^\top - f(W)] h(W_{OV})\|_{\max} \\ &\leq \epsilon/\text{poly}(L). \quad \text{(By [Alman and Song, 2023, Theorem 3])} \end{aligned}$$

\square

Lemma G.5 (Approximate $q(\cdot)$). Let $k_2 = L^{o(1)}$, $c(\cdot) \in \mathbb{R}^{L \times d}$ follow **Definition G.5** and let $q(W) := c(W)h(W_{OV})^\top \in \mathbb{R}^{L \times L}$ (follow **Definition G.6**). There exist two matrices $U_2, V_2 \in \mathbb{R}^{L \times k_2}$ such that $\|U_2 V_2^\top - q(W)\|_{\max} \leq \epsilon/\text{poly}(L)$. In addition, it takes $L^{1+o(1)}$ time to construct U_2, V_2 .

Proof of Lemma G.5. Our proof is built on [Alman and Song, 2023, Lemma D.3].

Let $\tilde{q}(\cdot)$ denote an approximation to $q(\cdot)$.

By **Lemma G.4**, $U_1 V_1^\top h(W_{OV}) - Y$ approximates $c(W)$ up to accuracy $\epsilon = 1/\text{poly}(L)$.

Thus, by setting $\tilde{q}(W) = h(W_{OV}) (U_1 V_1^\top h(W_{OV}) - Y)^\top$, we find a low-rank form for $\tilde{q}(\cdot)$:

$$\tilde{q}(W) = h(W_{OV}) (h(W_{OV}))^\top V_1 U_1^\top - h(W_{OV}) Y^\top,$$

such that

$$\begin{aligned}\|\tilde{q}(\underline{W}) - q(\underline{W})\|_{\max} &= \left\| h(W_{OV}) (U_1 V_1^\top h(W_{OV}) - Y)^\top - h(W_{OV}) Y^\top \right\|_{\max} \\ &\leq d \|h(W_{OV})\|_{\max} \|U_1 V_1^\top h(W_{OV}) - Y - c(\underline{W})\|_{\max} \\ &\leq \epsilon/\text{poly}(L).\end{aligned}$$

By $k_1, d = L^{o(1)}$, compute $\underbrace{(h(W_{OV}))^\top}_{d \times L} \underbrace{V_1}_{L \times k_1} \underbrace{U_1^\top}_{k_1 \times L}$ takes only $L^{1+o(1)}$ time. This completes the proof. \square

G.1.3 Low-Rank Approximations of Building Blocks II

Now, we use the low-rank approximations of f, q, c to construct low-rank approximations for $p_1(\cdot), p_2(\cdot), p(\cdot)$.

Lemma G.6 (Approximate $p_1(\cdot)$). Let $k_1, k_2 = L^{o(1)}$. Suppose $U_1, V_1 \in \mathbb{R}^{L \times k_1}$ approximates $f(\underline{W}) \in \mathbb{R}^{L \times L}$ such that $\|U_1 V_1^\top - f(\underline{W})\|_{\max} \leq \epsilon/\text{poly}(L)$, and $U_2, V_2 \in \mathbb{R}^{L \times k_2}$ approximates the $q(\underline{W}) \in \mathbb{R}^{L \times L}$ such that $\|U_2 V_2^\top - q(\underline{W})\|_{\max} \leq \epsilon/\text{poly}(L)$. Then there exist two matrices $U_3, V_3 \in \mathbb{R}^{L \times k_3}$ such that $\|U_3 V_3^\top - p_1(\underline{W})\|_{\max} \leq \epsilon/\text{poly}(L)$. In addition, it takes $L^{1+o(1)}$ time to construct U_3, V_3 .

Proof of Lemma G.6. By tensor trick, we construct U_3, V_3 as tensor products of U_1, V_1 and U_2, V_2 , respectively, while preserving their low-rank structures. Then, we show the low-rank approximation of $p_1(\cdot)$ with bounded error by Lemma G.3 and Lemma G.5.

Let \otimes be *column-wise* Kronecker product such that $A \otimes B := [A[\cdot, 1] \otimes B[\cdot, 1] \mid \dots \mid A[\cdot, k_1] \otimes B[\cdot, k_1]] \in \mathbb{R}^{L \times k_1 k_2}$ for $A \in \mathbb{R}^{L \times k_1}, B \in \mathbb{R}^{L \times k_2}$.

Let $\tilde{f}(\underline{W}) := U_1 V_1^\top$ and $\tilde{q}(\underline{W}) := U_2 V_2^\top$ denote matrix-multiplication approximations to $f(\underline{W})$ and $q(\underline{W})$, respectively.

For the case of presentation, let $U_3 = \overbrace{U_1}^{L \times k_1} \otimes \overbrace{U_2}^{L \times k_2}$ and $V_3 = \overbrace{V_1}^{L \times k_1} \otimes \overbrace{V_2}^{L \times k_2}$. It holds

$$\begin{aligned}
& \|U_3 V_3^\top - p_1(\underline{W})\|_{\max} \\
&= \|U_3 V_3^\top - f(\underline{W}) \odot q(\underline{W})\|_{\max} \quad (\text{By } p_1(\underline{W}) = f(\underline{W}) \odot q(\underline{W})) \\
&= \|(U_1 \otimes U_2)(V_1 \otimes V_2)^\top - f(\underline{W}) \odot q(\underline{W})\|_{\max} \\
&= \|(U_1 V_1^\top) \odot (U_2 V_2^\top) - f(\underline{W}) \odot q(\underline{W})\|_{\max} \\
&= \|\tilde{f}(\underline{W}) \odot \tilde{q}(\underline{W}) - f(\underline{W}) \odot q(\underline{W})\|_{\max} \\
&\leq \underbrace{\|\tilde{f}(\underline{W}) \odot \tilde{q}(\underline{W}) - \tilde{f}(\underline{W}) \odot q(\underline{W})\|_{\max}}_{\leq \epsilon/\text{poly}(L)} + \underbrace{\|\tilde{f}(\underline{W}) \odot q(\underline{W}) - f(\underline{W}) \odot q(\underline{W})\|_{\max}}_{\leq \epsilon/\text{poly}(L)} \\
&\leq \epsilon/\text{poly}(L). \quad (\text{By Lemma G.3 and Lemma G.5})
\end{aligned}$$

Computationally, by $k_1, k_2 = L^{o(1)}$, computing U_3 and V_3 takes $L^{1+o(1)}$ time. This completes the proof. \square

Lemma G.7 (Approximate $p_2(\cdot)$). Let $k_1, k_2, k_4 = L^{o(1)}$. Let $p_2(\underline{W}) \in \mathbb{R}^{L \times L}$ follow **Definition G.7** such that its j_0 -th column is $p_2(\underline{W})_{j_0} = f(\underline{W})_{j_0} f(\underline{W})_{j_0}^\top q(\underline{W})_{j_0}$ for each $j_0 \in [L]$. Suppose $U_1, V_1 \in \mathbb{R}^{L \times k_1}$ approximates the $f(\underline{X})$ such that $\|U_1 V_1^\top - f(\underline{W})\|_{\max} \leq \epsilon/\text{poly}(L)$, and $U_2, V_2 \in \mathbb{R}^{L \times k_2}$ approximates the $q(\underline{W}) \in \mathbb{R}^{L \times L}$ such that $\|U_2 V_2^\top - q(\underline{W})\|_{\max} \leq \epsilon/\text{poly}(L)$. Then there exist matrices $U_4, V_4 \in \mathbb{R}^{L \times k_4}$ such that $\|U_4 V_4^\top - p_2(\cdot)\|_{\max} \leq \epsilon/\text{poly}(L)$. In addition, it takes $L^{1+o(1)}$ time to construct U_4, V_4 .

Proof of Lemma G.7. From **Definition G.7**,

$$p_2(\underline{W})_{j_0} := \overbrace{f(\underline{W})_{j_0} f(\underline{W})_{j_0}^\top q(\underline{W})_{j_0}}^{(II)}.$$

(I)

For (I), we show its low-rank approximation by observing the low-rank-preserving property of the multiplication between $f(\cdot)$ and $q(\cdot)$ (from **Lemma G.3** and **Lemma G.5**). For (II), we show its low-rank approximation by the low-rank structure of $f(\cdot)$ and (I).

Part (I). We define a function $r(\underline{W}) : \mathbb{R}^{d^2} \rightarrow \mathbb{R}^L$ such that the j_0 -th component $r(\underline{W})_{j_0} := (f(\underline{W})_{j_0})^\top q(\underline{W})_{j_0}$ for all $j_0 \in [L]$. Let $\tilde{r}(\underline{W})$ denote the approximation of $r(\underline{W})$ via decomposing

into $f(\cdot)$ and $q(\cdot)$:

$$\begin{aligned}\tilde{r}(\underline{W})_{j_0} &:= \left\langle \tilde{f}(\underline{W})_{j_0}, \tilde{q}(\underline{W})_{j_0} \right\rangle = (U_1 V_1^\top) [j_0, \cdot] \cdot [(U_2 V_2^\top) [j_0, \cdot]]^\top \\ &= U_1 [j_0, \cdot] \underbrace{V_1^\top}_{k_1 \times L} \underbrace{V_2}_{L \times k_2} (U_2 [j_0, \cdot])^\top,\end{aligned}\tag{G.6}$$

for all $j_0 \in [L]$. This allows us to write $p_2(\underline{W}) = f(\underline{W}) \text{diag}(r(\underline{W}))$ with $\text{diag}(\tilde{r}(\underline{W}))$ denoting a diagonal matrix with diagonal entries being components of $\tilde{r}(\underline{W})$.

Part (II). With $r(\cdot)$, we approximate $p_2(\cdot)$ with $\tilde{p}_2(\underline{W}) = \tilde{f}(\underline{W}) \text{diag}(\tilde{r}(\underline{W}))$ as follows.

Since $\tilde{f}(\underline{W})$ has low rank representation, and $\text{diag}(\tilde{r}(\underline{W}))$ is a diagonal matrix, $\tilde{p}_2(\cdot)$ has low-rank representation by definition. Thus, we set $\tilde{p}_2(\underline{W}) = U_4 V_4^\top$ with $U_4 = U_1$ and $V_4 = \text{diag}(\tilde{r}(\underline{W})) V_1$. Then, we bound the approximation error

$$\begin{aligned}& \|U_4 V_4^\top - p_2(\underline{W})\|_{\max} \\ &= \|\tilde{p}_2(\underline{W}) - p_2(\underline{W})\|_{\max} \\ &= \max_{j_0 \in [L]} \left\| \tilde{f}(\underline{W})_{j_0} \tilde{r}(\underline{W})_{j_0} - f(\underline{W})_{j_0} r(\underline{W})_{j_0} \right\|_{\max} \\ &\leq \max_{j_0 \in [L]} \left[\left\| \tilde{f}(\underline{W})_{j_0} \tilde{r}(\underline{W})_{j_0} - f(\underline{W})_{j_0} r(\underline{W})_{j_0} \right\|_{\max} + \left\| \tilde{f}(\underline{W})_{j_0} \tilde{r}(\underline{W})_{j_0} - f(\underline{W})_{j_0} r(\underline{W})_{j_0} \right\|_{\max} \right] \\ &\quad \text{(By triangle inequality)} \\ &\leq \epsilon / \text{poly}(L).\end{aligned}$$

Computationally, computing $V_1^\top V_2$ takes $L^{1+o(1)}$ time by $k_1, k_2 = L^{o(1)}$. Once we have $V_1^\top V_2$ precomputed, (G.6) only takes $O(k_1 k_2)$ time for each $j_0 \in [L]$. Thus, the total time is $O(L k_1 k_2) = L^{1+o(1)}$. Since U_1 and V_1 takes $L^{1+o(1)}$ time to construct and $V_4 = \underbrace{\text{diag}(\tilde{r}(\underline{W}))}_{L \times L} \underbrace{V_1}_{L \times k_1}$ also takes $L^{1+o(1)}$ time, U_4 and V_4 takes $L^{1+o(1)}$ time to construct. This completes the proof. \square

G.2 Proof of Theorem 4.1

Proof of Theorem 4.1. By the definitions of matrices $p(\cdot)$, $p_1(\cdot)$ and $p_2(\cdot)$ (Definition G.7), we have

$$p(\underline{W}) = p_1(\underline{W}) - p_2(\underline{W}).$$

By Lemma G.2, we have

$$\frac{dg_2}{d\underline{W}} = \text{vec} \left(A_1 p(\underline{W}) A_2^\top \right).\tag{G.7}$$

To show the existence of $L^{1+o(1)}$ algorithms for DiT backward computation **Problem 1**, we prove fast low-rank approximations for $A_1 p_1(\underline{W}) A_2^\top$ and $A_1 p_2(\underline{W}) A_2^\top$ as follows.

Let $\tilde{p}_1(\underline{W}), \tilde{p}_2(\underline{W})$ denote the approximations to $p_1(\underline{W}), p_2(\underline{W})$, respectively.

By **Lemma G.6**, it takes $L^{1+o(1)}$ time to construct $U_3, V_3 \in \mathbb{R}^{L \times k_3}$ such that

$$A_1 \tilde{p}_1(\underline{W}) A_2^\top = A_1 U_3 V_3^\top A_2^\top.$$

Then, computing $\underbrace{A_1}_{d \times L} \underbrace{U_3}_{L \times k_3} \underbrace{V_3^\top}_{k_3 \times L} \underbrace{A_2^\top}_{L \times d}$ takes $L^{1+o(1)}$ due to the fact that $d, k_1 k_3 = L^{o(1)}$.

Therefore, total running time for $A_1 p_1(\underline{W}) A_2^\top$ is $L \cdot L^{o(1)} = L^{1+o(1)}$.

For the same reason (by **Lemma G.7**), total running time for $A_1 p_2(\underline{W}) A_2^\top$ is $L \cdot L^{o(1)} = L^{1+o(1)}$.

Lastly, we have

$$\begin{aligned} & \left\| \frac{\partial g_2}{\partial \underline{W}} - \tilde{G}^{(W)} \right\|_{\max} \\ &= \left\| \text{vec} \left(A_1 \tilde{p}(\underline{W}) A_2^\top \right) - \text{vec} \left(A_1 \tilde{p}(\underline{W}) A_2^\top \right) \right\|_{\max} && \text{(By Lemma G.2)} \\ &= \left\| \left(A_1 \tilde{p}(\underline{W}) A_2^\top \right) - \left(A_1 \tilde{p}(\underline{W}) A_2^\top \right) \right\|_{\max} && \text{(By definition, } \|A\|_{\max} := \max_{i,j} |A_{ij}| \text{ for any matrix } A) \\ &\leq \left\| \left(A_1 [p_1(\underline{W}) - \tilde{p}_1(\underline{W})] A_2^\top \right) \right\|_{\max} + \left\| \left(A_1 [p_2(\underline{W}) - \tilde{p}_2(\underline{W})] A_2^\top \right) \right\|_{\max} && \text{(By Definition G.7 and triangle inequality)} \\ &\leq \|A_1\|_{\infty} \|A_2\|_{\infty} (\|p_1(\underline{W}) - \tilde{p}_1(\underline{W})\|_{\max} + \|p_2(\underline{W}) - \tilde{p}_2(\underline{W})\|_{\max}) && \text{(By the sub-multiplicative property of } \|\cdot\|_{\infty}) \\ &\leq \epsilon / \text{poly}(L). && \text{(By Lemma G.6 and Lemma G.7)} \end{aligned}$$

Set $\epsilon = 1/\text{poly}(L)$. We complete the proof. \square

References

- Josh Alman and Zhao Song. Fast attention requires bounded entries. *Advances in Neural Information Processing Systems (NeurIPS)*, 36, 2023.
- Josh Alman and Zhao Song. The fine-grained complexity of gradient computation for training large language models. *arXiv preprint arXiv:2402.04497*, 2024a.
- Josh Alman and Zhao Song. How to capture higher-order correlations? generalizing matrix softmax attention to kronecker computation. In *The Twelfth International Conference on Learning Representations (ICLR)*, 2024b.
- Luca Ambrogioni. In search of dispersed memories: Generative diffusion models are associative memory networks. *arXiv preprint arXiv:2309.17290*, 2023.
- Fan Bao, Chongxuan Li, Yue Cao, and Jun Zhu. All are worth words: a vit backbone for score-based diffusion models. In *NeurIPS 2022 Workshop on Score-Based Methods*, 2022.
- Joe Benton, Valentin De Bortoli, Arnaud Doucet, and George Deligiannidis. Nearly d-linear convergence bounds for diffusion models via stochastic localization. In *The Twelfth International Conference on Learning Representations (ICLR)*, 2024.
- Valentin De Bortoli. Convergence of denoising diffusion models under the manifold hypothesis. *Transactions on Machine Learning Research*, 2022. ISSN 2835-8856.
- Tom Brown, Benjamin Mann, Nick Ryder, Melanie Subbiah, Jared D Kaplan, Prafulla Dhariwal, Arvind Neelakantan, Pranav Shyam, Girish Sastry, Amanda Askell, et al. Language models are few-shot learners. *Advances in neural information processing systems*, 33:1877–1901, 2020.
- Junsong Chen, Jincheng YU, Chongjian GE, Lewei Yao, Enze Xie, Zhongdao Wang, James Kwok, Ping Luo, Huchuan Lu, and Zhenguo Li. Pixart- α : Fast training of diffusion transformer for photorealistic text-to-image synthesis. In *The Twelfth International Conference on Learning Representations (ICLR)*, 2024.
- Minshuo Chen, Xingguo Li, and Tuo Zhao. On generalization bounds of a family of recurrent neural networks. In *Proceedings of the Twenty Third International Conference on Artificial Intelligence and Statistics (AISTATS)*, volume 108, pages 1233–1243, 2020a.
- Minshuo Chen, Wenjing Liao, Hongyuan Zha, and Tuo Zhao. Distribution approximation and statistical estimation guarantees of generative adversarial networks. *arXiv preprint arXiv:2002.03938*, 2020b.
- Minshuo Chen, Kaixuan Huang, Tuo Zhao, and Mengdi Wang. Score approximation, estimation and distribution recovery of diffusion models on low-dimensional data. In *International Conference on Machine Learning (ICML)*, pages 4672–4712. PMLR, 2023a.

- Sitan Chen, Sinho Chewi, Jerry Li, Yuanzhi Li, Adil Salim, and Anru Zhang. Sampling is as easy as learning the score: theory for diffusion models with minimal data assumptions. In *The Eleventh International Conference on Learning Representations (ICLR)*, 2023b.
- Marek Cygan, Holger Dell, Daniel Lokshtanov, Dániel Marx, Jesper Nederlof, Yoshio Okamoto, Ramamohan Paturi, Saket Saurabh, and Magnus Wahlström. On problems as hard as cnf-sat. *ACM Transactions on Algorithms (TALG)*, 12(3):1–24, 2016.
- Huaian Diao, Zhao Song, Wen Sun, and David Woodruff. Sketching for kronecker product regression and p-splines. In *International Conference on Artificial Intelligence and Statistics (AISTATS)*, pages 1299–1308. PMLR, 2018.
- Huaian Diao, Rajesh Jayaram, Zhao Song, Wen Sun, and David Woodruff. Optimal sketching for kronecker product regression and low rank approximation. *Advances in neural information processing systems (NeurIPS)*, 32, 2019.
- Benjamin L Edelman, Surbhi Goel, Sham Kakade, and Cyril Zhang. Inductive biases and variable creation in self-attention mechanisms. In *International Conference on Machine Learning (ICML)*, pages 5793–5831. PMLR, 2022.
- Patrick Esser, Sumith Kulal, Andreas Blattmann, Rahim Entezari, Jonas Müller, Harry Saini, Yam Levi, Dominik Lorenz, Axel Sauer, Frederic Boesel, et al. Scaling rectified flow transformers for high-resolution image synthesis. *arXiv preprint arXiv:2403.03206*, 2024.
- Luciano Floridi and Massimo Chiriatti. Gpt-3: Its nature, scope, limits, and consequences. *Minds and Machines*, 30:681–694, 2020.
- Shanghua Gao, Pan Zhou, Ming-Ming Cheng, and Shuicheng Yan. Masked diffusion transformer is a strong image synthesizer. In *Proceedings of the IEEE/CVF International Conference on Computer Vision*, pages 23164–23173, 2023a.
- Yeqi Gao, Zhao Song, Weixin Wang, and Junze Yin. A fast optimization view: Reformulating single layer attention in llm based on tensor and svm trick, and solving it in matrix multiplication time. *arXiv preprint arXiv:2309.07418*, 2023b.
- Yeqi Gao, Zhao Song, and Shenghao Xie. In-context learning for attention scheme: from single softmax regression to multiple softmax regression via a tensor trick. *arXiv preprint arXiv:2307.02419*, 2023c.
- Jiuxiang Gu, Yingyu Liang, Zhenmei Shi, Zhao Song, and Yufa Zhou. Tensor attention training: Provably efficient learning of higher-order transformers. *arXiv preprint arXiv:2405.16411*, 2024.
- Jiaqi Guan, Xiangxin Zhou, Yuwei Yang, Yu Bao, Jian Peng, Jianzhu Ma, Qiang Liu, Liang Wang, and Quanquan Gu. Decompdiff: diffusion models with decomposed priors for structure-based drug design. *arXiv preprint arXiv:2403.07902*, 2024.

- Jonathan Ho, Ajay Jain, and Pieter Abbeel. Denoising diffusion probabilistic models. *Advances in neural information processing systems*, 33:6840–6851, 2020.
- Benjamin Hoover, Hendrik Strobelt, Dmitry Krotov, Judy Hoffman, Zsolt Kira, and Duen Horng Chau. Memory in plain sight: A survey of the uncanny resemblances between diffusion models and associative memories. *arXiv preprint arXiv:2309.16750*, 2023.
- Jerry Yao-Chieh Hu, Donglin Yang, Dennis Wu, Chenwei Xu, Bo-Yu Chen, and Han Liu. On sparse modern hopfield model. In *Thirty-seventh Conference on Neural Information Processing Systems (NeurIPS)*, 2023.
- Jerry Yao-Chieh Hu, Pei-Hsuan Chang, Haozheng Luo, Hong-Yu Chen, Weijian Li, Wei-Po Wang, and Han Liu. Outlier-efficient hopfield layers for large transformer-based models. In *Forty-first International Conference on Machine Learning (ICML)*, 2024a.
- Jerry Yao-Chieh Hu, Bo-Yu Chen, Dennis Wu, Feng Ruan, and Han Liu. Nonparametric modern hopfield models. *arXiv preprint arXiv:2404.03900*, 2024b.
- Jerry Yao-Chieh Hu, Thomas Lin, Zhao Song, and Han Liu. On computational limits of modern hopfield models: A fine-grained complexity analysis. In *Forty-first International Conference on Machine Learning (ICML)*, 2024c.
- Russell Impagliazzo and Ramamohan Paturi. On the complexity of k-sat. *Journal of Computer and System Sciences*, 62(2):367–375, 2001.
- Yanrong Ji, Zhihan Zhou, Han Liu, and Ramana V Davuluri. Dnabert: pre-trained bidirectional encoder representations from transformers model for dna-language in genome. *Bioinformatics*, 37(15):2112–2120, 2021.
- Haotian Jiang and Qianxiao Li. Approximation theory of transformer networks for sequence modeling. *arXiv preprint arXiv:2305.18475*, 2023.
- Tokio Kajitsuka and Issei Sato. Are transformers with one layer self-attention using low-rank weight matrices universal approximators? *arXiv preprint arXiv:2307.14023*, 2023.
- Junghwan Kim, Michelle Kim, and Barzan Mozafari. Provable memorization capacity of transformers. In *The Eleventh International Conference on Learning Representations (ICLR)*, 2022.
- Yixin Liu, Kai Zhang, Yuan Li, Zhiling Yan, Chujie Gao, Ruoxi Chen, Zhengqing Yuan, Yue Huang, Hanchi Sun, Jianfeng Gao, Lifang He, and Lichao Sun. Sora: A review on background, technology, limitations, and opportunities of large vision models, 2024.
- Zhonghua Liu, Yue Lu, Zhihui Lai, Weihua Ou, and Kaibing Zhang. Robust sparse low-rank embedding for image dimension reduction. *Applied Soft Computing*, 113:107907, 2021.

- Zhengxiong Luo, Dayou Chen, Yingya Zhang, Yan Huang, Liang Wang, Yujun Shen, Deli Zhao, Jingren Zhou, and Tieniu Tan. Videofusion: Decomposed diffusion models for high-quality video generation. In *2023 IEEE/CVF Conference on Computer Vision and Pattern Recognition (CVPR)*, pages 10209–10218. IEEE, 2023.
- Nanye Ma, Mark Goldstein, Michael S Albergo, Nicholas M Boffi, Eric Vanden-Eijnden, and Saining Xie. Sit: Exploring flow and diffusion-based generative models with scalable interpolant transformers. *arXiv preprint arXiv:2401.08740*, 2024.
- Sadegh Mahdavi, Renjie Liao, and Christos Thrampoulidis. Memorization capacity of multi-head attention in transformers. *arXiv preprint arXiv:2306.02010*, 2023.
- Shentong Mo, Enze Xie, Ruihang Chu, Lanqing Hong, Matthias Niessner, and Zhenguo Li. Dit-3d: Exploring plain diffusion transformers for 3d shape generation. *Advances in Neural Information Processing Systems (NeurIPS)*, 36, 2023.
- Alex Nichol, Prafulla Dhariwal, Aditya Ramesh, Pranav Shyam, Pamela Mishkin, Bob McGrew, Ilya Sutskever, and Mark Chen. Glide: Towards photorealistic image generation and editing with text-guided diffusion models. *arXiv preprint arXiv:2112.10741*, 2021.
- Kazusato Oko, Shunta Akiyama, and Taiji Suzuki. Diffusion models are minimax optimal distribution estimators. In *International Conference on Machine Learning (ICML)*, pages 26517–26582. PMLR, 2023.
- William Peebles and Saining Xie. Scalable diffusion models with transformers. In *Proceedings of the IEEE/CVF International Conference on Computer Vision (ICCV)*, pages 4195–4205, 2023.
- Phillip Pope, Chen Zhu, Ahmed Abdelkader, Micah Goldblum, and Tom Goldstein. The intrinsic dimension of images and its impact on learning. *arXiv preprint arXiv:2104.08894*, 2021.
- Alec Radford, Jeffrey Wu, Rewon Child, David Luan, Dario Amodei, Ilya Sutskever, et al. Language models are unsupervised multitask learners. *OpenAI blog*, 1(8):9, 2019.
- Aditya Ramesh, Prafulla Dhariwal, Alex Nichol, Casey Chu, and Mark Chen. Hierarchical text-conditional image generation with clip latents. *arXiv preprint arXiv:2204.06125*, 1(2):3, 2022.
- Hubert Ramsauer, Bernhard Schaf, Johannes Lehner, Philipp Seidl, Michael Widrich, Thomas Adler, Lukas Gruber, Markus Holzleitner, Milena Pavlovic, Geir Kjetil Sandve, et al. Hopfield networks is all you need. *arXiv preprint arXiv:2008.02217*, 2020.
- Robin Rombach, Andreas Blattmann, Dominik Lorenz, Patrick Esser, and Björn Ommer. High-resolution image synthesis with latent diffusion models. In *Proceedings of the IEEE/CVF conference on computer vision and pattern recognition (CVPR)*, pages 10684–10695, 2022.
- Yang Song and Stefano Ermon. Generative modeling by estimating gradients of the data distribution. *Advances in neural information processing systems (NeurIPS)*, 32, 2019.

- Bing Su and Ying Wu. Learning low-dimensional temporal representations. In *International Conference on Machine Learning (ICML)*, pages 4761–4770. PMLR, 2018.
- Arash Vahdat, Karsten Kreis, and Jan Kautz. Score-based generative modeling in latent space. In *Advances in Neural Information Processing Systems (NeurIPS)*, volume 34, pages 11287–11302, 2021.
- Xinyou Wang, Zaixiang Zheng, Fei Ye, Dongyu Xue, Shujian Huang, and Quanquan Gu. Diffusion language models are versatile protein learners. *arXiv preprint arXiv:2402.18567*, 2024a.
- Yan Wang, Lihao Wang, Yuning Shen, Yiqun Wang, Huizhuo Yuan, Yue Wu, and Quanquan Gu. Protein conformation generation via force-guided se (3) diffusion models. *arXiv preprint arXiv:2403.14088*, 2024b.
- Yihan Wang, Jatin Chauhan, Wei Wang, and Cho-Jui Hsieh. Universality and limitations of prompt tuning. *Advances in Neural Information Processing Systems (NeurIPS)*, 36, 2023.
- Andre Wibisono, Yihong Wu, and Kaylee Yingxi Yang. Optimal score estimation via empirical bayes smoothing. *arXiv preprint arXiv:2402.07747*, 2024.
- Virginia Vassilevska Williams. On some fine-grained questions in algorithms and complexity. In *Proceedings of the international congress of mathematicians: Rio de janeiro 2018*, pages 3447–3487. World Scientific, 2018.
- Dennis Wu, Jerry Yao-Chieh Hu, Teng-Yun Hsiao, and Han Liu. Uniform memory retrieval with larger capacity for modern hopfield models. In *Forty-first International Conference on Machine Learning (ICML)*, 2024a.
- Dennis Wu, Jerry Yao-Chieh Hu, Weijian Li, Bo-Yu Chen, and Han Liu. STanhop: Sparse tandem hopfield model for memory-enhanced time series prediction. In *The Twelfth International Conference on Learning Representations (ICLR)*, 2024b.
- Chulhee Yun, Srinadh Bhojanapalli, Ankit Singh Rawat, Sashank Reddi, and Sanjiv Kumar. Are transformers universal approximators of sequence-to-sequence functions? In *International Conference on Learning Representations (ICLR)*, 2020.
- Hongkai Zheng, Weili Nie, Arash Vahdat, and Anima Anandkumar. Fast training of diffusion models with masked transformers. *arXiv preprint arXiv:2306.09305*, 2023.
- Xiangxin Zhou, Xiwei Cheng, Yuwei Yang, Yu Bao, Liang Wang, and Quanquan Gu. Decompt: Controllable and decomposed diffusion models for structure-based molecular optimization. *arXiv preprint arXiv:2403.13829*, 2024a.
- Xiangxin Zhou, Dongyu Xue, Ruizhe Chen, Zaixiang Zheng, Liang Wang, and Quanquan Gu. Antigen-specific antibody design via direct energy-based preference optimization. *arXiv preprint arXiv:2403.16576*, 2024b.

- Zhihan Zhou, Yanrong Ji, Weijian Li, Pratik Dutta, Ramana Davuluri, and Han Liu. Dnabert-2: Efficient foundation model and benchmark for multi-species genome. *arXiv preprint arXiv:2306.15006*, 2023.
- Zhihan Zhou, Weimin Wu, Harrison Ho, Jiayi Wang, Lizhen Shi, Ramana V Davuluri, Zhong Wang, and Han Liu. Dnabert-s: Learning species-aware dna embedding with genome foundation models. *ArXiv*, 2024c.
- Zhenyu Zhu, Francesco Locatello, and Volkan Cevher. Sample complexity bounds for score-matching: Causal discovery and generative modeling. *Advances in Neural Information Processing Systems (NeurIPS)*, 36, 2023.